HIGH-THROUGHPUT METHODS TO DETERMINE INTERMOLECULAR
ASSOCIATION AND LIPOPHILICITY

by

Zhi Chen

B.S., Xiamen University, 2000

M.S. University of Pittsburgh, 2006

Submitted to the Graduate Faculty of

Arts and Sciences in partial fulfillment

of the requirements for the degree of

Doctor of Philosophy

University of Pittsburgh

2007

UNIVERSITY OF PITTSBURGH

FACULTY OF ARTS AND SCIENCES

This dissertation was presented

by

Zhi Chen

It was defended on

April 23, 2007

and approved by

Stephen G. Weber, Professor, Department of Chemistry

Shigeru Amemiya, Assistant Professor, Department of Chemistry

Stephane Petoud, Assistant Professor, Department of Chemistry

Billy Day, Professor, Department of Pharmaceutical Sciences

Dissertation Advisor: Stephen G. Weber, Professor, Department of Chemistry

HIGH-THROUGHPUT METHODS TO DETERMINE INTERMOLECULAR ASSOCIATION AND LIPOPHILICITY

ZHI CHEN, PhD

University of Pittsburgh, 2007

Noncovalent intermolecular associations are omnipresent in chemical and biochemical systems. Binding constants provide a fundamental measure of the affinity of a solute to a ligand; hence their determination has been an important step in describing and understanding molecular interactions. A high-throughput method based on the concept of phase distribution has been developed to determine binding constants. The solute distribution coefficients between a polymer phase and an aqueous phase are measured in a 96-well format, in the presence and absence of the ligand in one of the two phases. Binding constants are then calculated through linear or nonlinear fitting analyses. The polymer is plasticized poly(vinyl chloride). This high-throughput approach has been employed in several applications. In the first one, the partition ratios (no ligand in either phase) of neutral solutes have been correlated with their lipophilicities (octanol-water partition coefficients). The established linear correlation between their logarithmic values can be used as a calibration curve to predict the lipophilicity of compounds with unknown lipophilicity values. The pK_a value of a charged compound and the distribution coefficient of the ionic form can also be determined by this approach. In the second application, binding constants in the film phase have been determined for the fast evaluation of enantioselectivity of potential chiral selectors. The technique identified one chiral selector for the target econazole from a small library of twelve cyclopropyl dipeptide isosteres. Compared to other screening approaches, this protocol does not require the covalent attachment of either the target of the selector candidate hence

iv

decreases the time and labor required for screening. In addition, the amount of the potential chiral selector (~100 μg) needed is significantly reduced. Similarly, intermolecular association can be determined in the aqueous phase. In the last application, binding constants of drug-cyclodextrin complex formation have been measured at various cyclodextrin concentration and pH conditions with various cyclodextrins. Again, high throughput and low mass requirement are advantages of the method.

TABLE OF CONTENTS

LIST OF TABLES

LIST OF FIGURES

ACKNOWLEDGEMENTS

"Pursue excellence; strive for perfection." – Mr. Tan Kae-Kee

First and foremost, I would like to thank my research advisor, Prof. Stephen G. Weber. It was a great and pleasant experience to work with him and learn from him. With his vast knowledge of science, he has always provided me with proper guidance and valuable advice and for that I am eternally grateful.

Scientific research is inherently collaborative. I would like to thank Prof. Peter Wipf and Dr. Stefan Werner for providing me with chemical libraries to discover. I am also thankful to members of my research group for their helpful discussions and kind spirits.

The supporting cast in the Chemistry Department is fantastic. I would like to express my special acknowledgement to Dr. Kasi Somayajula, former director of the Mass Spectrometry Lab. I have worked with him to operate the facility and gained my expertise in mass spectrometry through that experience.

I am eternally indebted to my parents and sister for their support and encouragement throughout this endeavor. Lastly, I would like to thank my girlfriend, Xiaoping, for her continuous loving support.

1.0   INTRODUCTION

1.1   METHODS FOR THE DETERMINATION OF BINDING CONSTANTS

1.1.1   Introduction

Noncovalent intermolecular associations are omnipresent in chemical and biochemical systems. Cyclodextrin-drug inclusion, protein-drug, peptide-peptide, carbohydrate-drug, and antigen-antibody binding are a few examples. Binding constants provide a fundamental measure of the affinity of a solute to a ligand; hence their determination has been an important step in describing and understanding molecular interactions.

Many conventional techniques have been developed to measure binding constants. They can be categorized into two groups: separation based and non-separation based methods.[1] The former category of methods physically separates the free solute and the bound solute, and evaluates their concentrations. Depending on how the separation is achieved, they can be further classified as heterogeneous or homogeneous. Chromatography,[2] dialysis,[3] ultrafiltration,[4] surface plasma resonance (SPR)[5] are heterogeneous methods. The free solute is separated from the bound one on the surface of a solid substrate. Affinity capillary electrophoresis (ACE)[6-9] and electrospray mass spectrometry (ESI-MS)[10] are homogeneous methods. The separation occurs either in solution or in the gas phase. Separation-free methods monitor the change in specific

physicochemical properties of the solute or ligand upon complexation. This category includes spectroscopy methods such as UV/VIS,[11-13] IR,[14] fluorescence[13, 14] and NMR;[15] electrochemical methods such as potentiometry,[16] conductometry[15] and polarography;[17] as well as phase-solubility[18] and hydrolysis kinetics.[19, 20]

Many of the above methods were thoroughly reviewed by Connors[21] twenty years ago, hence this selective review will emphasize ACE and ESI-MS methods that have been emerging in the last two decades, and recent development in phase-distribution approaches.

1.1.2   Affinity Capillary Electrophoresis

Affinity capillary electrophoresis (ACE) is a term referring to the separation by capillary electrophoresis of substances that participate in specific or non-specific affinity interactions during electrophoresis.[22] In the last two decades, ACE has been one of the most rapidly growing analytical techniques to study a variety of noncovalent interactions and in determining binding constants and stoichiometries.

A number of specialized and general ACE reviews have appeared.[6, 9, 22-49] Most of them cover the progress and innovation in ACE during a certain period with respect to biological-based molecular interactions. Other topics include combinatorial library screening,[28] chiral additive evaluation,[40] and cyclodextrin-drug inclusion.[35, 40] Detection sensitivity improvement[36] and miniaturization[48] are also continuing foci for technological innovations within ACE. The theoretical aspect of ACE has been reviewed by several papers,[9, 23, 24, 26, 36, 37, 43, 47] including a discussion of the advantages and limitations of various ACE methods.[24, 26, 36, 47]

ACE may be classified into two modes: dynamic equilibrium ACE and pre-equilibrated ACE. The former mode requires complex forming equilibria having a lifetime of less than the

order of seconds. In the latter mode, the solute and ligand are pre-equilibrated prior to injection. For non-kinetic methods the dissociation rate must be small relative to the separation time.

1.1.2.1 Dynamic equilibrium ACE

Mobility-shift ACE is one of the dynamic equilibrium ACE methods in which the binding constant is calculated from the dependence of apparent electrophoretic mobility of the injected solute on the ligand concentration in the running buffer. A number of related methods exist, including the Hummel–Dreyer method (HD), vacancy affinity capillary electrophoresis (VACE),[50, 51] and the vacancy peak method (VP). The details in experimental design and data analysis of each method will be discussed later. Except for VACE, all the other methods were primarily developed for high-performance liquid chromatography (HPLC) and transferred to CE. These methods can be subdivided according the way the binding constants are determined from the change of the electrophoretic mobility of the species (ACE, VACE) or from the solute (free and bound) concentration evaluated by the peak area (HD, VP).

Dynamic equilibrium ACE methods assume that the equilibrium between the solute and the ligand is established very quickly in the capillary. Most studies also assume that the stoichiometry of the binding between the target and the ligand is 1:1 to establish a simple model. Complex formation of the solute (S) and the ligand (L) with the binding constant $K_{1:1}$ is described by the following equation

$$S + L \underset{}{\overset{K_{1:1}}{\rightleftharpoons}} SL \tag{1.1}$$

Hence the binding constant is

$$K_{1:1} = \frac{[SL]}{[S] \cdot [L]} \tag{1.2}$$

where [S], [L], and [SL] are the concentrations of the free solute, free ligand, and solute-ligand complex.

1.1.2.1.1   Calculation of binding constants

1.1.2.1.1.1   Calculation from the change in electrophoretic mobility

In mobility-shift ACE and VACE, the apparent electrophoretic mobility of the solute, μ_i, is expressed as

$$\mu_i = \frac{[S]}{[S]+[SL]}\mu_f + \frac{[SL]}{[S]+[SL]}\mu_c \tag{1.3}$$

where μ_f and μ_c are the electrophoretic mobilities of the free solute and solute-ligand complex, respectively. From Eq. 1.2, Eq. 1.3 can be written as

$$\mu_i = \frac{\mu_f + \mu_c K_{1:1}[L]}{1 + K_{1:1}[L]} \tag{1.4}$$

Eq. 1.4 can be converted into

$$(\mu_i - \mu_f) = \frac{(\mu_c - \mu_f)K_{1:1}[L]}{1 + K_{1:1}[L]} \tag{1.5}$$

Evaluation of experimental data is easier when Eq. 1.5 is rearranged into a linear form, for instance, double reciprocal plot

$$\frac{1}{(\mu_i - \mu_f)} = \frac{1}{(\mu_c - \mu_f)K_{1:1}} \cdot \frac{1}{[L]} + \frac{1}{(\mu_c - \mu_f)} \tag{1.6}$$

If the solute has a much smaller concentration than the ligand, then [L] can be approximated by [L_{tot}], which is the total concentration of the ligand. Hence by plotting $\frac{1}{(\mu_i - \mu_f)}$ versus $\frac{1}{[L_{tot}]}$, the y-intercept of the linear fitting will give the value of $\frac{1}{(\mu_c - \mu_f)}$, and $K_{1:1} = $ intercept / slope.

Eq. 1.5 can be converted into other linear forms. For example, y-reciprocal plot

4

$$\frac{[L]}{(\mu_i - \mu_f)} = \frac{1}{(\mu_c - \mu_f)} \cdot [L] + \frac{1}{(\mu_c - \mu_f) \cdot K_{1:1}} \qquad (1.7)$$

and *x*-reciprocal plot

$$\frac{(\mu_i - \mu_f)}{[L]} = -K_{1:1} \cdot (\mu_i - \mu_f) + K_{1:1} \cdot (\mu_c - \mu_f) \qquad (1.8)$$

All these linearization methods have different statistical weights of the data points and are shown in Table 1.1. However, it is difficult to know the ideal weights in practical cases.[53] Moreover, when the binding constant is lower than ~5 M^{-1}, bias becomes significant in the three linearization methods and weighting does not remove the bias.[53] At high $K_{1:1}$ values ($K_{1:1}$ > ~1500 M^{-1}), the *y*-reciprocal method without weighting gives poorer precision than do the other methods, while bias is significant in the *x*-reciprocal plot and weighting the data does not alleviate the problem.[53] The maximum-response range may also greatly affect the error. For instance, when ($\mu_i - \mu_f$) is small, an *x*-reciprocal plot may give the wrong values for $K_{1:1}$.[54] Generally, nonlinear regression is more accurate and precise for the estimation of binding constants than linear regressions.[53-55] A detailed discussion of statistical errors can be found in references.[9, 26, 53-55]

1.1.2.1.1.2   Calculation from the change in peak area

The concentrations of the free and bound solute are determined by their peak (or vacancy peak) area in HD and VACE methods. Eq. 1.2 can be rearranged as[36, 56]

$$\frac{[SL]}{[S]} = -K_{1:1}[SL] + K_{1:1}[L_{tot}] \qquad (1.9)$$

Hence, the binding constant can be determined by plotting $\frac{[SL]}{[S]}$ versus [L_{tot}].

1.1.2.1.2   Experimental settings

1.1.2.1.2.1   Mobility-shift ACE

5

Table 1.1. Equations used in ACE and variances in the transformed y for the different

calculation methods.

(Adapted from reference.[54])

Calculation methods	Equations	$\sigma_{y'}^{2}$ [a]
nonlinear regression	$(\mu_i - \mu_f) = \dfrac{(\mu_c - \mu_f)K_{1:1}[L]}{1 + K_{1:1}[L]}$	σ_y^2
double reciprocal	$\dfrac{1}{(\mu_i - \mu_f)} = \dfrac{1}{(\mu_c - \mu_f)K_{1:1}} \cdot \dfrac{1}{[L]} + \dfrac{1}{(\mu_c - \mu_f)}$	$\dfrac{\sigma_y^2}{(\mu_i - \mu_f)^4}$
y-reciprocal	$\dfrac{[L]}{(\mu_i - \mu_f)} = \dfrac{1}{(\mu_c - \mu_f)} \cdot [L] + \dfrac{1}{(\mu_c - \mu_f) \cdot K_{1:1}}$	$\dfrac{[L]^2 \cdot \sigma_y^2}{(\mu_i - \mu_f)^4}$
x-reciprocal	$\dfrac{(\mu_i - \mu_f)}{[L]} = -K_{1:1} \cdot (\mu_i - \mu_f) + K_{1:1} \cdot (\mu_c - \mu_f)$	$\left(K_{1:1} + \dfrac{1}{[L]}\right)^2 \cdot \sigma_y^2$

[a] $\sigma_{y'}^{2}$ is the variance of the transformed y; σ_y^2 is the variance in $(\mu_i - \mu_f)$; the weight for each

point is equal to $1/\sigma_{y'}^{2}$.

A capillary is filled with buffer containing L in varying concentrations and a small amount of S is injected. Two peaks may appear in the electropherogram, as shown in Figure 1.1a. The positive peak corresponds to the injected S (both free and bound). The migration time of this peak is monitored for the calculation of μ_i, the apparent electrophoretic mobility of S.

1.1.2.1.2.2   HD method

A capillary is filled with buffer containing S in varying concentrations and a small amount of L is injected. Similarly, two peaks may appear in the electropherogram, as shown in Figure 1.1a. The negative peak is caused by the local deficiency of S in the buffer, and the peak area is directly related to the concentration of S bound to L. Hence both the free and bound solute concentration can be determined through a series of internal or external calibrations.[23]

1.1.2.1.2.3   VP and VACE

The capillary is filled with a buffer containing both S and L. The concentration of either S or L is fixed and the concentration of the other component is varied. The presence of S and L in the capillary causes a large background detector response. After a small plug of neat buffer is injected, the voltage is switched on and two negative peaks (Figure 1.1b) will appear in the electropherogram corresponding to free S and L caused by their decrease in local concentration. VP uses the area of the vacancy peak corresponding to free S to construct the binding isotherm. A change in mobility of S or L gives the binding information for VACE.

1.1.2.2 ACE for pre-equilibrated sample mixtures

Similar to the HD and VP methods, methods for pre-equilibrated sample mixtures give the equilibrium concentrations of the solute and ligand from the electropherogram. Hence the binding constant can be determined according to Eq. 1.2.

A   B
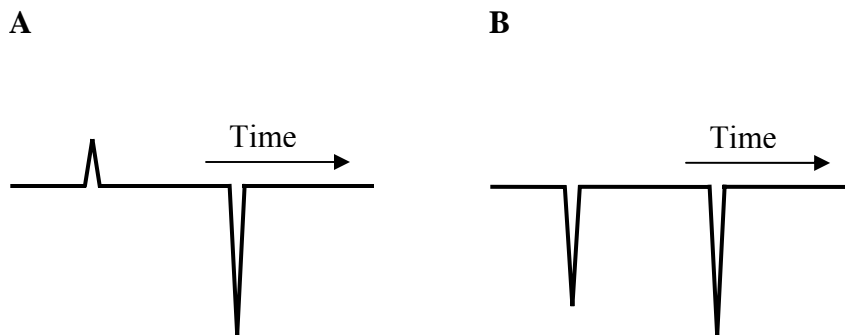
Figure 1.1. Simulated electropherograms of the methods: (A) mobility-shift ACE (HD);

(B) VP (VACE).

(Adapted from reference,[24] with permission from Elsevier)

1.1.2.2.1   Frontal Analysis (FA) and Frontal Analysis Continuous Capillary Electrophoresis (FACCE)

In the FA method, the capillary is filled with neat buffer and a large sample plug consisting of pre-equilibrated S and L is injected. Depending on the dimensions of the capillaries, the sample volume is typically between 20 and 200 nL, *i.e.*, 5-20% of the total capillary volume.[47] It is assumed that SL and L have approximately the same mobility and the mobility of S differs significantly. Another assumption is that the dissociation rate of the complex is slow enough that it can be neglected. Upon application of the electrical field, free S begins to separate from the mixture. Two plateaus will be detected, as shown in Figure 1.2. Plateau (a) corresponds to free S, and plateau (b) corresponds to $S + SL$. Hence the concentration of free S can be determined from its plateau height through an external calibration process.

FACCE differs from the FA method by the sample introduction step. The capillary inlet is immersed in the sample vial during electrophoresis; hence continuous sample introduction is achieved.   Apparently, FACCE requires free S to migrate faster than SL. Similar to the FA method, the plateau height corresponding to free S can be correlated to its concentration.

1.1.2.2.2   Kinetic CE methods

All the previously described methods assume equilibrium between interacting molecules. In dynamic equilibrium mode, equilibrium must be reached rapidly. For the FA and FACCE methods, the equilibrium is maintained locally. These assumptions may be theoretically wrong since separation disturbs equilibrium.[57] Considering the kinetics of the complex formation of S and L, Eq. 1.1 can be re-written as

$$S + L \underset{k_{\text{off}}}{\overset{k_{\text{on}}}{\rightleftharpoons}} SL$$

(1.10)
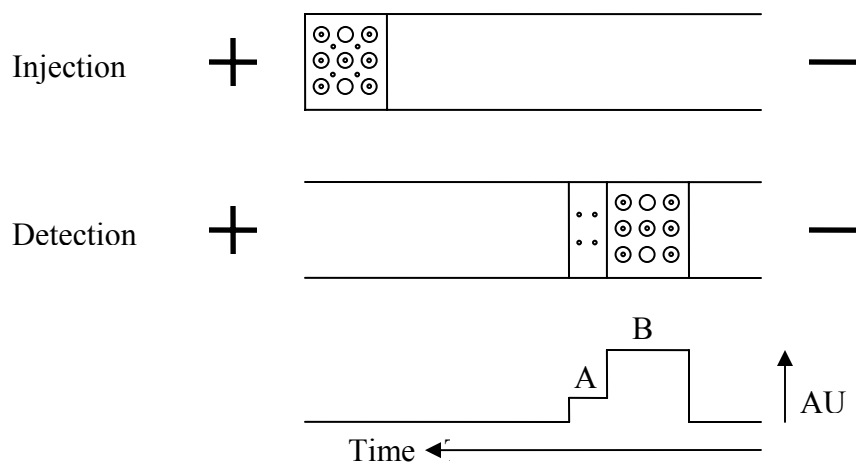
Figure 1.2. Schematic representation of frontal analysis with capillary electrophoresis.

Compounds: (·), solute; (○), ligand; (◉), solute-ligand complex. A: Signal height reflecting the

free solute concentration. B: Signal height reflecting the complex concentration.

(Adapted from reference,[9] with permission from Wiley)

where k_{on} and k_{off} are rate constants of complex formation and dissociation, respectively. Hence according to Eq. 1.2

$$K_{1:1} = k_{on} / k_{off} \qquad (1.11)$$

Whitesides was the first to explore ACE for kinetic studies.[58] Both the change in electrophoretic mobility and the shape (but not the area) of the peak were used for the determination of k_{on} and k_{off}, and thus $K_{1:1}$. Recently, Krylov has developed a series of kinetic CE methods by applying different experimental settings and data analysis approaches. Based on various initial and boundary conditions – the way interacting species enter and exit the capillary, a number of kinetic CE methods have been designed. A thorough review of these methods has been given in 2007.[59] Here one of the approaches with simple mathematics, non-equilibrium capillary electrophoresis of equilibrium mixtures (NECEEM), will be described briefly.

In NECEEM, neat buffer is used as the background electrolyte. A short plug of the equilibrium mixture of S and L is injected into the inlet of the capillary, and the complex SL continuously dissociates during electrophoresis. If the separation of S, L, and SL is efficient, re-association of S and L can be neglected. Hence the resulting electropherogram contains three peaks, as shown in Figure 1.3, representing S, L, and SL, and two exponential "smears" of S and L, which occur from the dissociation of SL. Figure 1.4 shows an experimental NECEEM electropherogram for the interaction between fluorescently labeled ssDNA and SSB protein. The dissociation constant and rate, K_d and k_{off}, respectively, can be calculated as

$$K_d = 1/K_{1:1} = \frac{[S]_0(1 + A_1/(A_2 + A_3)) - [L]_0}{1 + (A_2 + A_3)/A_1} \qquad (1.12)$$

$$k_{off} = \ln\left(\frac{A_2 + A_3}{A_1}\right)/t_{SL} \qquad (1.13)$$

11
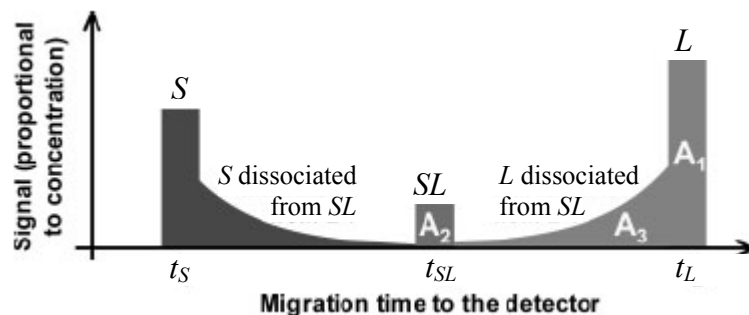
Figure 1.3. Simulated NECEEM electropherogram.

A_1 is the peak area of L that either was free in the equilibrium mixture (for NECEEM), A_2 is the peak area of intact SL at the time of its passing the detector, A_3 is the peak area of L dissociated from SL during the separation, t_L, t_{SL}, and t_S are migration times from the capillary inlet to the detector of L, SL, and S, respectively.

(Adapted from reference,[59] with permission from Wiley and the author)
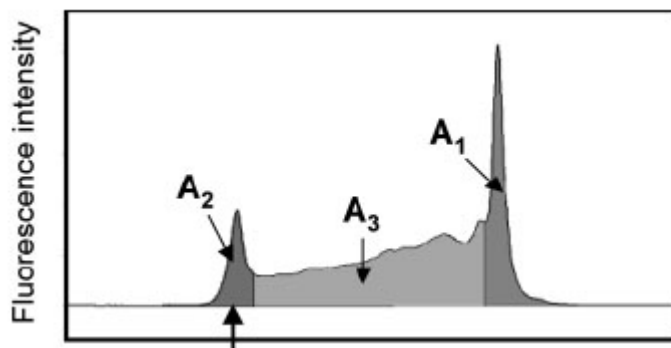
Figure 1.4. Experimental NECEEM electropherogram for the interaction between fluorescently labeled ssDNA and SSB protein.

(Reprinted from reference,[59] with permission from Wiley and the author)

12

where A_1 is the peak area corresponding to L, A_2 is the peak area corresponding to SL which was still intact at the time it passed through the detector. A_3 is the area of the exponential smear left by L dissociated from SL during the separation. Finally, t_{SL} is the migration time of the complex. $[S]_0$ and $[L]_0$ are total concentrations of S and L in the equilibrium mixture.

For NECEEM, as well as other kinetic CE methods, it is important to distinguish accurately the boundaries of the peaks. Two approaches have been proposed, by a control experiment and mathematical modeling, respectively.[59] The boundary between A_1 and A_3 can be found by comparing the peaks of free L in the presence and absence of S.[60] However, experimental errors in the range of 10% are inevitable.[59] In the approach that a mathematical model has been developed to simulate NECEEM electropherograms, various parameters, including k_{off}, v_L, v_{SL}, D_L, D_{SL} and $A_1 / (A_2 + A_3)$, are optimized in the regression analysis to minimize the deviation between the experimental and simulated traces using the least-squares method.[61] Here v_L and v_{SL} are the electrophoretic velocities of L and SL, respectively; D_L and D_{SL} are the diffusion coefficients of L and SL, respectively. This modeling approach clearly requires effort. Nevertheless, compared to conventional ACE methods, NECEEM only needs a single run to determine the binding constants. Moreover, the availability of other methods based on various initial and boundary conditions makes kinetic CE a multi-method toolbox not only to measuring binding parameters but also to testing hypotheses about the interaction mechanisms.[62] Conceptually, experimental electropherograms are obtained by multiple kinetic CE methods first. A hypothetical model of interactions between S and L is suggested and electropherograms based on the hypothesis are simulated. The experimental kinetic CE electropherograms are compared with simulated ones to obtain the best fits. If the quality of the fit is not satisfactory, a new hypothesis must be developed for the interaction. The procedure is repeated until a satisfying

13

hypothesis is found. The best fits for the accepted hypothesis lead to the determination of stoichiometric and kinetic parameters of the interaction.[62]

1.1.2.3 Comparison of ACE methods

As a homogeneous, separation based approach, ACE does not require immobilization of the ligand on a solid support with the risk of altering binding properties. Other advantages of ACE include low sample and reagent consumption, relatively short analysis time, and availability to study interactions under physiologically relevant conditions with respect to pH, ionic strength, and temperature. There are a number of experimental approaches for the determination of binding constants with ACE. Each of them exhibits specific ranges of applicability, advantages and limitations, and can often be considered as complementary rather than competitive to each other.

Mobility-shift ACE has several specific advantages compared to other approaches: (1) the injected sample need not be highly purified, and (2) binding constants of several samples can be determined simultaneously. However, the fluctuation of the electroosmotic flow (EOF) may adversely influence the observed electrophoretic mobility hence a careful control or correction of EOF is needed. Coating of the capillary inner wall is frequently useful to control EOF and to avoid solute adsorption on the inner wall of the capillary that may cause peak broadening and inaccurate mobility measurement. Alternatively, the mobility ratio (M) can be used to estimate binding constants[63]

$$M = \mu_{net} / \mu_{eof} = (\mu + \mu_{eof}) / \mu_{eof} \qquad (1.14)$$

where μ, μ_{net}, and μ_{eo} are the observed mobility, net mobility and electroosmotic mobility, respectively.

$$\frac{\Delta M}{[L]} = K_{1:1} \Delta M^{\max} - K_{1:1} \Delta M \qquad (1.15)$$

where ΔM is the change in migration ratio as a function of $[L]$, and $\Delta M^{\max}$ is the maximum change in migration ratio that can be achieved with the saturation of L for complexation. This analysis method is independent of the capillary length, the applied voltage, and the EOF mobility.

In addition, the accuracy of mobility-shift analysis depends on the stability of the complex relative to the separation time. The complex dissociation halftime, expressed as $\ln 2/k_{off}$, must be less than 1% of the peak appearance time.[64] When the on and off rates are too slow to ensure establishment of a dynamic equilibrium, broadened, split, undetectable peaks may be observed.[65] This rule holds true for other dynamic equilibrium approaches, *i.e.*, HD, VP, and VACE methods.

For methods that use the change in peak area or plateau height for the determination of the free and bound solute concentrations, and thus the binding constant, special care must be taken to assure that the total solute concentration is known accurately, since the bound solute concentration is usually calculated as the difference between the total and free concentrations of the solute. Thus, it is assumed that no solute is lost due to capillary wall adsorption or other nonspecific phenomena (precipitation, *etc.*).[66] and that the concentration in the sample corresponds to the concentration during electrophoresis (*i.e.*, no stacking occurs) or at least is corrected based on a standard curve obtained under identical conditions.[47] These requirements are more restrictive than the ones applied for mobility-shift ACE.

Contrary to dynamic equilibrium ACE methods, FA and FACCE usually require the complex to be quite stable so that a subsequent quantitation of the free S plateau height reflects the free S concentration in the sample. For molecular interactions characterized by relatively

15

rapid binding kinetics, the validity of using these two approaches should be verified. This may be accomplished by inspection of both the ascending and descending solute boundaries,[67] which is possible in FA but not in FACCE. These two methods are suitable to measure $K_{1:1}$ values in the range from 10^3 to 10^8 M^{-1}.[68] For weak interactions, the height difference between the two frontal zones may be too small. In this case, mobility-shift ACE may be preferred for the determination of binding constant. If $K_{1:1}$ is too large, the plateau height for free S may be too small to be measured.[37]

An attractive feature of FA and FACCE is that they are insensitive to changes or fluctuations in migration times, EOF, and applied voltage.[69] Low detection limit is also an advantage of these two methods. Compared to FA, FACCE requires greater sample consumption (*e.g.*, 500 nL)[70] but has been proposed to be advantageous since the continuous sampling may avoid perturbation of the binding equilibrium.[71] Moreover, FACCE usually provides a broader plateau than FA that may be easier for quantitation.[47] One of the requirements for FA and FACCE is that the mobilities of L and SL must be equal otherwise the free S plateau does not reflect the true free solute concentration at equilibrium.[24, 67] This may potentially limit the application of FA and FACCE. The mobility requirements for other ACE methods (*i.e.*, mobility-shift ACE, HD, VP, VACE) have been thoroughly discussed elsewhere.[24] The availability of various approaches to study multiple equilibria has also been discussed there.[24]

Kinetic CE methods can determine $K_{1:1}$, k_{off}, and k_{on} from a single electrophoresis experiment when 1:1 binding stoichiometry has been verified. One of the most attractive features of kinetic CE is that it is a multi-method tool based on various initial and boundary conditions; hence some proposed affinity mechanisms for a specific approach can be validated by a series of comparison studies. A potential problem of kinetic CE is the difficulty in distinguishing the

16

equilibrium fractions of corresponding components, which may lead to uncertainty in the estimate of the binding parameters.[47] The applications of kinetic CE methods to higher order equilibria are also expected.

There are certainly some inherent limitations to all ACE methods for evaluating binding constants. For instance, it may be difficult to evaluate the association of two or more neutral molecules. In addition, with a few exceptions,[72] applications of ACE have not been extended to interaction studies in non-aqueous solvents.[9]

1.1.3 Electrospray Ionization Mass Spectroscopy

Electrospray ionization mass spectrometry (ESI-MS) provides a soft ionization procedure that allows the transfer of weakly bound complexes from solution to the gas phase for mass analysis, and hence has been frequently used to study the binding behavior of a wide variety of noncovalent complexes.[73-75] Specificity, sensitivity, and speed are several advantages of ESI-MS.[76] Moreover, ESI-MS can provide the stoichiometric information of the complex directly and detect multiple components simultaneously.

To determine the binding constant of a complex quantitatively through ESI-MS, one of the most frequently used approaches is the titration method. Generally, the solute concentration in the solution is kept constant while the ligand concentration is varied over a range of about two orders of magnitude.[76] The gas phase ion intensities of the free and bound solute are monitored, and can be fit to association models for the calculation of binding constants.

Considering a 1:1 system

$$K_{1:1} = \frac{[SL]}{[S] \cdot [L]} = \frac{[SL]}{[S] \cdot ([L_{tot}] - [SL])} \tag{1.16}$$

where $[L_{tot}]$ is the total concentration of the solute. Since

$$[SL] = [S_{tot}] \cdot \frac{[SL]}{[S]+[SL]} \qquad (1.17)$$

Eq. 1.16 can be converted into

$$K_{1:1} = \frac{[SL]}{[S]} \cdot \frac{1}{[L_{tot}]-[S_{tot}] \cdot \dfrac{1}{\dfrac{[S]}{[SL]}+1}} \qquad (1.18)$$

Define

$$\frac{[S]}{[SL]} = \frac{i_S / f_S}{i_{SL} / f_{SL}} = \frac{i_S}{i_{SL}} \cdot \frac{f_{SL}}{f_S} = IF \qquad (1.19)$$

where i_S and i_{SL} are the ion intensities of the free and bound solute, respectively; f_S and f_{SL} are the response factors of the free and bound solute, respectively. Hence Eq. 1.18 can be converted into

$$(IF)^2 K_{1:1}[L_{tot}] + IF(K_{1:1}[L_{tot}] - K_{1:1}[S_{tot}] - 1) - 1 = 0 \qquad (1.20)$$

Eq. 1.20 can be further converted into various linear forms, for instance

$$\frac{1}{IF} = K_{1:1}[L_{tot}] - \frac{K_{1:1}[S_{tot}]}{IF+1} \qquad (1.21)$$

By plotting $\dfrac{1}{IF}$ versus $[L_{tot}]$, the slope of the linear fitt will give the value of $K_{1:1}$.

The ratio of ion intensities (I) can be obtained from the mass spectrum for each concentration point. However, there is no valid method that is suitable to determine the response factor of the complex (f_{SL}) and thus the ratio of response factors (F). It is often assumed that the response factors of the free and bound solutes are similar, and then F can be approximated to unity. However, different molecular species may undergo different vaporization and ionization efficiencies. This represents one of the biggest disadvantages of the ESI-MS method for binding

18

constant determination. In addition, ESI is not an instantaneous process, thus changes can occur when non-covalent complexes are transferred from the solution phase to the gas phase. For instance, when the kinetics of dissociation is in the same timescale of the evaporation process, evaporation of the droplet can cause a displacement of the complexation equilibrium towards association.[75] The limitations of the ESI-MS method described above can be partially improved by competition approaches. Basically, a reference compound is mixed with the solute for complexation with the ligand. The reference should have a similar structure to the solute and its binding behavior with the ligand should be known. Therefore the binding constant between the solute and ligand can be indirectly obtained by comparing the two binding systems.[76] From a practical point of view, ESI-MS should be used to determine relative binding affinities (selectivities) rather than absolute values.

1.1.4   Phase-Distribution Method

Phase-distribution methods monitor the dependence of the solute distribution coefficient between two phases on the ligand concentration in one phase to determine the solute-ligand binding constant. Usually, one of the phases is aqueous and the other is organic. The binding equilibrium can be studied in either phase. This method has been applied to measure binding constants for the complex formation of caffeine/ benzoic acid,[77] solute/cyclodextrin,[2, 78-85] metal ion/anion,[86] and drug/chiral selector.[87]

Eq. 1.1 describes the formation of 1:1 complex. For consecutive complexation

$$\text{S-L}_{i-1} + \text{L} \xrightleftharpoons{K_{1:i}} \text{S-L}_i \tag{1.22}$$
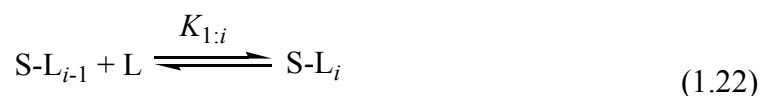
The binding constant ($K_{1:i}$) is defined as

$$K_{1:i} = \frac{[S \cdot L_i]}{[S \cdot L_{i-1}][L]}$$ (1.23)

The distribution of the free solute between phase 1 and phase 2 is determined by the partition ratio D_0

$$D_0 = \frac{[S]_1}{[S]_2}$$ (1.24)

where $[S]_1$ and $[S]_2$ are the free solute concentrations in phase 1 and phase 2, respectively. When the ligand is added to phase 1, the solute distribution coefficient is

$$D = \frac{[S]_1 + \sum_{i=1}^{n}[S \cdot L_i]_1}{[S]_2}$$ (1.25)

where n is the stoichiometry, $[S\text{-}L_i]$ ($i = 1$ to n) is the concentration of solute-ligand complex in phase 1 in various forms. Dividing Eq. 1.25 by Eq. 1.24

$$\frac{D}{D_0} = 1 + \sum_{i=1}^{n}\frac{[S \cdot L_i]}{[S]}$$ (1.26)

From Eq. 1.23, one obtains

$$[S \cdot L_i] = [S][L]^i \prod_{j=1}^{i} K_{1:j}$$ (1.27)

Here

$$K_{1:j} = \frac{[S \cdot L_j]}{[S \cdot L_{j-1}][L]}$$ (1.28)

Inserting Eq. 1.27 to Eq. 1.26

$$\frac{D}{D_0} = 1 + \sum_{i=1}^{n}\left([L]^i \prod_{j=1}^{i} K_{1:j}\right)$$ (1.29)

20

Plotting D/D_0 versus [L], the stoichiometry and the binding constants can be obtained from polynomial fitting analyses.

The phase distribution method provides an alternative approach to measure binding constants of complex formation. Advantages of this method include relatively low sample requirement, availability to measure binding constants relevant to physiological properties (*e.g.*, pH, temperature, ionic strength). However, there are several disadvantages that have to be taken into consideration. The mutual solubility of the two phases may interfere and complicate the binding equilibrium. It is even possible that some organic solvent may function as a competitor to bind the ligand (*e.g.*, octanol/cyclodextrin),[85] which should be carefully investigated to prevent from misinterpretation of the calculated binding parameters.[2] In addition, all species present in phase 1 (*e.g.*, free solute, free ligand, complexes) may partition to the second phase. The model described above assumes the partitioning of only the free solute hence has been over-simplified. Octanol has been the most frequently used solvent as the organic phase in phase-distribution studies. In this case, entrainment and emulsion can be severe problems when very hydrophobic compounds are studied.[88]

1.2   HIGH-THROUGHPUT SOLID-PHASE EXTRACTION

One of the most important strategies in the pharmaceutical field is to reduce time and labor needed for research and development of new drugs. This has led to the movement of pharmaceutical and biotechnology companies toward high-throughput screening (HTS) of small-molecule compounds for their discovery programs.[89] More compounds have become available

for further investigations. Consequently, high-throughput technologies are demanded in the post-synthetic stages in the research and development process.

Since its introduction in the mid-eighties, solid phase extraction (SPE) has been a routine sample preparation technique used to pre-concentrate drugs present at low levels of concentration and to remove interfering components from complex matrices prior to quantitative analysis. Compared to traditional liquid extraction methods, SPE presents the following advantages: higher recovery, better reproducibility, faster, and easier for automation.[90] The high throughput concept has also been embedded into SPE techniques in the last decade.[91, 92] Except for sample preparation, high-throughput SPE technologies have been employed for synthesis using affinity tags,[93] in-gel digestion of proteins,[94] immunosorbent development,[95] and chiral selector screening.[96-98]

Solid phase microextraction (SPME) is a special version of SPE in which the extraction media is a small coated fiber or tip. SPME does not have some common disadvantages of SPE such as clogging problems. It is especially designed for subsequent analysis by methods such as gas chromatography and capillary electrophoresis that have low mass detection limits.[99] Recently, a high-throughput SPME assay has been developed as a phase-distribution method to measure binding constant of complex formation.[87,100]

1.3   OUTLINE

The high-throughput SPE assay developed in our lab has been employed in various applications including the determination of intermolecular association and drug lipophilicity. Figure 1.5 illustrates the general procedure of the assay. Briefly, plasticized poly(vinyl chloride) (PVC)

films are prepared in 96-well microplates. Aqueous solutions are then dispensed. The partition

coefficient (P_{pw}) of a solute between the polymer phase and the aqueous phase can be correlated

to its lipophilicity, *i.e.*, octanol-water partition coefficient (P_{ow}). Chapter 2 of this dissertation

will focus on the development of this application. When ligand compounds are dissolved either

in the polymer films or in the aqueous solutions, the distribution coefficient (D_{pw}) of the solute

that may be different from P_{pw} can be used to calculate the binding constant of the solute-ligand

complex formation. A screening method based on this concept for fast evaluation of the

enantioselectivity of potential chiral selectors will be described in Chapter 3. The complex

formation of the chiral selectors with the target solutes are studied in the film phase. Similarly,

intermolecular association can be determined in the aqueous phase. Chapter 4 will introduce such

an example by measuring binding constant of drug-cyclodextrin inclusion complex formation.

Add polymer/plasticizer in THF
with/without solute
with/without ligand

96-well plate
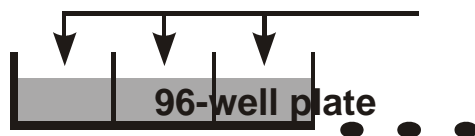
Evaporate THF
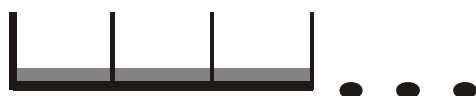
Add aqueous solution
with/without solute
with/without ligand
Equilibrate (const. T)
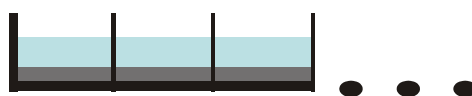
Transfer supernatant
Measure solute conc.

by plate reader or HPLC
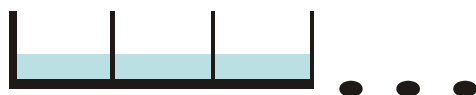
Figure 1.5. General procedure of the high-throughput method to determine

intermolecular association and lipophilicity.

24

1.4   REFERENCE

(1)   Klotz, I. M. *Ligand-Receptor Energetics: A Guide for the Perplexed*; John Wiley & Sons: New York, 1997.

(2)   Masson, M.; Sigurdardottir, B. V.; Matthiasson, K.; Loftsson, T. *Chemical & Pharmaceutical Bulletin* **2005**, *53*, 958-964.

(3)   Sideris, E. E.; Georgiou, C. A.; Koupparis, M. A.; Macheras, P. E. *Analytica Chimica Acta* **1994**, *289*, 87-95.

(4)   Kokugan, T.; Yudiarto, A.; Takashima, T.; Dewi, E. *Journal of Chemical Engineering of Japan* **1998**, *31*, 640-643.

(5)   Wikstroem, A.; Deinum, J. *Analytical Biochemistry* **2007**, *362*, 98-107.

(6)   Schou, C.; Heegaard, N. H. H. *Electrophoresis* **2006**, *27*, 44-59.

(7)   Schipper, B. R.; Ramstad, T. *Journal of Pharmaceutical Sciences* **2005**, *94*, 1528-1537.

(8)   Karakasyan, C.; Taverna, M.; Millot, M.-C. *Journal of Chromatography, A* **2004**, *1032*, 159-164.

(9)   Rundlett, K. L.; Armstrong, D. W. *Electrophoresis* **2001**, *22*, 1419-1427.

(10)   Beni, S.; Szakacs, Z.; Csernak, O.; Barcza, L.; Noszal, B. *European Journal of Pharmaceutical Sciences* **2007**, *30*, 167-174.

(11)   Archontaki, H. A.; Vertzoni, M. V.; Athanassiou-Malaki, M. H. *Journal of Pharmaceutical and Biomedical Analysis* **2002**, *28*, 761-769.

(12)   Koopmans, C.; Ritter, H. *Journal of the American Chemical Society* **2007**, *129(12)*, 3502-3503.

(13)   Fini, P.; Catucci, L.; Castagnolo, M.; Cosma, P.; Pluchinotta, V.; Agostiano, A. *Journal of Inclusion Phenomena and Macrocyclic Chemistry* **2007**, *57*, 663-668.

(14)   Tang, J.; Luan, F.; Chen, X. *Bioorganic & Medicinal Chemistry* **2006**, *14*, 3210-3217.

(15)   Sheehy, P. M.; Ramstad, T. *Journal of Pharmaceutical and Biomedical Analysis* **2005**, *39*, 877-885.

(16)   Kahle, C.; Holzgrabe, U. *Chirality* **2004**, *16*, 509-515.

(17)   Khan, F.; Khan, F. *Journal of the Chinese Chemical Society (Taipei, Taiwan)* **2005**, *52*, 569-573.

(18)   Higuchi, T.; Connors, K. A. *Advan. Anal. Chem. Instr.* **1965**, *4*, 117-212.

(19)   Loukas, Y. L. *Pharmaceutical Sciences* **1997**, *3*, 343-346.

(20)   Loukas, Y. L.; Vraka, V.; Gregoriadis, G. *International Journal of Pharmaceutics* **1996**, *144*, 225-231.

(21)   Connors, K. A. *Binding Constants*; John Wiley & Sons., Inc., 1987.

(22)   Heegaard, N. H. H.; Nilsson, S.; Guzman, N. A. *Journal of Chromatography, B: Biomedical Sciences and Applications* **1998**, *715*, 29-54.

(23)   Busch, M. H. A.; Carels, L. B.; Boelens, H. F. M.; Kraak, J. C.; Poppe, H. *Journal of Chromatography, A* **1997**, *777*, 311-328.

(24)   Busch, M. H. A.; Kraak, J. C.; Poppe, H. *Journal of Chromatography, A* **1997**, *777*, 329-353.

(25)   Rippel, G.; Corstjens, H.; Billiet, H. A. H.; Frank, J. *Electrophoresis* **1997**, *18*, 2175-2183.

(26)   Rundlett, K. L.; Armstrong, D. W. *Electrophoresis* **1997**, *18*, 2194-2202.

(27)   Shimura, K.; Kasai, K.-I. *Analytical Biochemistry* **1997**, *251*, 1-16.

(28)   Chu, Y.-H.; Zang, X.; Tu, J. *Journal of the Chinese Chemical Society (Taipei)* **1998**, *45*, 713-720.

(29)   Colton, I. J.; Carbeck, J. D.; Rao, J.; Whitesides, G. M. *Electrophoresis* **1998**, *19*, 367-382.

(30)   Gao, J.; Mrksich, M.; Mammen, M.; Whitesides, G. M. *Chemical Analysis (New York)* **1998**, *146*, 947-972.

(31)   Heegaard, N. H. H. *Journal of Molecular Recognition* **1998**, *11*, 141-148.

(32)   Heegaard, N. H. H.; Shimura, K. *Quantitative Analysis of Biospecific Interactions* **1998**, 15-34.

(33)   Oravcova, J.; Lindner, W. *Quantitative Analysis of Biospecific Interactions* **1998**, 191-226.

(34)   Heegaard, N. H. H.; Kennedy, R. T. *Electrophoresis* **1999**, *20*, 3122-3133.

(35)   Larsen, K. L.; Zimmermann, W. *Journal of Chromatography, A* **1999**, *836*, 3-14.

(36)   Guijt-Van Duijn, R. M.; Frank, J.; Van Dedem, G. W. K.; Baltussen, E. *Electrophoresis* **2000**, *21*, 3905-3918.

(37)   Tanaka, Y.; Terabe, S. *Journal of Chromatography, B: Analytical Technologies in the Biomedical and Life Sciences* **2002**, *768*, 81-92.

(38)   Tseng, W.-L.; Chang, H.-T.; Hsu, S.-M.; Chen, R.-J.; Lin, S. *Electrophoresis* **2002**, *23*, 836-846.

(39)   Vollmerhaus, P. J.; Tempels, F. W. A.; Kettenes-Van den Bosch, J. J.; Heck, A. J. R. *Electrophoresis* **2002**, *23*, 868-879.

(40)   Blaschke, G.; Chankvetadze, B. *Drugs and the Pharmaceutical Sciences* **2003**, *128*, 175-209.

(41)   Galbusera, C.; Chen, D. D. Y. *Current Opinion in Biotechnology* **2003**, *14*, 126-130.

(42)   Heegaard, N. H. H. *Electrophoresis* **2003**, *24*, 3879-3891.

(43)   Ruettinger, H.-H. *Drugs and the Pharmaceutical Sciences* **2003**, *128*, 23-43.

(44)   Berezovski, M. V.; Okhonin, V.; Petrov, A.; Krylov, S. N. *Proceedings of SPIE-The International Society for Optical Engineering* **2005**, *5969*, 59690Y/59691-59690Y/59613.

(45)   Gayton-Ely, M.; Pappas, T. J.; Holland, L. A. *Analytical and Bioanalytical Chemistry* **2005**, *382*, 570-580.

(46)   Jia, Z. *Current Pharmaceutical Analysis* **2005**, *1*, 41-56.

(47)   Oestergaard, J.; Heegaard, N. H. H. *Electrophoresis* **2006**, *27*, 2590-2608.

(48)   Vlckova, M.; Stettler, A.; Schwarz, M. *Journal of Liquid Chromatography & Related Technologies* **2006**, *29*, 1047-1076.

(49)   Zavaleta, J.; Chinchilla, D.; Brown, A.; Ramirez, A.; Calderon, V.; Sogomonyan, T.; Gomez, F. A. *Current Analytical Chemistry* **2006**, *2*, 35-42.

(50)   Erim, F. B.; Kraak, J. C. *Journal of Chromatography, B: Biomedical Sciences and Applications* **1998**, *710*, 205-210.

(51)   Busch, M. H. A.; Boelens, H. F. M.; Kraak, J. C.; Poppe, H. *Journal of Chromatography, A* **1997**, *775*, 313-326.

(52)   Pedersen, M.; Edelsten, M.; Nielsen, V. F.; Scarpellini, A.; Skytte, S.; Slot, C. *International Journal of Pharmaceutics* **1993**, *90*, 247-254.

(53)   Bowser, M. T.; Chen, D. D. Y. *Journal of Physical Chemistry A* **1998**, *102*, 8063-8071.

(54)   Bowser, M. T.; Chen, D. D. Y. *Journal of Physical Chemistry A* **1999**, *103*, 197-202.

(55)   Rundlett, K. L.; Armstrong, D. W. *Journal of Chromatography, A* **1996**, *721*, 173-186.

(56)   Busch, M. H. A.; Boelens, H. F. M.; Kraak, J. C.; Poppe, H.; Meekel, A. A. P.; Resmini,
M. *Journal of Chromatography, A* **1996**, *744*, 195-203.

(57)   Krylov, S. N. *Journal of Biomolecular Screening* **2006**, *11*, 115-122.

(58)   Avila, L. Z.; Chu, Y. H.; Blossey, E. C.; Whitesides, G. M. *Journal of medicinal
chemistry* **1993**, *36*, 126-133.

(59)   Krylov Sergey, N. *Electrophoresis* **2007**, *28*, 69-88.

(60)   Berezovski, M.; Nutiu, R.; Li, Y.; Krylov Sergey, N. *Analytical Chemistry* **2003**, *75*,
1382-1386.

(61)   Okhonin, V.; Krylova, S. M.; Krylov, S. N. *Analytical Chemistry* **2004**, *76*, 1507-1512.

(62)   Petrov, A.; Okhonin, V.; Berezovski, M.; Krylov Sergey, N. *Journal of the American
Chemical Society* **2005**, *127*, 17104-17110.

(63)   Kawaoka, J.; Gomez, F. A. *Journal of Chromatography, B: Biomedical Sciences and
Applications* **1998**, *715*, 203-210.

(64)   Horejsi, V.; Ticha, M. *Journal of Chromatography* **1986**, *376*, 49-67.

(65)   Heegaard, N. H. H. *Journal of Chromatography, A* **1994**, *680*, 405-412.

(66)   Tao, L.; Kennedy, R. T. *Electrophoresis* **1997**, *18*, 112-117.

(67)   Winzor, D. J. *Analytical Biochemistry* **2006**, *349*, 285-291.

(68)   McDonnell, P. A.; Caldwell, G. W.; Masucci, J. A. *Electrophoresis* **1998**, *19*, 448-454.

(69)   Oestergaard, J.; Hansen, S. H.; Jensen, H.; Thomsen, A. E. *Electrophoresis* **2005**, *26*,
4050-4054.

(70)   Gao, J. Y.; Dubin, P. L.; Muhoberac, B. B. *Analytical Chemistry* **1997**, *69*, 2945-2951.

(71)   Hattori, T.; Kimura, K.; Seyrek, E.; Dubin, P. L. *Analytical Biochemistry* **2001**, *295*, 158-
167.

(72)   Peddicord, M. B.; Weber, S. G. *Electrophoresis* **2002**, *23*, 431-436.

(73)   Brodbelt, J. S. *International Journal of Mass Spectrometry* **2000**, *200*, 57-69.

(74)   Di Marco, V. B.; Bombi, G. G. *Mass Spectrometry Reviews* **2006**, *25*, 347-379.

(75)   Di Tullio, A.; Reale, S.; De Angelis, F. *Journal of Mass Spectrometry* **2005**, *40*, 845-865.

(76)   Daniel, J. M.; Friess, S. D.; Rajagopalan, S.; Wendt, S.; Zenobi, R. *International Journal of Mass Spectrometry* **2002**, *216*, 1-27.

(77)   Higuchi, T.; Zuck, D. A. *Journal of the American Pharmaceutical Association (1912-1977)* **1952**, *41*, 10-13.

(78)   Eli, W.; Chen, W.; Xue, Q. *Journal of Inclusion Phenomena and Macrocyclic Chemistry* **2000**, *38*, 37-43.

(79)   Andreaus, J.; Draxler, J.; Marr, R.; Hermetter, A. *Journal of Colloid and Interface Science* **1997**, *193*, 8-16.

(80)   Andreaus, J.; Draxler, J.; Marr, R.; Lohner, H. *Journal of Colloid and Interface Science* **1997**, *185*, 306-312.

(81)   Tachibana, M.; Furusawa, M.; Kiba, N. *Journal of Inclusion Phenomena and Molecular Recognition in Chemistry* **1995**, *22*, 313-329.

(82)   Menges, R. A.; Armstrong, D. W. *Analytica Chimica Acta* **1991**, *255*, 157-162.

(83)   Nakai, Y.; Yamamoto, K.; Terada, K.; Horibe, H. *Journal of Inclusion Phenomena* **1984**, *2*, 523-531.

(84)   Nakai, Y.; Yamamoto, K.; Terada, K.; Horibe, H. *Chemical & Pharmaceutical Bulletin* **1982**, *30*, 1796-1802.

(85)   Nakajima, T.; Sunagawa, M.; Hirohashi, T. *Chemical & Pharmaceutical Bulletin* **1984**, *32*, 401-408.

(86)   Xia, Y.; Friese, J. I.; Moore, D. A.; Rao, L. *Journal of Radioanalytical and Nuclear Chemistry* **2006**, *268*, 445-451.

(87)   Chen, Z.; Yang, Y.; Werner, S.; Wipf, P.; Weber, S. G. *Journal of the American Chemical Society* **2006**, *128*, 2208-2209.

(88)   Poole, S. K.; Poole, C. F. *Journal of Chromatography, B: Analytical Technologies in the Biomedical and Life Sciences* **2003**, *797*, 3-19.

(89)   Eldridge, G. R.; Vervoort, H. C.; Lee, C. M.; Cremin, P. A.; Williams, C. T.; Hart, S. M.; Goering, M. G.; O'Neil-Johnson, M.; Zeng, L. *Analytical Chemistry* **2002**, *74*, 3963-3971.

(90)   Krishnan, T. R.; Ibraham, I. *Journal of Pharmaceutical and Biomedical Analysis* **1994**, *12*, 287-294.

(91)   Janiszewski, J.; Schneider, R. P.; Hoffmaster, K.; Swyden, M.; Wells, D.; Fouda, H. *Rapid Communications in Mass Spectrometry* **1997**, *11*, 1033-1037.

(92)   Allanson, J. P.; Biddlecombe, R. A.; Jones, A. E.; Pleasance, S. *Rapid Communications in Mass Spectrometry* **1996**, *10*, 811-816.

(93)   Fukase, K.; Zhang, S.-Q.; Fukase, Y.; Umesako, N.; Kusumoto, S. *ACS Symposium Series* **2005**, *892*, 87-98.

(94)   Nissum, M.; Schneider, U.; Kuhfuss, S.; Obermaier, C.; Wildgruber, R.; Posch, A.; Eckerskorn, C. *Analytical Chemistry* **2004**, *76*, 2040-2045.

(95)   Nevanen, T. K.; Simolin, H.; Suortti, T.; Koivula, A.; Soederlund, H. *Analytical Chemistry* **2005**, *77*, 3038-3044.

(96)   Wu, Y.; Wang, Y.; Yang, A.; Li, T. *Analytical Chemistry* **1999**, *71*, 1688-1691.

(97)   Wang, Y.; Bluhm, L. H.; Li, T. *Analytical Chemistry* **2000**, *72*, 5459-5465.

(98)   Bluhm, L. H.; Wang, Y.; Li, T. *Analytical Chemistry* **2000**, *72*, 5201-5205.

(99)   Li, S.; Weber, S. G. *Analytical Chemistry* **1997**, *69*, 1217-1222.

(100)   Chen, Z.; Weber, S. G. **In preparation**.

2.0   A HIGH-THROUGHPUT METHOD FOR LIPOPHILICITY MEASUREMENT

2.1   ABSTRACT

A high-throughput method has been developed for lipophilicity measurement. It measures the partition coefficient of a solute between a polymer phase and an aqueous phase (P_{pw}) in a 96-well format. The polymer is plasticized poly(vinyl chloride) (PVC), which is widely used as a material for clinical containers and ion-selective electrodes. The composition is 2:1 (w/w) dioctyl sebacate and PVC. With six repeats, log P_{pw} values of 15 solutes have been determined in one 96-well microplate in 4 h. A linear relationship between log P_{pw} and log P_{ow} (octanol-water partition coefficient) values exists with a correlation coefficient of 0.979. The slope and intercept of the log P_{pw} vs log P_{ow} plot are statistically indistinguishable from 1 and 0, respectively. Similar to the HPLC method, by using the correlation line as a calibration curve, the measured log P_{pw} values can be used to predict log P_{ow}. This protocol is faster than the HPLC method. Moreover, it is straightforward to extend the protocol to the determination of the distribution coefficient and pK_a of charged solutes. We show that the log P_{pw} of the neutral form of racemic econazole is 4.83($\pm$0.06), for the cationic form (presumably as a dihydrogen phosphate ion pair)

33

1.68(±0.04), and the pK_a is 6.15(±0.04). This method has great flexibility as well and is potentially fully automated.

2.2   INTRODUCTION

Lipophilicity represents the affinity of a molecule or a moiety for a lipophilic environment.[1, 2] Over a century ago, Overton[3] and Meyer's[4] pioneering work demonstrated that the lipophilicity of a compound could be related quantitatively to its biological activity. As suggested by Collander[5] and by Hansch,[6, 7] the logarithmic value of the 1-octanol/water partition coefficient, log P_{ow}, has been widely recognized in the pharmaceutical, biomedical, and environmental sciences to describe the lipophilicity of various compounds. Numerous experimental methods exist to measure log P_{ow} values. The shake-flask procedure is a standard method[8] to determine log P_{ow} in the range of −2 to 4, but it is time and labor consuming, and requires relatively large amounts of pure compounds.[9, 10] In addition, entrainment and octanol/water emulsions can be severe problems for compounds having a log P_{ow} value larger than 4.[11] The HPLC method is an indirect way to estimate log P_{ow} values in the range of 0 to 6, and has also become a standard procedure.[12, 13] A series of reference compounds is injected onto a C_{18} column. The compounds' retention factors are used to create a calibration curve with their known log P_{ow} values. Compounds with unknown log P_{ow} values are then injected, and their retention factors are used to predict log P_{ow} from the calibration curve. However, this technique is only valid for neutral molecules since charged molecules have a far more complex retention behavior than simple partitioning. HPLC and other separation based methods to determine log P_{ow} have been reviewed.[11, 14, 15] Responding to the need for more speed and accuracy, workers have used other

clever approaches over the last decade. Valko[16] introduced a chromatographic hydrophobicity index based on a fast-gradient RP-HPLC method. Tsang[17] made silica-encapsulated magnetic nanoparticles to adsorb a tiny amount of n-octanol and measured the sample partition coefficient from water to the new phase. Solid-phase microextraction (SPME) has also been applied by several research groups to estimate log P_{ow}.[18-24] All of the above methods achieved satisfactory correlation with log P_{ow}, even for very hydrophobic compounds (log P_{ow} >6).[24] There are also some theoretical approaches to calculate log P_{ow} of a compound, but their reliability for new chemical entities and/or novel structures is not satisfactory.[25]

With the development of combinatorial synthesis, high-throughput technologies have become the paradigm in pharmaceutical industry. Although accuracy remains a goal, small sample usage, ultra-fast analysis, and automation, are becoming important factors for the determination of physico-chemical properties in early drug discovery.[11] To increase the throughput of log P_{ow} measurement, an attempt has been made to transfer the traditional shake-flask method to a 96-well format.[26] However, restrictions of the shake-flask method still remained, and the yield was limited to one plate per day due to the detection bottleneck. An indirect method based on transportation experiments through octanol layers in 96-well filter plates has also been introduced,[27] yet an unstable octanol membrane could be a problem for reproducibility. Recently, our group developed a high-throughput screening method for chiral selectors, which was modeled after the protocol for biological screening of combinatorial libraries.[28] This method was based on target partitioning between a selector-containing polymer-film phase and an aqueous phase. The polymer used was plasticized poly(vinyl chloride) (PVC). Due to its wide use in plastic containers such as catheters and infusion bags, the partitioning of drugs, environmental contaminants and food components into PVC has caught the interest of many researchers.[29-35]

Plasticized PVC is also the material for ion-selective electrodes, and the lower detection limit of these electrodes can be dependent on the solute lipophilicity in plasticized PVC.[36, 37] Plasticized PVC films have seen application to microextraction.[38-40] Moreover, studies on PVC containers have shown a reasonable linear correlation between P_{pw} (polymer-water partition coefficient) and P_{ow}.[33-36, 41] Here we introduce a high-throughput method to measure P_{pw} in a 96-well format. A linear correlation between log P_{pw} and log P_{ow} for 15 standard references has been established, which can be used as a calibration curve for indirect determination of log P_{ow}. This application has also been extended to the determination of distribution coefficient and pK_a of a charged solute.

2.3   EXPERIMENTAL SECTION

Chemicals and Materials. HPLC grade tetrahydrofuran (THF) and acetonitrile were purchased from Aldrich (Milwaukee, WI). PVC (high molecular weight, Selectophore) and dioctyl sebacate (DOS; Selectophore) were purchased from Fluka (Ronkonkoma, NY). Water used in all the experiments was purified with a Milli-Q Synthesis A10 system (Millipore, Bedford, MA). All the solutes were purchased from commercial sources with purities greater than 99%. Costar polypropylene 96-well microplates (flat bottom, 330-μL well volume), BD Falcon UV-transparent 96-well microplates (370-μL well volume), and thermal adhesive sealing films were purchased from Fisher Scientific Co. (Pittsburgh, PA).

Equipment. A Deep Well Maximizer (or BioShaker) (model M·BR-022 UP, made by Taitec and distributed by Bionexus Inc., Oakland, CA) was used to speed up the solute distribution kinetics and control the temperature for better reproducibility. UV spectra were acquired with a

SpectraMax M2 microplate reader (Molecular Devices, Sunnyvale, CA) in UV-transparent microplates. An X-LC (Jasco Inc.) HPLC system was used to measure the retention factors of 15 standard compounds on a C_{18} column (Prevail C18, 4.6 × 100 mm, particle size 3 μM, Alltech Associates, Inc., Deerfield, IL). For high-throughput determination of econazole concentration, the same HPLC system with a UPLC C_{18} column (1.0 × 50 mm, particle size 1.7 μM, Waters, Milford, MA) was used.

General Procedure for P_{pw} Determination. Figure 2.1 gives the sequence of operations for the P_{pw} determination. The plasticized PVC films were prepared in polypropylene 96-well microplates. Aliquots of the solute solution were then dispensed. The plates were covered by adhesive sealing films and incubated in a shaker (500 rpm, 25 °C). In order to determine the equilibration time, a kinetic study was performed. The concentration of solute remaining in the aqueous phase was measured as a function of time. All other data generated were at equilibrium. To determine the solute concentration, the supernatant from each well was transferred to a UV-transparent microplate. A microplate reader was used for UV absorbance measurement. The partition coefficient, P_{pw}, was then calculated as

$$P_{pw} = \frac{C_0 - C_1}{C_1 \cdot \Phi} \tag{2.1}$$

Here C_0 is the initial solute concentration in the aqueous phase, C_1 is the concentration at equilibrium, and Φ is the phase ratio.

Preparation of Plasticized PVC films. PVC (1.67 g) and DOS (3.33 g) were dissolved in 200 mL THF in a volumetric flask. A multi-channel pipette was used to dispense the solution to the wells of a polypropylene 96-well microplate. The plate was placed in the hood for 6 hours for evaporation of the THF, and the films were formed at the bottom of each well. The volume of each film was estimated as

Add PVC/plasticizer in THF
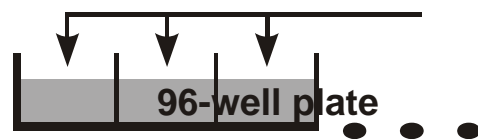
Evaporate THF
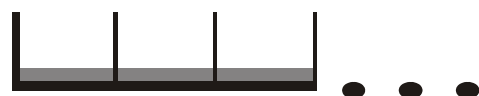
Add target, equilibrate (const. T)
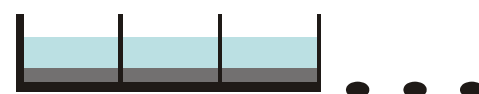
Transfer target to a UV-transparent plate, measure absorbance of target

96-well plate
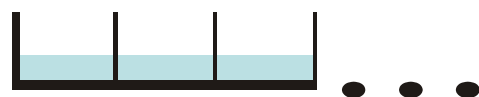
Figure 2.1. General procedure for P_{pw} determination.

$$V_{film} = \frac{5g/200mL \times V_{solution}}{d_{film}} \approx \frac{V_{solution}}{100\mu L} \times 2.5\mu L \qquad (2.2)$$

Here $V_{solution}$ is the volume of the THF solution used in each well and d_{film} is the density of the film, which is estimated as 1 g/mL. In this paper, 100 μL of the THF solution was dispensed in each well, so the volume of each film was ~2.5 μL.

Protocol to determine the P_{pw} values of the 15 reference solutes. Fifteen compounds were dissolved in water at the concentration of 0.5 mM. The solutions were then filtered. As shown in Table 2.1, aliquots of the solutions were dispensed to the polypropylene microplate in which the plasticized PVC films were made. The volume of the dispensed aqueous solution in each well was 200 μL, and six repeats were performed. The plate was then sealed by an adhesive film and equilibrated in the shaker (500 rpm, 25 °C) for 4 h. At the same time, aliquots of 100 μL of each standard solution were dispensed to a UV-transparent microplate. Again, six repeats were performed. The UV absorbance of each standard was measured at its maximum absorbance wavelength by the microplate reader. Note that, for all the measurements, the same amount of water in the wells was used as reference for background deduction. For standard i, A_{i0} (i = 1-15) is defined as its average absorbance. The UV absorbance of the standards at partition equilibrium was measured similarly: After 4 h, from each well of the polypropylene plate, 100 μL of the supernatant was transferred to a UV-transparent plate. The corresponding UV absorbance data were again collected by the microplate reader. A_i is defined as the average absorbance for standard i at equilibrium. As shown in Table 2.1, there was no solute in wells H7-12. The UV absorbance in those wells (A_b) was due to the small aqueous solubility of DOS. Thus, the partition coefficient for standard i could be calculated as

$$P_{pw} = \frac{A_{i0} - (A_i - A_b)}{(A_i - A_b) \cdot \Phi} \qquad (2.3)$$

Table 2.1. Layout of the 15 reference solutes in the 96-well microplate

	1-6	7-12
A	4-acetylpyridine	acetophenone
B	aniline	methyl benzoate
C	acetanilide	4-chlorophenol
D	benzyl alcohol	ethyl benzoate
E	4-methoxyphenol	2,3-dichloroaniline
F	phenol	ethylbenzene
G	benzonitrile	benzophenone
H	phenylacetonitrile	water

Here, $\Phi = 2.5\ \mu\text{L}\ /\ 200\ \mu\text{L} = 1\ /\ 80$.

The protocols to measure the P_{pw} values of other solutes are similar.

HPLC method to determine the k values of the 15 reference solutes. The retention factors of the 15 standard references were measured on the Alltech C_{18} column. The mobile phase was water/acetonitrile (50/50), with a flow rate of 0.6 mL/min. The back pressure was ~2550 psi. Two repeats were performed for each solute.

Protocol to determine the D_{pw} values of econazole at different pH. To measure distribution coefficient, D_{pw}, the protocol had some minor modifications. The solute was initially prepared in the polymer film. The solute econazole was dissolved in THF at 200 μM. Each well received 200 μL of the solution. The PVC/DOS solution was then dispensed, and the same procedures as previously described were followed to make the films. For distribution experiments, 10 mM phosphate buffer solutions with various pH values were added to the films. The econazole concentration in the supernatant at equilibrium (C) was determined both by HPLC and by UV absorbance as above. The distribution coefficient at a specific pH could be calculated as

$$D_{pw}{}^{pH} = \frac{C_0{}^{pH} - C^{pH}}{C^{pH} \cdot \Phi} \tag{2.4}$$

Here, $C_0 = 200\ \mu\text{M}$.

The HPLC method to determine econazole concentration. To minimize the ionized form, econazole samples in acidic buffer (pH <4) were diluted 20 times by 25% ACN + 37.5 mM Na_2HPO_4 solution; samples in near-neutral buffer (6 < pH < 8) were diluted twice by 50 mM Na_2HPO_4 solution. The column used was the Waters UPLC C_{18} column. The mobile phase was 50 mM Na_2HPO_4/acetonitrile (65/35), with a flow rate of 0.2 mL/min. The back pressure was ~6400 psi. To ensure reproducibility, the full-load injection mode was used (injection volume 30

41

μL; loop volume 1 μL). The peak area of econazole was used for the calibration and determination of its concentration. The time per analysis is ~60 s.

2.4   RESULTS AND DISCUSSION

When a solute partitions from the aqueous phase to the film phase, its UV absorbance in the aqueous phase should continually decrease until equilibrium. As shown in Figure 2.2, 4 h is needed for the partitioning of solutes to reach equilibrium. Careful inspection of the curves shows that the equilibration time is longer for more hydrophobic compounds. In this paper, all the solutes (except econazole) have log P_{ow} values in the range of 0-3.2, so all the partitioning experiments were performed for 4 h, if not stated otherwise.

The Organization for Economic Co-operation and Development has recommended the 15 compounds listed in Table 2.2 as the reference substances for the HPLC method.[13] As shown in Figure 2.3, they span a wide range in hydrogen bond basicity and acidity. Figure 2.4 shows the correlation between the log P_{ow} values and the log P_{pw} values for these 15 compounds. The least-squares regression equation of log P_{pw} versus log P_{ow} (Table 2.2) leads to

$$\log P_{pw} = 0.933(\pm 0.054)\log P_{ow} + 0.185(\pm 0.108) \quad \begin{array}{cccc} n & r & se & p \\ 15 & 0.979 & 0.170 & <0.0001 \end{array}$$

$$(2.5)$$

where n is the number of compounds studied, r is the correlation coefficient, and se is the standard error of the regression. This regression line can be used as the calibration curve for indirect determination of log P_{ow} as in the HPLC method. Briefly, for compounds that have
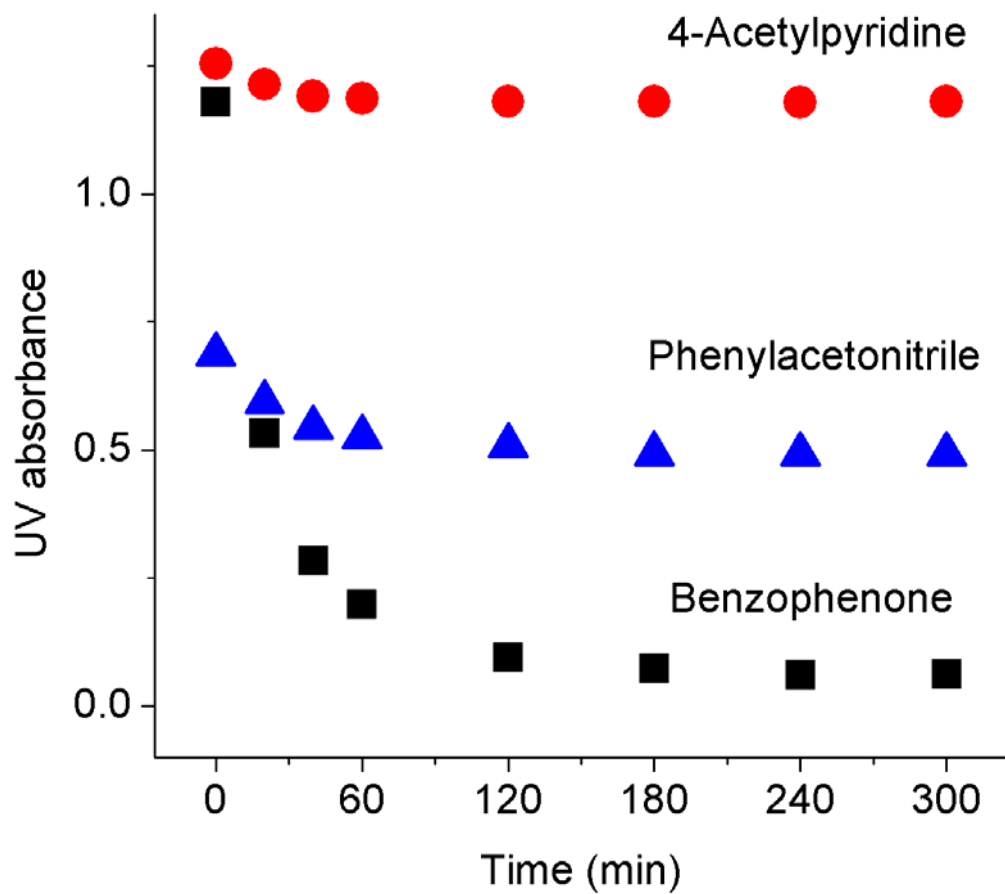
Figure 2.2. Kinetic UV absorbance of solutes in the aqueous phase during the partition

equilibration process.

Table 2.2. The 15 reference solutes and their values of log P_{ow}, log P_{pw}, and log k

Number	Standards	log P_{ow}	log P_{pw}	log k
1	4-acetylpyridine	0.5	0.70 ± 0.07	0.234 ± 0.015
2	aniline	0.9	1.28 ± 0.20	−0.130 ± 0.002
3	acetanilide	1.0	1.06 ± 0.11	−0.046 ± 0.002
4	benzyl alcohol	1.1	0.95 ± 0.32	−0.052 ± 0.002
5	4-methoxyphenol	1.3	1.42 ± 0.06	−0.082 ± 0.002
6	phenol	1.5	1.48 ± 0.09	−0.002 ± 0.002
7	phenylacetonitrile	1.6	1.50 ± 0.06	0.288 ± 0.001
8	benzonitrile	1.6	1.66 ± 0.06	0.278 ± 0.001
9	acetophenone	1.7	1.84 ± 0.11	0.278 ± 0.001
10	methyl benzoate	2.1	2.45 ± 0.04	0.464 ± 0.001
11	4-chlorophenol	2.4	2.16 ± 0.05	0.264 ± 0.002
12	ethyl benzoate	2.6	2.67 ± 0.05	0.658 ± 0.002
13	2,3-dichloroaniline	2.8	2.81 ± 0.10	0.620 ± 0.001
14	ethylbenzene	3.2	3.19 ± 0.28	0.913 ± 0.005
15	benzophenone	3.2	3.17 ± 0.19	0.786 ± 0.006
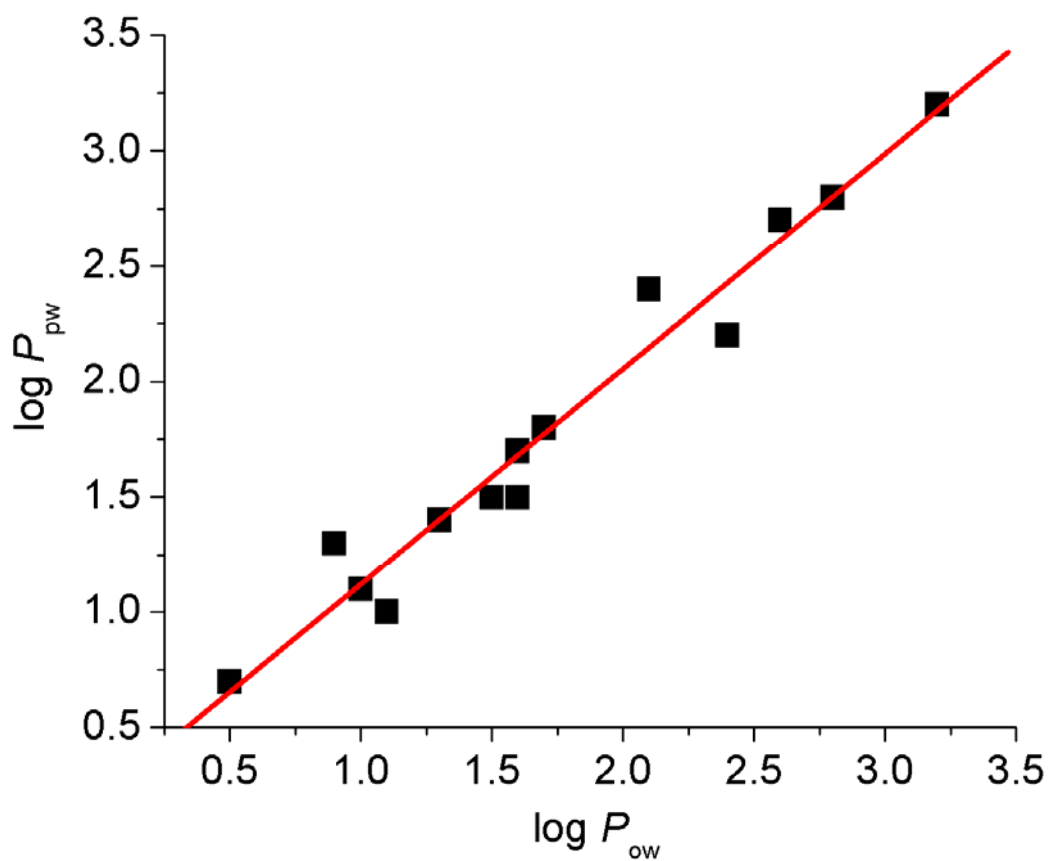
Figure 2.3. Linear correlation of log P_{pw} - log P_{ow} for the 15 reference solutes.
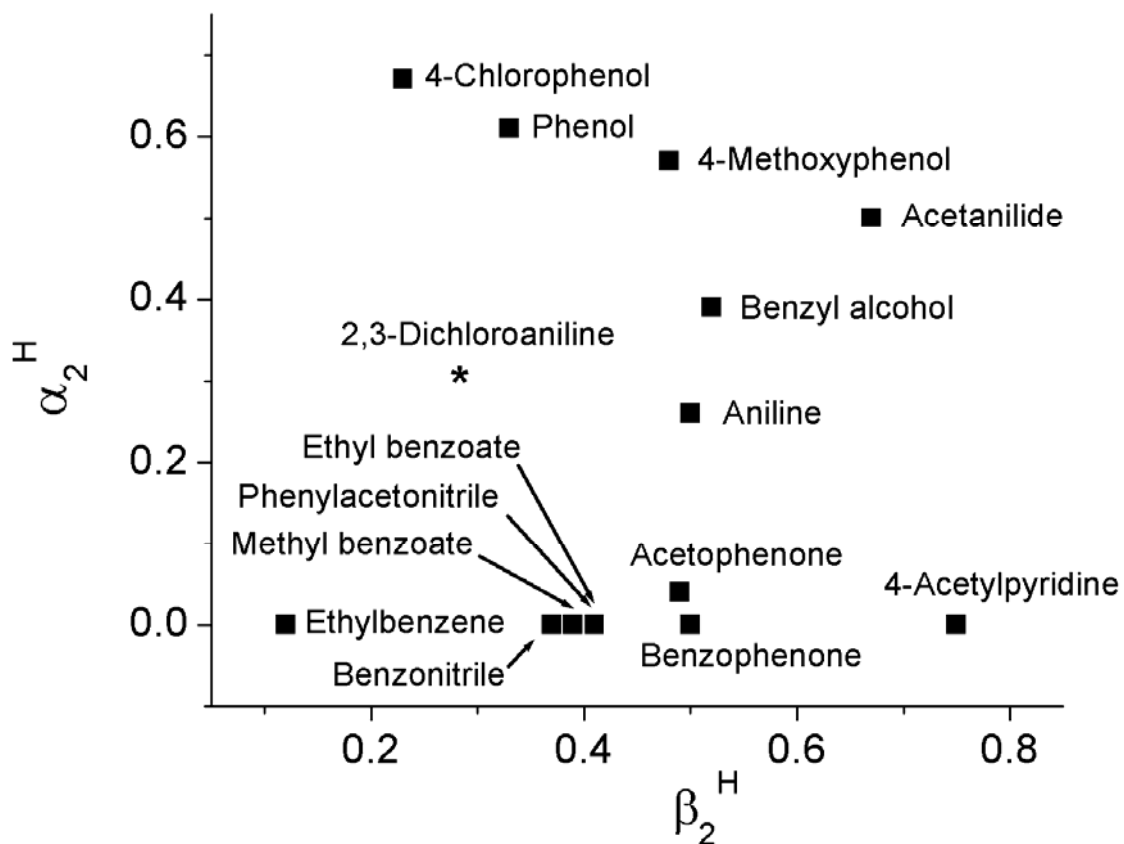
Figure 2.4. Hydrogen bond acidity (α_2^H) and basicity (β_2^H) map of the 15 reference solutes.

($\blacksquare$)[42,49,50] (*) Estimated (2-chloroaniline, $\alpha_2^H = 0.25$, $\beta_2^H = 0.31$; 3-chloroaniline, $\alpha_2^H = 0.30$, β_2^H

$= 0.30$. 2,3-Dichloroaniline should be slightly more acidic but less basic than both of them)

unknown log P_{ow} values, measure their log P_{pw} values and use the regression line to predict their log P_{ow} values.

Figure 2.5 gives the correlation between the log k (RPLC) and log P_{ow} values of the same 15 reference solutes. The least-squares regression equation is

$$\log k = 0.41(\pm 0.04)\log P_{ow} - 0.49(\pm 0.08)$$

$$\begin{array}{cccc} n & r & s.e. & p \\ 14 & 0.952 & 0.110 & < 0.0001 \end{array}$$

$$(2.6)$$

Note that the data point of 4-acetylpyridine is not used for regression analysis since it is an obvious outlier. The linear correlation coefficient would decrease to 0.879 if that point had been included. The r values of the two correlations (after discarding the outlier) are similar, indicating that the precision of our method is similar to the HPLC method for indirect determination of log P_{ow}. However, as the slope of the HPLC method is lower, the precision in the slope of the polymer-based method is better than that of the HPLC method based on comparing the relative standard deviation of the two slopes. Besides lipophilicity, H-bonding also plays an important role in determining the P_{ow} value of a solute. As a result, due to the diversity of the H-bonding ability of PVC/DOS (1:2) ($\beta = 0.53$, $\alpha = 0$),[40] n-octanol ($\beta = 0.45$, $\alpha = 0.33$)[42] and C18 ($\beta = 0$, $\alpha = 0$), the linear correlations are not perfect among systems when the solutes have various numbers of H-bond donors and acceptors. Note that P_{ow} is just a term to picture lipophilicity. Actually, to describe lipophilicity, the ideal partition system should use an organic phase that is free of polar binding forces, and a hydrocarbon solvent such as cyclohexane or hexadecane[43] should serve as a better reference than octanol. However, some practical issues hindered their popularity. Furthermore, one of the most important reasons making P_{ow} a standard term to describe lipophilicity is the large number of data measured.
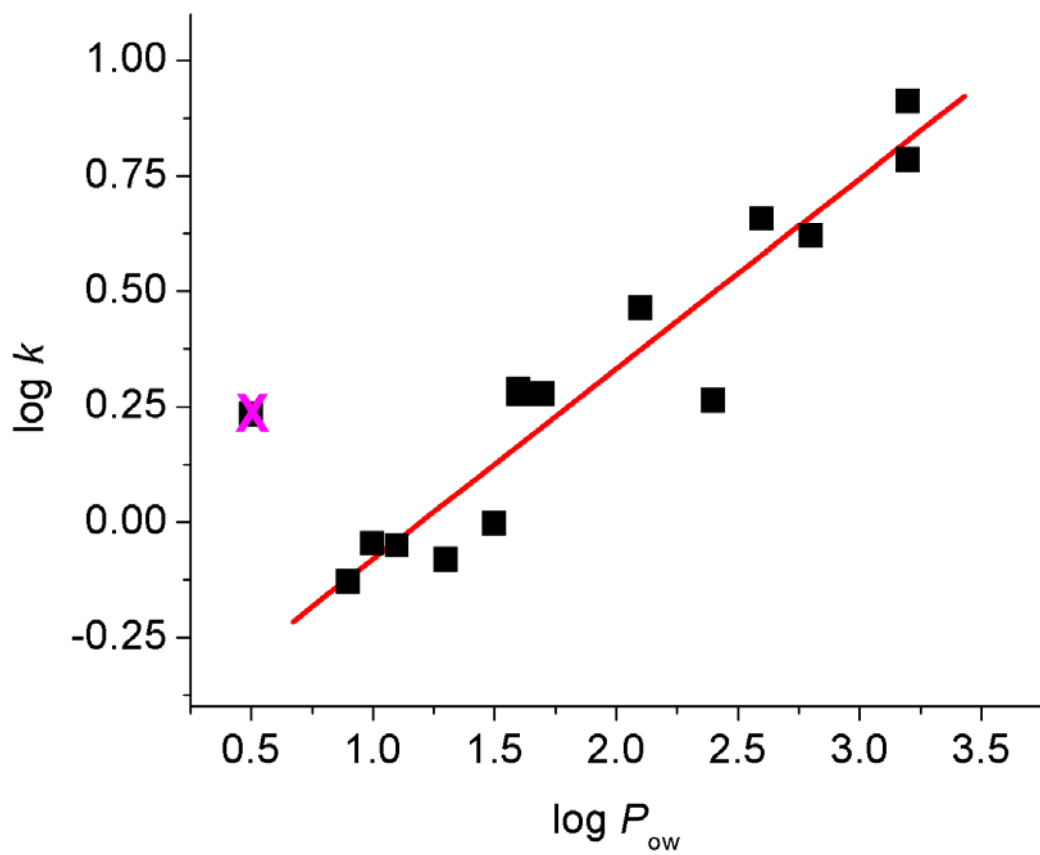
Figure 2.5. Linear correlation of log k - log P_{ow} for the 15 reference solutes.

Studies in drug partitioning behavior in polymers have shown that the slope of the log P_{pw} - log P_{ow} correlation line has an inverse linear relationship to the polarity or the solubility parameter of the polymer,[44, 45] which can be used to predict drug solubility in polymers. It also reflects how sensitive the solvent system is to changes in lipophilicity of solutes.[7] In Eq. 2.5, the slope is close to 1 ($t = 1.24$, $p = 0.24$), indicating that the polymer material (PVC:DOS = 1:2) (π^* = 0.64)[40] has a similar polarity to octanol (π^* = 0.40).[42] The intercept of the log P_{pw} - log P_{ow} correlation line can be used as a measure of the polymer lipophilicity.[7] The intercept of Eq. 2.5 is close to 0 ($t = 1.71$, $p = 0.11$), indicating that DOS plasticized PVC (PVC:DOS = 1:2) has a similar lipophilicity to octanol. The intercept is also linearly related to the solubility of water in the polymer phase.[7, 44, 45]

In another application, log P_{pw} values of the three positional isomers of nitroanisole were measured and correlated to their experimental log P_{ow} values. The linear regression equation is:

$$\log P_{pw} = 1.054(\pm 0.041)\log P_{ow} + 0.210(\pm 0.082)$$

n	r	s.e.	p
3	0.9992	0.013	0.025

$$(2.7)$$

For isomers that have the same functional groups, the partition behavior is more similar than for a set of compounds that have different functional groups. The measured log P_{pw} values, as well as the experimental log P_{ow} values from the literature, and the estimated log P_{ow} values from online-software calculations, are listed in Table 2.3. Obviously, the order of the three experimental log P_{ow} values of the isomers matched the order of the three log P_{pw} values very well: 3-nitroanisole > 4-nitroanisole > 2-nitroanisole. For the calculated log P_{ow} values, the orders did not match. This mismatch of the calculated data with the experimental data confirms our statement in the introduction, that theoretical calculations of log P_{ow} sometimes are not very accurate.

Table 2.3. Log P_{ow} and log P_{pw} values of the 3 isomers of nitroanisole

Targets	log P_{pw}	log P_{ow}		
		Exp.	esc.syrres.com	logP.com
2-nitroanisole	2.03 ± 0.03	1.73	1.89	1.90
3-nitroanisole	2.49 ± 0.06	2.17	1.89	1.97
4-nitroanisole	2.36 ± 0.07	2.03	1.89	2.02

For a homologous series of solutes, the free energy for the partitioning process linearly increases with increasing number of methylene groups in a straight chain. Figure 2.6 confirms this relationship by examing the log Ppw and log Pow values of four alkyl 4-hydroxybenzoates. Since methyl 4-hydroxybenzoate has no methylene group, only three points from each data set were used for the regression analysis. The least-squares regression equations are

$$\log P_{pw} = 0.480(\pm 0.012)m + 1.373(\pm 0.025)$$

n	r	s.e	p
3	0.9997	0.016	0.015

$$(2.8)$$

$$\log P_{ow} = 0.550(\pm 0.012)m + 1.927(\pm 0.025)$$

n	r	s.e.	p
3	0.9998	0.016	0.013

$$(2.9)$$

The two slopes are not significantly different ($t = 4.12$, $p = 0.15$). The free energies required for a methylene group to transfer from the organic phases to the aqueous phase are 2.74($\pm$0.06) kJ/mol from the polymer phase to water and 3.13($\pm$0.06) kJ/mol from octanol to water.

Compared to the HPLC method, which requires ~5-20 min for determining the retention factor of 1 sample, the new technique is more suitable for a large number of solutes, for instance, combinatorial libraries. The time needed to prepare one plate of PVC films is ~6 h. Increasing the number of plates will not significantly change the processing time since the bottleneck of the film-making procedure is THF evaporation. The equilibration time is 4 h, regardless of the number of plates. Dispensing solutes to one plate takes ~15 min, and UV absorbance reading adds another 15 min. As described above, the time scale for both methods is about the same if the log P values of only 30 samples are to be determined. However, if the analysis of more compounds is required, this technique will save time. Moreover, it has the potential to build a larger database for P_{pw} than for P_{ow}.
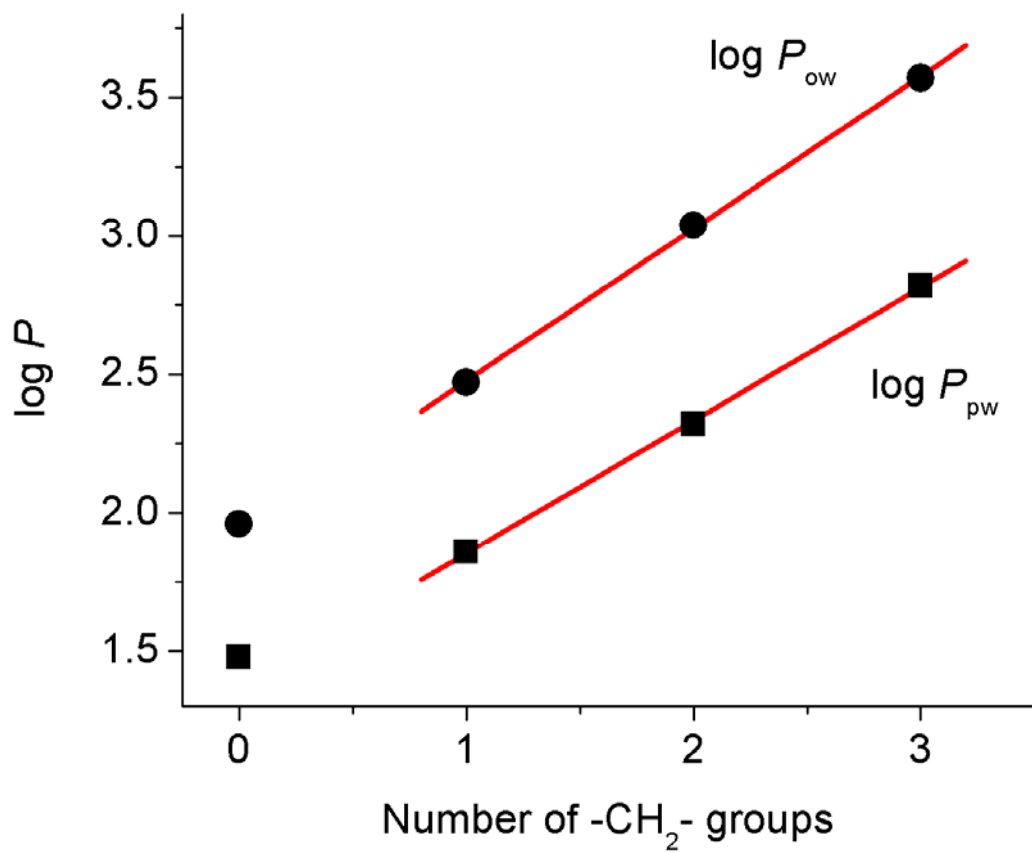
Figure 2.6. Linear correlation of the log P_{pw} and log P_{ow} values versus the number of

methylene groups in alkyl 4-hydroxybenzoates.

The method assumes that partitioning only occurs between the two phases: aqueous and polymer. Loss of solute to the microplates due to sorption can lead to misinterpretation. Polypropylene is a good packaging material for drug-like compounds because the sorption effect is small or nonexistent.[46-48] We tested the concentration stability of the solutes in the polypropylene plate and didn't see any apparent loss. Therefore, we have assumed that solute loss to the plate during the equilibration process is negligible. Solute adsorption on the surface of the plasticized PVC film should also be considered. Calculations show that if a monolayer of well-packed solute (M.W. ~ 200) had been adsorbed on the film surface, only about 0.3% of the solute would be lost from the aqueous solution at 0.5 mM. If a lower solute concentration is used, this could become more of a problem. When using the UV-transparent plate, buffering sometimes may be needed since mass loss of basic compounds to polystyrene materials could be severe.[46] Attentions should also be paid to volatile solutes: instant covering and quick action to measure UV absorbance in the plate are needed.

Figure 2.7 shows the estimated measurement error associated with the calculated log P_{pw} value, based on the following assumptions: (1) Concentrations are measured by optical absorbance in the aqueous phase; (2) $A_{i0} = 1$, $s_{Ai0}/A_{i0} = 0.015$; (3) $A_b = 0.06$, $s_{Ab} = 0.006$; (4) $s_{Ai}/A_i = 0.037$ ($s_{Ai} \geq 0.003$); (5) four repeats are performed for each measurement. s_{Ai0}, s_{Ab}, and s_{Ai} are the standard deviations of A_{i0}, A_b, and A_i, respectively. The selected values of s_{Ai0}/A_{i0}, A_b, s_{Ab}, and s_{Ai}/A_i are the averages obtained from experiments. P_{pw} values are calculated from Eq. 2.3 with various A_i values. The standard deviation, s, is primarily a result of pipetting errors during the processes of film preparation, solute dispensing, and supernatant transferring, but not from the determination of UV absorbance. With a more precise liquid-handling technique, it is possible to reduce the pipetting errors, as well as the propagated error of log P_{pw}. At one fixed phase ratio, it

53
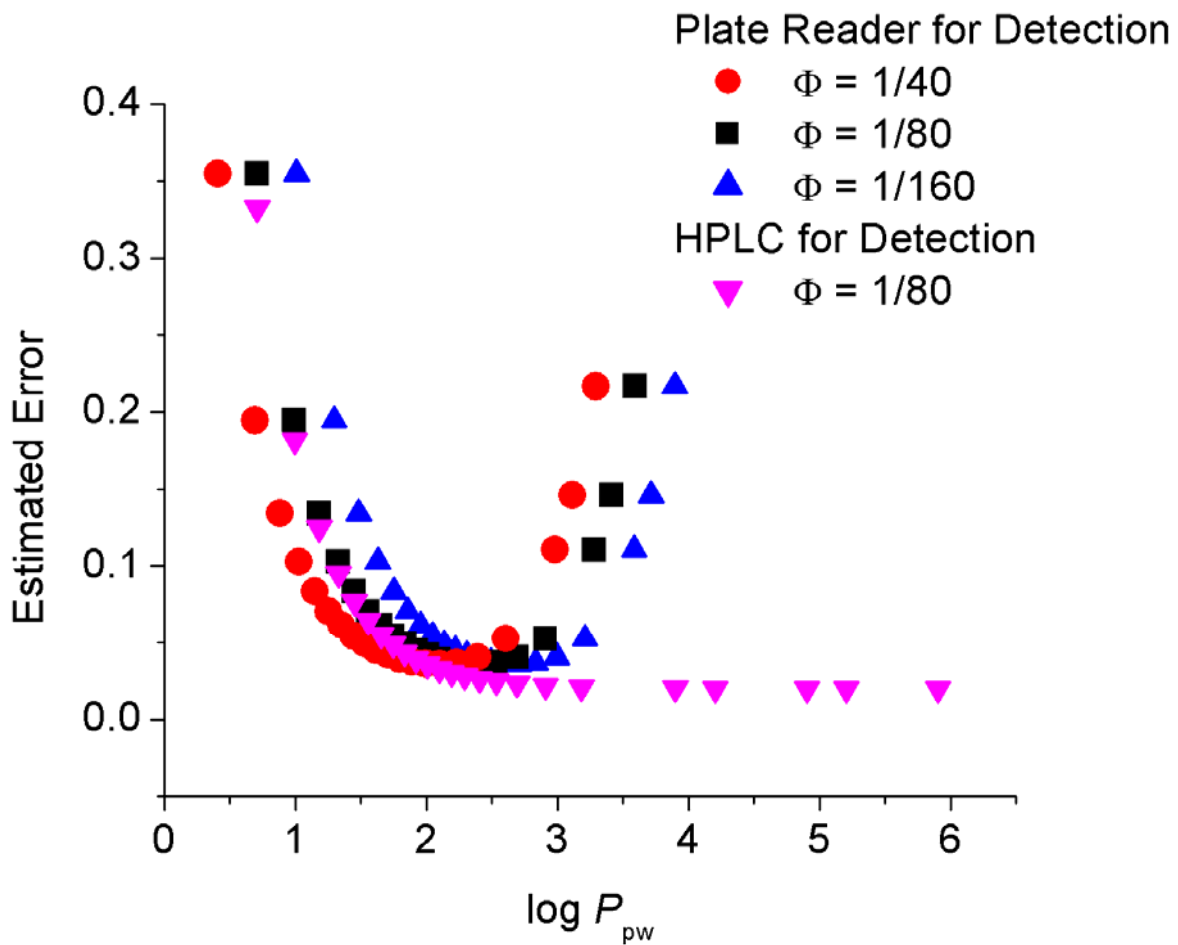
Figure 2.7. Estimated error of log P_{pw} at various phase ratios (Φ).

is possible to obtain precise measurement results ($s_{\log Ppw} < 0.2$. $s_{\log Ppw}$ is the standard deviation of log P_{pw}) for ~2.6 log P_{pw} units. Changing the phase ratio will greatly extend the applicable range, *e.g.*, by doubling or halving the phase ratio, the boundaries will be 0.3 unit larger or smaller, respectively. This strategy is similar to changing the strength of the mobile phase or the length of column to adjust the retention time when using the HPLC method.

Increasing the number of independent determination, which is very easy when using a microtiter plate, will also help to decrease measurement error. Therefore, depending on the acceptable precision, an operator performing the protocol can flexibly choose the necessary phase ratio and determination repeats.

This high-throughput technique can also be applied to determine the distribution coefficient (D_{pw}) of a substance at various pH values. Some minor modifications of the protocol, as shown in the experimental section, made the measurement even more convenient and extended the range of log D_{pw} accessible at a single phase ratio. Figure 2.8 shows an example of the application. Econazole (Figure 2.9) is a basic compound that has two ionizable groups, with only one of them ionizable at pH $\geq$ 1 (pK$_a$ = 6.69, log P_{ow} = 5.32, calculated using Advanced Chemistry Development (ACD/Labs) Software V8.14 for Solaris). Thus its log D_{pw} value increases with increasing pH of the buffer, and can be further elucidated by the log D estimation formula for bases:

$$D(pH) = \frac{P}{1+10^{pK_a-pH}} + \frac{P'}{1+10^{pH-pK_a}} \qquad (2.10)$$

where P is the partition coefficient of the neutral form while P' is that of the ionized form. The equilibration time was 6 h. Two parallel experiments were performed, using the plate reader and HPLC to determine the econazole concentration at equilibrium, and two sets of log D_{pw} values were correspondingly acquired. Applying nonlinear least-squares curve fitting, as shown in
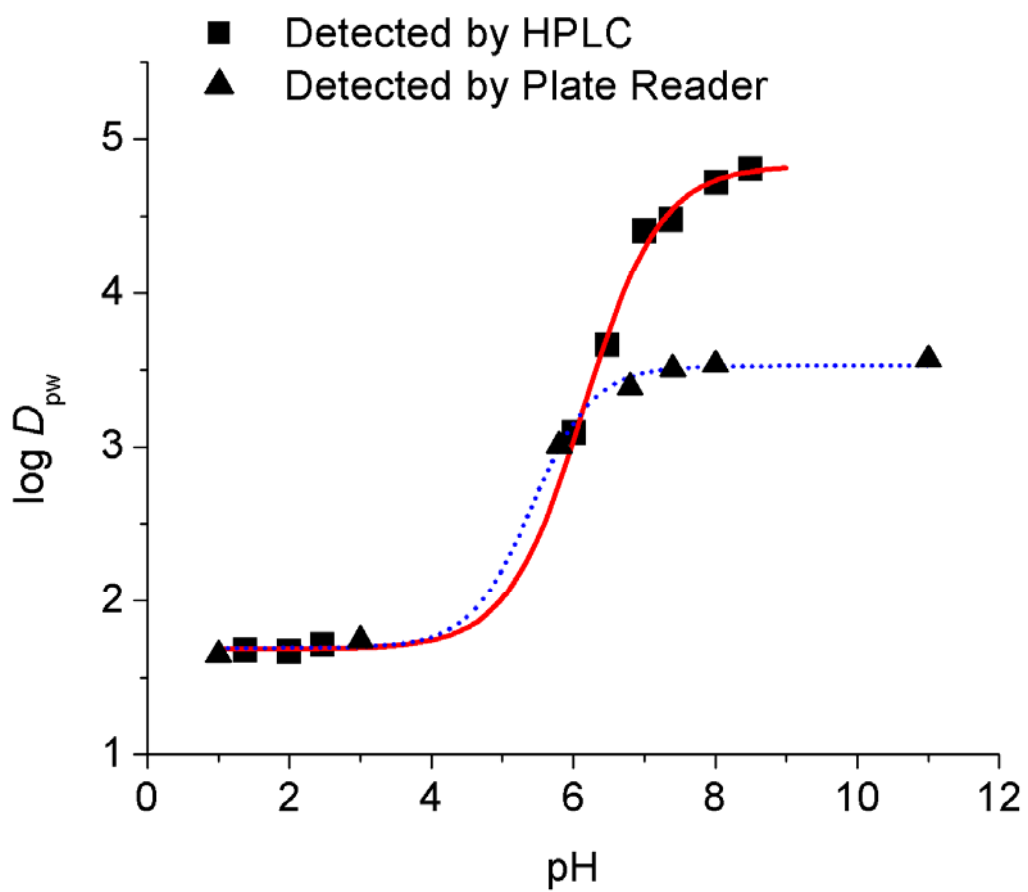
Figure 2.8. Log D_{pw} of econazole at various values of pH.
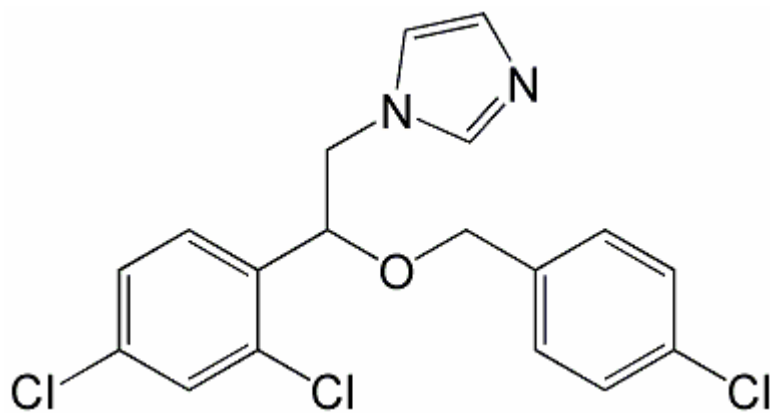
Figure 2.9. Econazole structure

56

Figure 2.8, the log P_{pw}, log P'_{pw}, and pK_a values of econazole can all be obtained, which are 3.53(±0.03), 1.69(±0.04), and 5.41(±0.06), respectively, when the plate reader was used, and 4.83(±0.06), 1.68(±0.04), and 6.15(±0.04), respectively, when the HPLC was used. Apparently the latter set of data are more accurate. The two fitting curves almost overlap at low pH, but have a clear variance when pH >7, where log D_{pw} values are larger than 3.5. This is in good agreement with our previous calculation about the applicable range of log P_{pw} when using the plate readeras the detection tool. The plate reader can only quantitate the econazole concentration above 10 μM, which limits the measurable range of log D_{pw} to 3.5, while HPLC on-column preconcentration helped to quantitate econazole concentration as low as 0.03 μM, with the extension of the measurable range of log P_{pw} and log D_{pw} to 5.7. The estimated error associated with log P_{pw} (or log D_{pw}) is again shown in Figure 6, based on the following assumptions: (1) Solute concentrations in the aqueous phase are measured by HPLC with on-column preconcentration; (2) $C_0 = 1$, $s_{C0}/C_0 = 0.015$; (3) $s_C/C = 0.037$ (when $C > 0.0001$); (4) four repeats are performed for each measurement. C_0 is the initial relative concentration of the solute and C is the relative solute concentration at equilibrium. s_{C0} and s_C are the standard deviations of C_0 and C, respectively. P_{pw} values are calculated from Eq. 2.1. For more straightforward comparison, the selected values of s_{C0}/C_0 and s_C/C are the same as s_{Ai0}/A_{i0} and s_{Ai}/A_i, as in the previous estimation of log P_{pw} error when using the plate reader to measure solute concentration. Apparently, with HPLC as the detection tool, the errors at high log P_{pw} are much smaller. For quantitative analysis of the solutes, one HPLC run needs ~30-60 s. Although slower than the plate reader, it is still reasonably rapid. Again, depending on the desired application, an operator performing the protocol can flexibly choose the most suitable detection technique. Since the traditional HPLC method for lipophilicity measurement is usually inaccurate for charged

compounds, the applicability of the system for the determination of log D and pK_a values is another advantage over it.

2.5   CONCLUSIONS

A new method for lipophilicity measurement using high-throughput technologies was successfully developed. In this method, the partition coefficient of a substance between a polymer phase and an aqueous phase (P_{pw}) in is measured 96-well microplates. With 6 repeats, The log P_{pw} values of 15 compounds can be determined simultaneously with six replicates per data point. A linear relationship between log P_{pw} and log P_{ow} has been established. By using the correlation line as a calibration curve, the measured log P_{pw} values can be used to predict log P_{ow}. This method proven to be more accurate than some software for the estimation of log P_{ow}. It can also help to understand the partition mechanism among different solvent systems. Compared to the HPLC method, our protocol is more time-saving for combinatorial libraries, and it is not only applicable for the partition coefficient determination of neutral compounds but can also be utilized as a tool for distribution coefficient and pK_a measurement. This method has great flexibility as well, as instruments exist to make it fully automated.

2.6   REFERENCE

(1)   Van De Waterbeemd, H.; Carter, R. E.; Grassy, G.; Kubinyi, H.; Martin, Y. C.; Tute, M. S.; Willett, P. *Annual Reports in Medicinal Chemistry* **1998**, *33*, 397-409.

(2)   Wermuth, C.-G.; Ganellin, C. R.; Lindberg, P.; Mitscher, L. A. *Annual Reports in Medicinal Chemistry* **1998**, *33*, 385-395.

(3)   Overton, E. *Studien uber die Narkose.*; Fischer: Jena, 1901.

(4)   Meyer, H. *Arch. Exp. Pathol. Pharmacol.* **1899**, *42*, 109-118.

(5)   Collander, R. *Acta Chemica Scandinavica* **1951**, *5*, 774-780.

(6)   Hansch, C.; Fujita, T. *Journal of the American Chemical Society* **1964**, *86*, 1616-1626.

(7)   Leo, A.; Hansch, C.; Elkins, D. *Chemical Reviews* **1971**, *71*, 525-616.

(8)   *OECD Guidelines for the Testing of Chemicals*, Test No. 107; Organisation for Economic Co-operation and Development (OECD): Paris, 1995.

(9)   Danielsson, L.-G.; Zhang, Y.-H. *TrAC, Trends in Analytical Chemistry* **1996**, *15*, VIII.

(10)   Sangster, J. *Octanol-water Partition Coefficients: Fundamentals and Physical Chemistry*; Wiley: New York, 1997.

(11)   Poole, S. K.; Poole, C. F. *Journal of Chromatography, B: Analytical Technologies in the Biomedical and Life Sciences* **2003**, *797*, 3-19.

(12)   *Product Properties Test Guidelines.* OPPTS 830.7570; U.S. Environmental Protection Agency, U.S. Government printing Office: Washington, DC, 1996.

(13)   Welch, C. J.; Fleitz, F.; Antia, F.; Yehl, P.; Waters, R.; Ikemoto, N.; Armstrong, J. D., III; Mathre, D. J. *Organic Process Research & Development* **2004**, *8*, 186-191.

(14)   Valko, K. *Journal of Chromatography, A* **2004**, *1037*, 299-310.

(15)   Berthod, A.; Carda-Broch, S. *Journal of Chromatography, A* **2004**, *1037*, 3-14.

(16)   Valko, K.; Bevan, C.; Reynolds, D. *Analytical Chemistry* **1997**, *69*, 2022-2029.

(17)   Gao, X.; Yu, C. H.; Tam, K. Y.; Tsang, S. C. *Journal of Pharmaceutical and Biomedical Analysis* **2005**, *38*, 197-203.

(18)   Dean, J. R.; Tomlinson, W. R.; Makovskaya, V.; Cumming, R.; Hetheridge, M.; Comber, M. *Analytical Chemistry* **1996**, *68*, 130-133.

(19)   Paschke, A.; Popp, P. *Applications of Solid Phase Microextraction* **1999**, 140-155.

(20)   Wang, Y.; Wang, X.; Lee, F. S. C. *Sepu* **1999**, *17*, 424-426.

(21)   Doong, R.-A.; Chang, S.-M. *Analytical Chemistry* **2000**, *72*, 3647-3652.

(22)   Mayer, P.; Vaes, W. H. J.; Hermens, J. L. M. *Analytical Chemistry* **2000**, 72, 459-464.

(23)   Paschke, A.; Popp, P. *Journal of Chromatography, A* **2003**, *999*, 35-42.

(24)   Kong, X. Q.; Shea, D.; Gebreyes, W. A.; Xia, X.-R. *Analytical Chemistry* **2005**, *77*, 1275-1281.

(25)   Morris, J. J.; Bruneau, P. P. *Methods and Principles in Medicinal Chemistry* **2000**, *10*, 33-58.

(26)   Hitzel, L.; Watt, A. P.; Locker, K. L. *Pharmaceutical Research* **2000**, *17*, 1389-1395.

(27)   Faller, B.; Grimm, H. P.; Loeuillet-Ritzler, F.; Arnold, S.; Briand, X. *Journal of Medicinal Chemistry* **2005**, *48*, 2571-2576.

(28)   Chen, Z.; Yang, Y.; Werner, S.; Wipf, P.; Weber, S. G. *Journal of the American Chemical Society* **2006**, *128*, 2208-2209.

(29)   Jenke, D. R. *Journal of Parenteral Science and Technology* **1991**, *45*, 233-238.

(30)   Jenke, D. R.; Hayward, D. S.; Kenley, R. A. *Journal of Chromatographic Science* **1990**, *28*, 609-612.

(31)   Jenke, D. R. *Journal of Pharmaceutical Sciences* **1993**, *82*, 1134-1139.

(32)   Leggett, D. C.; Parker, L. V. *Environmental Science and Technology* **1994**, *28*, 1229-1233.

(33)   Illum, L.; Bundgaard, H.; Davis, S. S. *International Journal of Pharmaceutics* **1983**, *17*, 183-192.

(34)   Atkinson, H. C.; Duffull, S. B. *Journal of Pharmacy and Pharmacology* **1991**, *43*, 374-376

(35)   Roberts, M. S.; Kowaluk, E. A.; Polack, A. E. *Journal of Pharmaceutical Sciences* **1991**, *80*, 449-455.

(36)   Mohr, G. J.; Spichiger, U. E.; Jona, W.; Langhals, H. *Analytical Chemistry* **2000**, *72*, 1084-1087.

(37)   Mohr, G. J.; Demuth, C.; Spichiger-Keller, U. E. *Analytical Chemistry* **1998**, *70*, 3868-3873.

(38)   Li, S.; Sun, L.; Chung, Y.; Weber, S. G. *Analytical Chemistry* **1999**, *71*, 2146-2151.

(39)   Li, S.; Weber, S. G. *Analytical Chemistry* **1997**, *69*, 1217-1222.

(40)   Zhang, X.; Zhao, H.; Chen, Z.; Nims, R.; Weber, S. G. *Analytical Chemistry* **2003**, *75*, 4257-4264.

(41)   Smith, J. C.; Davies, M. C.; Melia, C. D.; Denyer, S. P.; Derrick, M. R. *Biomaterials* **1996**, *17*, 1469-1472.

(42)   Kamlet, M. J.; Doherty, R. M.; Abraham, M. H.; Marcus, Y.; Taft, R. W. *Journal of Physical Chemistry* **1988**, *92*, 5244-5255.

(43)   Li, J.; Carr, P. W. *Analytical Chemistry* **1993**, *65*, 1443-1450.

(44)   Bao, Y. T.; Samuel, N. K. P.; Pitt, C. G. *Journal of Polymer Science, Part C: Polymer Letters* **1988**, *26*, 41-46.

(45)   Foreman, P.; Luciano, A.; Yang, H.; Jacobson, S. *Drug Delivery Technology* **2005**, *5*, 46,48-51.

(46)   Palmgren, J. J.; Moenkkoenen, J.; Korjamo, T.; Hassinen, A.; Auriola, S. *European Journal of Pharmaceutics and Biopharmaceutics* **2006**, *64*, 369-378.

(47)   Wong, M.; Marion, R.; Reed, K.; Wang, Y. *International Journal of Pharmaceutics* **2006**, *307*, 163-167.

(48)   Salomies, H. E. M.; Heinonen, R. M.; Toppila, M. A. I. *International Journal of Pharmaceutics* **1994**, *110*, 197-201.

3.0   A SCREENING METHOD FOR CHIRAL SELECTORS THAT DOES NOT

REQUIRE COVALENT ATTACHMENT

Part of this work has been published in *Journal of the American Chemical Society* **2006**, *128(7)*, 2208-2209. Reproduced with permission from *Journal of the American Chemical Society.* Copyright by American Chemical Society.

3.1   ABSTRACT

A high throughput screening protocol for chiral selector discovery was developed based on target distribution between an aqueous phase and an organic phase. Screening for intermolecular association was carried out by partitioning experiments in the presence and absence of a chiral selector in the organic phase. A novel partition ratio measurement system was developed using 96-well microplates. This protocol was validated and applied to a small library. Among 12 cyclopropyl dipeptide isosteres that were screened, eight bound econazole, and one had measurable chiral selectivity. The advantages of the method are that it does not require the covalent attachment of either the analyte or the selector, and the required amount of the potential chiral selector (~ 0.1 mg) is significantly reduced.

3.2   INTRODUCTION

The enantiomers of a chiral drug often differ significantly in their pharmacological,[1] pharmacodynamic and pharmacokinetic effects.[2] For safety, efficacy and efficiency, the demand for enantiopure drugs over the racemic form has been increasing rapidly.[3] The process cost for a reaction/separation sequence is much lower than for an enantioselective synthesis,[4] thus chiral separation of racemic compounds has been a focus of interest in the pharmaceutical industry. At the analytical to semi-preparative scale, particularly in drug discovery, liquid chromatography (LC) on chiral stationary phases (CSPs) has been the most widely utilized technique for chiral separations.[5] Numerous CSPs have been developed by research groups worldwide, and some commercial sources have introduced various broadly applied CSPs.[5] However, there are still many racemic compounds that can not be separated or separated well by currently available columns. The desire for more generality, better selectivity, more robustness and predictability drives the search for new CSPs.[6]

Amino acids and their derivatives, as well as peptides, due to their many structural forms and their ease of modification and immobilization, are natural sources for CSPs.[7] Pirkle pioneered using amino acid derivatives in the development of CSPs based on charge-transfer interactions.[8] CSPs based on synthetic peptides have also been widely used in LC. Work in this field has been reviewed.[9, 10] New CSPs based on peptidomimetics have also been introduced.[11] Recently, parallel synthesis and combinatorial studies of peptides as well as peptidomimetics libraries have been developed rapidly.[12-15] These peptidomimetics not only have demonstrated some clinical utility,[16] but also they provide a diverse chiral pool from which chiral selectors may be obtained. For development and application of new chiral selectors, it is essential to have knowledge of the chiral recognition mechanism. Though many models have been established and

predictions have been made towards the chiral recognition mechanism, for instance, three-point interactions[17] for Pirkle-type CSPs, host-guest chemistry[18] for cyclodextrin-based CSPs, there is yet no thorough understanding at the molecular level in this very complicated subject.[19] Today most CSP designs are still based on previous experience or some semi-empirical theories. In order to find good chiral selectors from a large library, the safest way is to have a universal screening method.

The reciprocal principle (if a CSP derived from (+)-A can distinguish between (+)-B and (−)-B, then a CSP derived from (+)-B may distinguish (+)-A from (−)-A) was introduced by Pirkle for the screening of new CSPs.[20, 21] The target was attached to a stationary phase and the candidate selectors were resolved on the column. This principle avoids immobilizing every selector to a stationary phase. It has been applied successfully by subsequent researchers. However, the range of targets could be used successfully for screening was limited due to "tether effects".[22] Welch *et al.*[22] used LC/MS to check the enantioenrichment of the target after adsorption by a CSP. Isotopically labeled enantiomers were required for the screen to Welch. Li *et al.* were also very active in the development of a new screening method for chiral selectors.[23-26] Similar to the Welch's group, the target was allowed to adsorb on the CSP and enantioenrichment in the supernatant was analyzed by multiple detection methods. We note that all the current screening methods require the immobilization of either the target or the selector to a stationary phase; some of them also require packing and using the CSP in a column. These steps require time, labor and material. It would be extremely useful to have a library screening protocol for chiral selector discovery that would function within the standard regimen for biological screening of combinatorial libraries. That means using sub-mg quantities of candidate selectors in DMSO solution in 96- or 384-well microtiter plates.

Here, such a method based on target distribution between an aqueous phase and an organic (film) phase in a microtiter plate is introduced.[27-29] Partitioning experiments are performed in the presence and the absence of a candidate selector in the organic phase. The difference in the observed distribution of the target reports on the binding of the target to the selector. Since ordinary organic solvents are difficult to work with, especially at low volume, thin polymer films are preferred as the organic phase. Plasticized polyvinyl (PVC) films have been used to study molecular recognition,[30-32] so it is naturally a good choice for chiral recognition. Figure 3.1 gives the sequence of operations for the screening procedure. In this design, the aqueous phase contains target initially. Alternatively, target and selector may be combined in the film phase initially. The applicability of this method is validated using a known chiral selector and target analyte, *N*-(3,5-dinitrobenzoyl)-phenylglycine (DNBPG; Figure 3.2, **1**) and 2,2,2-trifluoro-1-(9-anthryl)ethanol (TFAE; Figure 3.2, **2**). TFAE is defined as the selector, and observe the release of DNBPG from the PVC/DOS film to the aqueous buffer solution, with or without the selector in the film. This method was then used to screen a small library of potential chiral selectors for econazole (Figure 3.2, **3**), an antifungal agent.
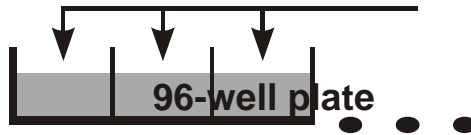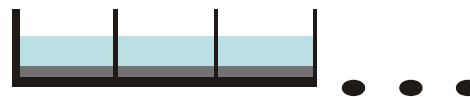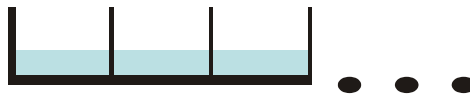
Figure 3.1. Screening protocol.
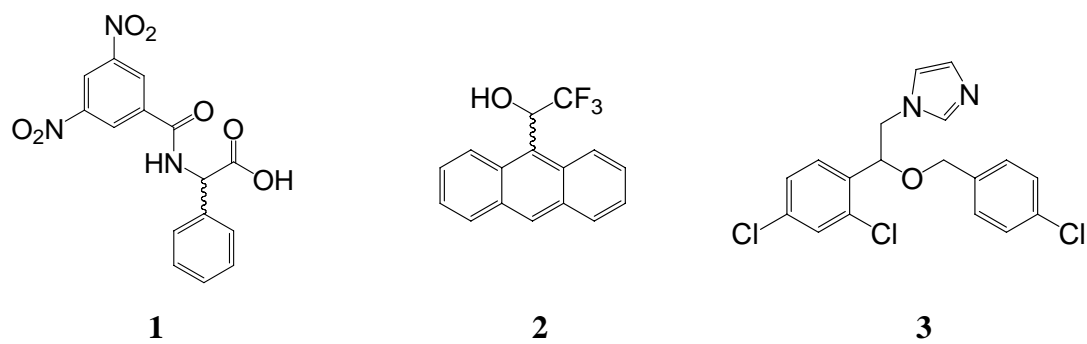
Figure 3.2. *N*-(3,5-dinitrobenzoyl)phenylglycine (DNBPG; **1**), 2,2,2-trifluoro-1-(9-anthryl)ethanol (TFAE; **2**), and econazole (**3**).

3.3   EPERIMENTAL SECTION

Chemicals and Materials.   (*R*)- and (*S*)-2,2,2-trifluoro-1-(9-anthryl)-1-ethanol (TFAE), (*R*)- and (*S*)-*N*-(3,5-dinitrobenzoyl)phenylglycine (DNBPG), econazole nitrite, HPLC grade tetrahydrofuran (THF), sulfated-β-cyclodextrin were purchased from Aldrich (Milwaukee, WI). Poly(vinyl) chloride (PVC; high molecular weight, Selectophore) and dioctyl sebacate (DOS; Selectophore) were purchased from Fluka (Ronkonkoma, NY). Water used in all the experiments was purified with a Milli-Q Synthesis A10 System (Millipore, Bedford, MA). The library of cyclopropyl dipeptide isosteres was provided by the University of Pittsburgh Center for Chemical Methodologies and Library Development (UPCMLD). Costar polypropylene 96-well microplates (flat-bottom, 330-μL well-volume), BD Falcon UV-transparent 96-well microplates (370-μL well-volume) and thermal adhesive sealing films were purchased from Fisher Scientific Co. (Pittsburgh, PA).

Equipment.   A Deep Well Maximizer (or BioShaker) (model M·BR-022 UP, made by Taitec and distributed by Bionexus Inc., Oakland, CA) was used to speed up the target distribution kinetics and control the temperature for better reproducibility. UV spectra were acquired with a SpectraMax M2 microplate reader (Molecular Devices, Sunnyvale, CA) in UV-transparent microplates. CE experiments were performed using a BioFocus 3000 (BioRad, Hercules, CA). A coated capillary with zero EOF (MicroSolv, Eatontown, NJ) was used to separate econazole racemates.

General Procedure for Screening. Figure 3.1 gives the sequence of operations for the screening procedure. The plasticized PVC films were prepared in polypropylene 96-well

microplates. In this design, the aqueous phase contains target initially. Alternatively, target and selector may be combined in the film phase initially. After the target distribution between the two phases reached equilibrium, the supernatant was transferred to a UV-transparent microplate and the UV absorbance data were collected by a microplate reader to determine the target concentration in the aqueous phase. The partition coefficient, K_p, and target-selector complex formation constant, K_f, were then calculated based on the target concentrations at equilibrium.

Detailed Protocol for Validation. PVC (2.5 g) and 2.5 g DOS were dissolved in 200 mL THF. 0.125 mg/mL (*R*)- and (*S*)-DNBPG, respectively, and 1 mg/mL (*R*)- and (*S*)-TFAE, respectively, were also prepared in THF. Polypropylene 96-well microplates were used to prepare the film phase. The volume of TFAE solution dispensed to each well is shown in Table 3.1. A multi-channel pipette was used to dispense the solution. Three such plates were prepared. In plate 1 and 2, 100 μL of the (*R*)- and (*S*)-DNBPG solution, respectively, was dispensed to each well. There was no DNBPG in plate 3. All three plates were placed in the hood for 6 hours for evaporation of the THF. Two hundred μL of the PVC/DOS solution was then dispensed to each well. The plates were again placed in the hood for 6 hours for evaporation of the THF. Plate 4 was prepared similarly, except for the contents in the wells, as shown in Table 3.2. After the films formed at the bottom of each well, 200 μL of 10 mM HCl was added. To speed up the kinetics, the microplate was placed in a shaker (500 rpm). This process was also temperature-controlled at 25 ˚C to achieve better reproducibility. A thermal adhesive sealing film was used to cover the plate to prevent water from evaporation. One hundred μL of the supernatant from each well was then transferred to UV-transparent plates. A plate reader was used for UV absorbance measurements. Note that plate 3 and columns 5 and 6 of plate 4 were used for background subtraction.

Table 3.1. Layout of TFAE dispensed in the 96-well microplate for the validation (plates 1-3).

	1	2	3	4	5	6	7	8	9	10	11	12
A												
B												
C												
D	(*R*)-TFAE		(*R*)-TFAE		(*R*)-TFAE		(*S*)-TFAE		(*S*)-TFAE		(*S*)-TFAE	
E	50 µL		100 µL		150 µL		50 µL		100 µL		150 µL	
F												
G												
H												

Table 3.2. Layout of plate 4 for the validation.

	1	2	3	4	5	6	7	8	9	10	11	12
A												
B	(*R*)-		(*S*)-									
C	DNBPG		DNBPG									
D	100 µL		100 µL		PVC/DOS		NOT USED					
E					200 µL							
F	PVC/DOS		PVC/DOS									
G	200 µL		200 µL									
H												

Detailed Protocol for Screening. In the application of the screening, candidate selectors dissolved in DMSO were dispensed to the wells shown as in Table 3.3. Each well contains 50 nmol of the candidate selector. DMSO is evaporated under vacuum and 200 μL of the PVC/DOS solution is then dispensed to each well of the plate. After evaporation of the THF, racemic econazole solutions (200 μL of 120 μM) prepared in phosphate buffer (25 mM, pH 3.0), and the buffer only, are added to the plate (Table 3.4). Again, after the equilibration in the shaker, 100 μL of the supernatant from each well is transferred to a UV-transparent plate and the UV absorbance is measured by the plate reader. Buffer-only wells are for background subtraction.

Calculations. The volume of each film was estimated as

$$V_{film} = \frac{5g/200mL \times V_{solution}}{d_{film}} \approx \frac{V_{solution}}{100\mu L} \times 2.5\mu L \tag{3.1}$$

Here $V_{solution}$ is the volume of the PVC/DOS solution used in each well, and d_{film} is the density of the film which is estimated as 1 g/mL. In this work, 200 μL of PVC/DOS solution was dispensed in each well, so the volume of each film was about 5 μL.

The concentration of the selector and target in the film, respectively, can be calculated as

$$C_S = \frac{V_S \times Conc_S / M_S}{V_{film}} \tag{3.2}$$

$$C_T = \frac{V_T \times Conc_T / M_T}{V_{film}} \tag{3.3}$$

Here V_S, $Conc_S$ and M_S are the dispensed volume of the selector solution, the selector concentration in the solution and the selector molecular weight, respectively; V_T, $Conc_T$ and M_T are the dispensed volume of the target solution, the target concentration in the solution and the target molecular weight, respectively.

The partition coefficient of the target, K_p, can be calculated as

$$K_p = \frac{C_0 - C_1}{C_1 \cdot \Phi} = \frac{A_0 - (A_1 - A_b)}{(A_1 - A_b) \cdot \Phi} \tag{3.4}$$

where C_0 is the initial target concentration in the aqueous phase (or the target concentration after all target partitions to the aqueous phase, when it is initially dissolved in the film phase), C_1 is the target concentration at equilibrium, A_0 and $(A_1 - A_{b1})$ are the UV absorbance corresponding to C_0 and C_1, respectively, A_{b1} is the UV absorbance due to small aqueous solubility of DOS, and Φ is the phase ratio.

If the target forms a 1:1 complex with the selector in the film phase, the binding constant of the complex can be calculated as

$$K_f \cong \left. \left(\frac{C_0 - C_2}{C_2 \cdot \Phi \cdot K_p} - 1 \right) \middle/ C_r \right. = \left. \left(\frac{A_0 - (A_2 - A_{b2})}{(A_2 - A_{b2}) \cdot \Phi \cdot K_p} - 1 \right) \middle/ C_r \right. \tag{3.5}$$

where C_r is the selector concentration in the film, C_2 is the target concentration at equilibrium (when the film phase contains the selector), $(A_2 - A_{b2})$ is the UV absorbance corresponding to C_2, A_{b1} is the UV absorbance due to small aqueous solubility of DOS and the selector. It is assumed that the selector is much more abundant than the target in the film and the selector concentration will not be apparently affected by the complex formation with the target.

Capillary Electrophoresis (CE) Separation of Econazole Racemate   Run buffer: 25 mM phosphate, pH 2.18, 4% (w/v) sulfated-β-CD; capillary: 60 cm in length, 50 cm to detection window, 50 μM i.d., 365 μM o.d., zero EOF ; E = - 15 kV; T = 25 ºC. Migration times were reasonably reproducible, but during a single run sometimes drifted (as did the current).

73

Table 3.3. Layout of the selector candidates in the 96-well microplate for the screening application.

	1	2	3	4	5	6	7	8	9	10	11	12
A							I		V		IX	
B												
C							II		VI		X	
D												
E							III		VII		XI	
F												
G							IV		VIII		XII	
H												

Table 3.4. Layout of the target solutions in the 96-well microplate for the screening application.

	1	2	3	4	5	6	7	8	9	10	11	12
A							Buffer		Buffer		Buffer	
B	Buffer			Econazole			Econazole		Econazole		Econazole	
C							Buffer		Buffer		Buffer	
D							Econazole		Econazole		Econazole	
E							Buffer		Buffer		Buffer	
F							Econazole		Econazole		Econazole	
G							Buffer		Buffer		Buffer	
H							Econazole		Econazole		Econazole	

3.4   RESULTS AND DISCUSSION

As a validation of the method prior to application, a known pair of chiral selector and target was considered. When attached to a stationary support, DNBPG has a selectivity (α) of 1.3 ~ 1.6 to TFAE.[8, 33] TFAE was defined as the selector, and the DNBPG release from the PVC/DOS film to the aqueous buffer solution was observed, with or without the selector in the film. As shown in Figure 3.3, ~4 h is needed for the distribution of DNBPG to reach equilibrium. Apparently, when the film contained the selector, less target solute was released. Compared to (*S*)-TFAE, (*R*)-TFAE as the selector kept more (*R*)-DNBPG in the film phase. In this work, all the distribution experiments in the validation process were performed for 5 h to ensure equilibration.

Figure 3.4 shows the dependence of the concentration of target in the aqueous phase at equilibrium on the selector concentration in the PVC/DOS film. Both selectors hindered the release of target in a concentration-dependent manner. At all selector concentrations, compared with (*R*)-TFAE, the use of (*S*)-TFAE caused more (*R*)-DNBPG to remain in the film phase; when (*S*)-DNBPG was the target, the opposite held true. The higher the selector concentration, the greater was the difference. Since a relatively low selector concentration minimizes the effect of TFAE self-association in the film (if it occurs), we determined K_f, (the formation constant for the (+)- and (-)-targets with the selector) and the selectivity, α, at the selector concentration of 36 mM, and K_p (partition ratio) with no selector present. Table 3.5 shows the results.

The formation constants are extremely small, yet complex formation influences partitioning. In a case like this, where material supply is not limited, we were able to perform a number of repeat measurements, adding significance to the measured absorbance differences.
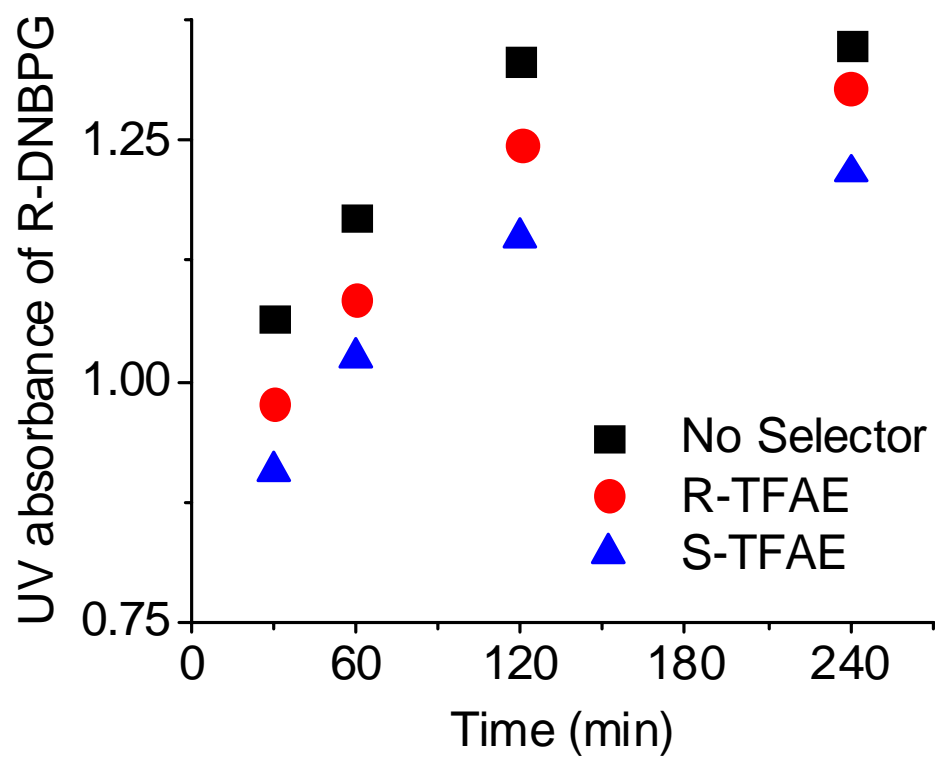
Figure 3.3. Kinetic UV absorbance of (*R*)-DNBPG in the aqueous phase during the distribution

equilibration process.
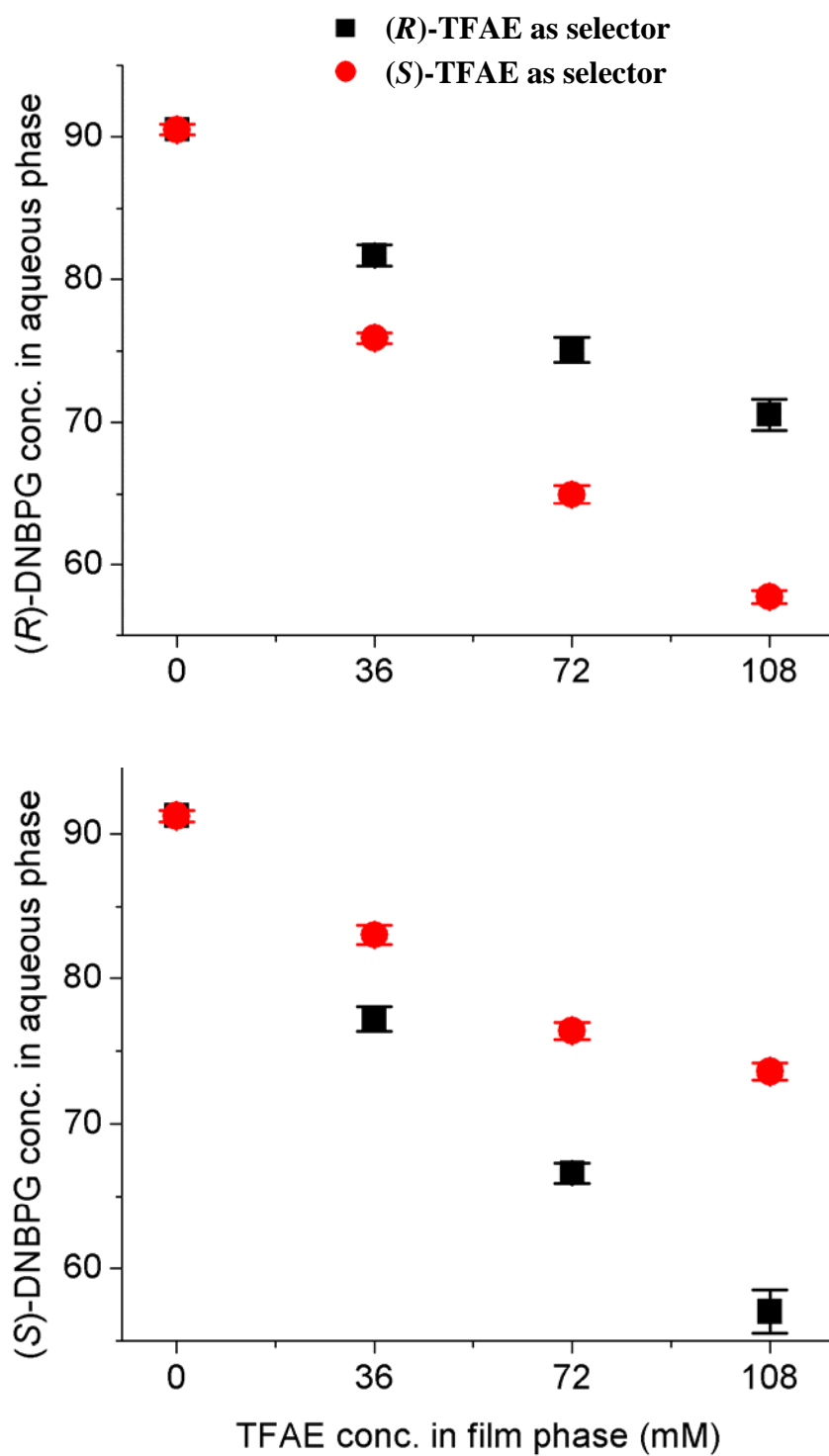
Figure 3.4. Effect of TFAE concentration in the film phase on DNBPG equilibrium

concentration in the aqueous phase.

Eight repeats were performed, and the error bars show the standard errors of the mean (SEM).

Table 3.5. Values of K_p for DNBPG going from PVC/DOS (1:1 w/w) film phase to 10 mM HCl

phase and its K_f with TFAE in the film.

K_p	K_f (M^{-1})		α
	R-R or S-S	R-S or S-R	
39.2 ± 0.2	5.8 ± 0.6	10.5 ± 0.6	1.8 ± 0.2

The value of selectivity is significant, and similar to the value found in chromatography cited above. It is likely that in normal organic solvents, the formation constants would be larger.[30, 34-36] In order for the solute distribution process to reveal binding, the solute partition coefficient K_p (distribution without selector) must be in a certain range (which depends on phase ratio). For accurate calculation of K_f, the selector should not be soluble in water and should have no self-association in film. The effect of partitioning of selector into the aqueous phase is to reduce the sensitivity of the measurement to binding.

This method was used to screen a small library of potential chiral selectors for econazole. This small library contained 12 cyclopropyl dipeptide isosteres. Racemic econazole solutions (120 μM) were prepared in phosphate buffer (25 mM, pH 3.0) and equilibrated with PVC/DOS films (phase ratio, Φ = 40), without selector and with selectors I-XII (Figure 3.5). The equilibrium optical absorbances in the aqueous phase for candidate selectors I-XII were compared to the control using the z distribution (Table 3.6; refer to Appendix A for a detailed discussion of Z-test). Eight of the 12 compounds show significant binding to econazole at the 99% confidence level.

As the racemate was used, chiral capillary electrophoresis (CE) was needed to determine the selectivity of econazole distribution. Among the 8 compounds, only selector X showed measurable enantioselective binding (Table 3.7). As indicated by the Peak 1/Peak 2 area ratio in the chiral CE trace (Figure 3.6), selector X binds the two enantiomers of econazole differently. Assuming no selector X was back-extracted to the aqueous phase, the selectivity is calculated to be 1.2. Though the selectivity is too low to use this compound as a chiral selector, it is remarkable that in this small sample we identified a selector.
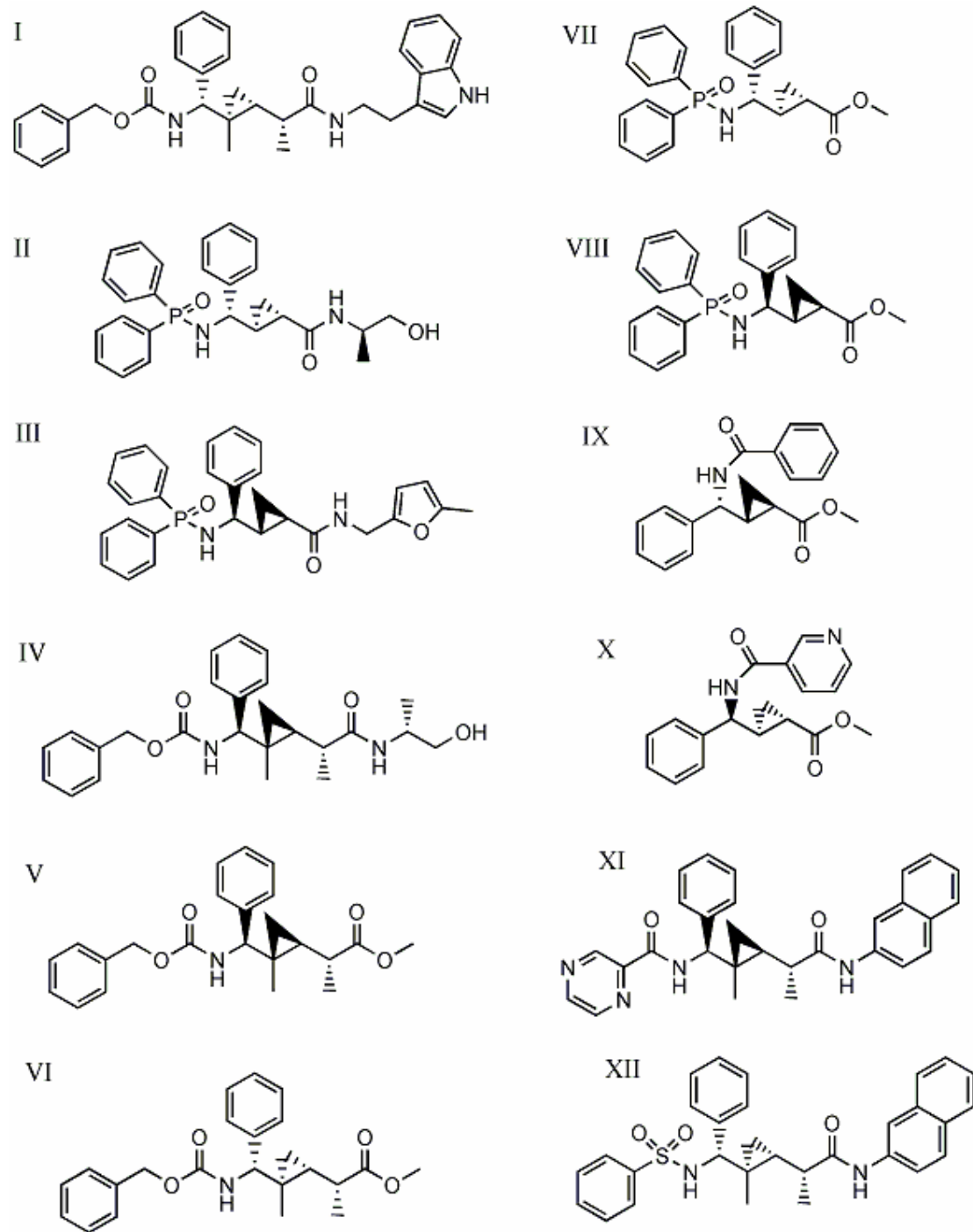
Figure 3.5. Chemical structures of the library of 12 potential selectors.

Table 3.6. Binding of econazole to the potential selectors.

Selector	UV abs. (218nm)	N^a	z^b	K_f (M^{-1})
NO	0.737	24		
I	0.724	2	1.36	--
II	0.685	2	5.43	48 ± 9
III	0.68	2	5.96	53 ± 9
IV	0.661	2	7.94	73 ± 10
V	0.741	2	0.418	--
VI	0.724	2	1.36	--
VII	0.677	2	6.27	57 ± 9
VIII	0.641	2	10.0	96 ± 11
IX	0.696	2	4.29	38 ± 9
X	0.502	2	24.6	298 ± 17
XI	0.676	2	6.38	58 ± 9
XII	0.714	2	2.40	--

[a]Number of repeats [b]Difference in absorbances divided by the error of the difference in absorbances (Appendix A).

Table 3.7. Peak area ratios from CE of econazole.

Econazole		Area Ratio (Peak 1 / Peak 2)	SEM	n
Before extraction		0.980	0.002	6
After extraction	No selector	0.973	0.003	6
	Selector X	1.051	0.009	16
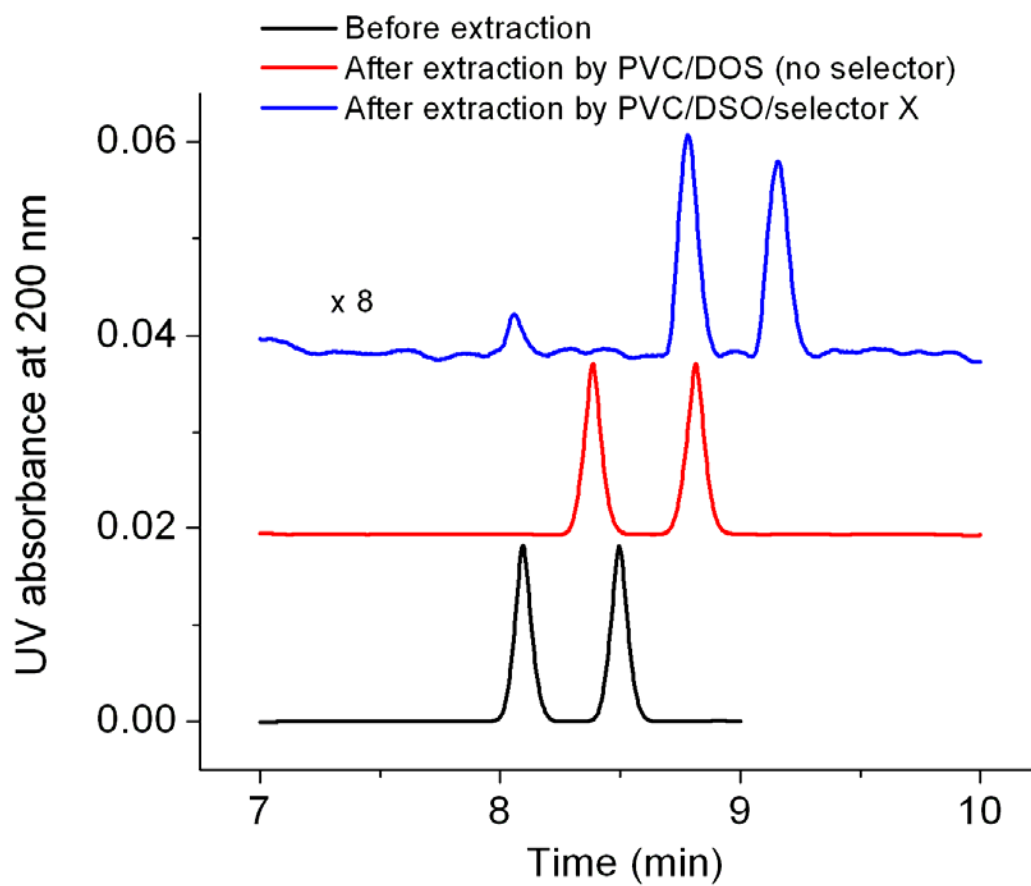
Figure 3.6. Chiral capillary electrophoresis separation of econazole nitrate.

There is a great deal of flexibility in this system. The sensitivity of the technique can be adjusted. While applicability to small values of α was demonstrated, it is also possible to set up a system in which a particular combination of K_f and α is discovered. In this high throughput screening application, only 200 nmol (<100 μg) of each library member was used. Because of the small mass requirements, it opens up huge numbers of compounds as candidate selectors. The same procedures can be used to test one selector vs. many solutes (*i.e.*, generality). A detailed comparison of this method to the other approaches is shown in Table 3.8.

Table 3.8. Comparison of screening methods for chiral stationary phases.

Screening Principle	Preparation		Detection	Selector amount
HPLC separation on synthesized CSP	Covalent attachment of each selector to the solid phase	N column packing	HPLC separation	According to column size
	Covalent attachment of the target analyte to the solid phase[20, 37]	One column packing	HPLC separation	According to column size
Selector-analyte complex formation	Covalent attachment of each selector to the solid phase[22]	Analyte adsorption equilibrium	LC/MS for isotopically labeled enantiomers	~ 50 mg
	Covalent attachment of each selector to the solid phase[23, 25, 26]	Analyte adsorption equilibrium (3 hours)	Circular Dichroism or HPLC	~ 15 mg (0.030 mmol)
	Membrane preparation (<12 hours, including 10 hours' waiting time)	Analyte distribution (1-5 hours)	UV absorbance (Plate reader, 10 min for 96 readings)	~ 0.1 mg (200 nmol)

3.5   CONCLUSIONS

A new screening method for chiral selectors based on target distribution between a film phase and an aqueous phase is described. This method was validated by a known pair of chiral selector and target – TFAE and DNBPG, and applied to a small library of cyclopropyl dipeptide isosteres to screen chiral selectors for econazole. Compared to current screening methods, this format does not require any covalent attachment of either the target or the potential chiral selector to the stationary phase, which saves time and labor. Moreover, the amount of the selector required by this method is at the microgram scale, which is about two orders of magnitude less than the amount needed by current screening processes.[22]

3.6   REFERENCE

(1)   Islam, M. R.; Mahdi, J. G.; Bowen, I. D. *Drug Safety* **1997**, *17*, 149-165.

(2)   Drayer, D. E. *Clinical Pharmacology & Therapeutics (St. Louis, MO, United States)* **1986**, *40*, 125-133.

(3)   De Camp, W. H. *Journal of Pharmaceutical and Biomedical Analysis* **1993**, *11*, 1167-1172.

(4)   Rekoske, J. E. *AIChE Journal* **2001**, *47*, 2-5.

(5)   Francotte, E. R. *Journal of Chromatography A* **2001**, *906*, 379-397.

(6)   Huang, J.; Zhang, P.; Chen, H.; Li, T. *Analytical Chemistry* **2005**, *77*, 3301-3308.

(7)   Hare, P. E.; Gil-Av, E. *Science* **1979**, *204*, 1226-1228.

(8)   Pirkle, W. H.; Finn, J. M.; Schreiner, J. L.; Hamper, B. C. *Journal of the American Chemical Society* **1981**, *103*, 3964-3966.

(9)   Allenmark, S. G.; Andersson, S. *Journal of Chromatography, A* **1994**, *666*, 167-179.

(10)   Bluhm, L.; Huang, J.; Li, T. *Analytical and Bioanalytical Chemistry* **2005**, *382*, 592-598.

(11)   Burguete, M. I.; Frechet, J. M. J.; Garcia-Verdugo, E.; Janco, M.; Luis, S. V.; Svec, F.; Vicent, M. J.; Xu, M. *Polymer Bulletin (Berlin, Germany)* **2002**, *48*, 9-15.

(12)   Wipf, P.; Coleman, C. M.; Janjic, J. M.; Iyer, P. S.; Fodor, M. D.; Shafer, Y. A.; Stephenson, C. R. J.; Kendall, C.; Day, B. W. *Journal of Combinatorial Chemistry* **2005**, *7*, 322-330.

(13)   Wipf, P.; Stephenson, C. R. J. *Organic Letters* **2005**, *7*, 1137-1140.

(14)   Wipf, P.; Xiao, J. *Organic Letters* **2005**, *7*, 103-106.

(15)   Xiao, J.; Weisblum, B.; Wipf, P. *Journal of the American Chemical Society* **2005**, *127*, 5742-5743.

(16)   Janjic, J. M.; Mu, Y.; Kendall, C.; Stephenson, C. R. J.; Balachandran, R.; Raccor, B. S.; Lu, Y.; Zhu, G.; Xie, W.; Wipf, P.; Day, B. W. *Bioorganic & Medicinal Chemistry* **2004**, *13*, 157-164.

(17)   Pirkle, W. H.; Sikkenga, D. L. *Journal of Organic Chemistry* **1977**, *42*, 1370-1374.

(18)   Lipkowitz, K. B.; Stoehr, C. M. *Chirality* **1996**, *8*, 341-350.

(19)   Aboul-Enein, H. Y.; Ali, I. *Chiral Separations by Liquid Chromatography and Related Technologies*; Marcel Dekker, Inc.: New York, 2003.

(20)   Pirkle, W. H.; House, D. W.; Finn, J. M. *Journal of Chromatography* **1980**, *192*, 143-158.

(21)   Pirkle, W. H.; Hyun, M. H.; Bank, B. *Journal of Chromatography* **1984**, *316*, 585-604.

(22)   Welch, C. J. *Chirality* **2001**, *13*, 425-427.

(23)   Wu, Y.; Wang, Y.; Yang, A.; Li, T. *Analytical Chemistry* **1999**, *71*, 1688-1691.

(24)   Wang, Y.; Li, T. *Analytical Chemistry* **1999**, *71*, 4178-4182.

(25)   Bluhm, L. H.; Wang, Y.; Li, T. *Analytical Chemistry* **2000**, *72*, 5201-5205.

(26)   Wang, Y.; Bluhm, L. H.; Li, T. *Analytical Chemistry* **2000**, *72*, 5459-5465.

(27)   Kim, S. B.; Cho, H. C.; Cha, G. S.; Nam, H. *Analytical Chemistry* **1998**, *70*, 4860-4863.

(28)   Dai, S.; Ye, Q.; Wang, E.; Meyerhoff, M. E. *Analytical Chemistry* **2000**, *72*, 3142-3149.

(29)   Welch, C. J.; Shaimi, M.; Biba, M.; Chilenski, J. R.; Szumigala, R. H., Jr.; Dolling, U.; Mathre, D. J.; Reider, P. J. *Journal of Separation Science* **2002**, *25*, 847-850.

(30)   Li, S.; Sun, L.; Chung, Y.; Weber, S. G. *Analytical Chemistry* **1999**, *71*, 2146-2151.

(31)   Zhang, X.; Zhao, H.; Weber, S. G. *Analytical Chemistry* **2002**, *74*, 2184-2189.

(32)   Zhang, X.; Zhao, H.; Chen, Z.; Nims, R.; Weber, S. G. *Analytical Chemistry* **2003**, *75*, 4257-4264.

(33)   Malyshev, O. R.; Vinogradov, M. G. *Journal of Chromatography, A* **1999**, *859*, 143-151.

(34)   Valenta, J. N.; Sun, L.; Ren, Y.; Weber, S. G. *Analytical Chemistry* **1997**, *69*, 3490-3495.

(35)   Li, S.; Weber, S. G. *Analytical Chemistry* **1997**, *69*, 1217-1222.

(36)   Sun, L.; Weber, S. G. *Journal of Molecular Recognition* **1998**, *11*, 28-31.

(37)   Pirkle, W. H.; Hyun, M. H.; Tsipouras, A.; Hamper, B. C.; Banks, B. *Journal of Pharmaceutical and Biomedical Analysis* **1984**, *2*, 173-181.

4.0 HIGH-THROUGHPUT PHASE-DISTRIBUTION METHOD TO DETERMINE DRUG-CYCLODEXTRIN BINDING CONSTANTS

4.1 ABSTRACT

A high-throughput method has been developed to measure drug-cyclodextrin binding constants. It measures the distribution coefficient of a drug between a polymer film (polyvinyl chloride (PVC) with 67% (w/w) dioctyl sebacate (DOS)) and a cyclodextrin-containing buffer in a 96-well format. Measurements of distribution coefficient at several cyclodextrin concentrations lead to binding constants. Binding constants for econazole with six CDs have been determined in one 96-well microplate with four replications of each condition in 10 hours. The $K_{1:1}$ values are 1662±159 M^{-1}, 1964±51 M^{-1}, 19600±5100 M^{-1}, 373±77 M^{-1}, 13190±300 M^{-1}, 3100±160 M^{-1}, with (2-hydroxyethyl)-β-cyclodextrin, (2-hydroxypropyl)-β-cyclodextrin, 2,6-di-o-methyl-β-cyclodextrin, heptakis(2,3,6-tri-o-methyl)-β-cyclodextrin, α-cyclodextrin, β-cyclodextrin, respectively. It is likely that 1:2 complexes are also formed in some cases. This method has also been applied to study the binding behavior as a function of the drug concentration and pH. Binding weakens at higher drug concentration which may be due to the self-association of the drug. An acidic environment decreases the binding constant of CD with the basic econazole. The formation of the 1:2 complex is completely suppressed in acid as well. This protocol is faster

than the phase-solubility method. Moreover, the material requirement is up to 4 orders of magnitude lower.

4.2 INTRODUCTION

Aqueous solubility is one of the fundamental determinants in developing new chemical entities as successful drugs.[1] Multiple formulation techniques exist to increase the apparent solubility of lipophilic compounds without decreasing their optimized potency. These techniques include particle size reduction, pH adjustment, addition of solubilising excipients, solid dispersion, microemulsification, nanocrystallization, inclusion complex formation, etc.[2] Cyclodextrins (CDs) are bucket-shaped oligosaccharides produced from starch, with a hydrophilic outer surface and a lipophilic inner cavity. They are able to form water-soluble inclusion complexes with many lipophilic compounds. They are commonly used in pharmaceutical formulations to enhance drug solubility, stability and bioavailability.[3, 4] To date, there are more than 20 marketed drugs that contain CDs,[5] and numerous publications are emerging every year studying the use of CDs for drug formulation and delivery. Although higher order complexes are not uncommon, the simplest and most frequent stoichiometry of drug-cyclodextrin (S-CD) complexes is 1:1

$$S + CD \overset{K_{1:1}}{\rightleftharpoons} S\text{-}CD$$

The binding constant ($K_{1:1}$) is defined as

$$K_{1:1} = \frac{[S\text{-}CD]}{[S][CD]} \tag{4.1}$$

where [S], [CD], [S-CD] are the concentrations of the free drug, free CD, and drug-CD complex, respectively. For consecutive complexation

$$S\text{-}CD_{i\text{-}1} + CD \underset{\xrightarrow{\hspace{1cm}}}{\overset{K_{1:i}}{\rightleftharpoons}} S\text{-}CD_i$$

The binding constant ($K_{1:i}$) is defined as

$$K_{1:i} = \frac{[S\text{-}CD_i]}{[S\text{-}CD_{i-1}][CD]} \qquad (4.2)$$

The binding forces within the drug-CD complexes may involve hydrophobic, van der Waals, hydrogen bonding, or dipole interactions.[6] Depending on the cavity size and functional groups, CDs vary in their ability to form inclusion complexes with specific guest compounds.[7] The stoichiometry and binding constant are important in any investigation to assess the value of a CD for the formulation of a specific drug.[8]

Grounded on the basic principles of medicinal chemistry, one of the most reliable methods to increase *in vitro* potency of drug candidates is to add lipophilic moieties at appropriate positions of the lead compound.[1] Hence the recent development of combinatorial synthesis and high-throughput technologies has led to an increasing number of poorly soluble compounds from combinatorial libraries being investigated for their therapeutic activities.[9] To develop a formulation technique that works within the combinatorial screening regimen, it would be beneficial to have a universal protocol that can measure the binding constant of drug-CD complexes in a high-throughput manner. Various techniques exist to measure drug-CD binding. They can be generally classified into two groups: separation based and non-separation based. The former separates the free and complexed drug and quantifies their concentrations. Chromatography,[10] affinity capillary electrophoresis (ACE),[11-14] dialysis,[15], and electrospray mass spectroscopy (ESI-MS)[16] methods are separation based techniques. The latter group of methods monitors the change in specific physicochemical properties of the drug or CD upon complexation. This category includes for example spectroscopy,[17, 18] NMR, conductometry,[19]

potentiometry,[20] phase-solubility,[21] and hydrolysis kinetics.[22, 23] Each type of measurement is limited to a certain set of compounds. The most common method to determine $K_{1:1}$ for drug-CD binding is the Higuchi-Connors phase-solubility method.[21] This method measures the effect of CD concentration on the apparent solubility of the drug; the intrinsic solubility (S_0) and the slope of the solubility vs. CD-content diagram are then used to calculate $K_{1:1}$. There are also a few reports using phase-distribution methods to determine binding constants for CD complexes.[24, 25] High-throughput technologies have been employed in protein binding measurement using homogeneous and cell-based assays.[26, 27] However, unique assays are required for each target, which leads to long development time and high cost.[26] As to the author's knowledge, there is no genuine high-throughput approach that has been developed for the determination of drug-CD complexation.

Recently, we have developed a high-throughput method that can determine the partition and distribution behavior of drug candidates between a polymer phase and an aqueous phase.[28] This method has also been applied to measure intermolecular association in the polymer phase to screen chiral selectors.[29] Here the application of this high-throughput method for the determination of drug-CD binding constants in the aqueous phase is reported. The polymer phase is composed of poly(vinyl chloride) (PVC) and dioctyl sebacate (DOS) at the ratio of 1:2 (w/w). Econazole and miconazole (Figure 4.1), both anti-fungal agents, were used as the test drugs. Their abilities to form water-soluble complexes with various CDs were determined under various concentration and pH conditions.
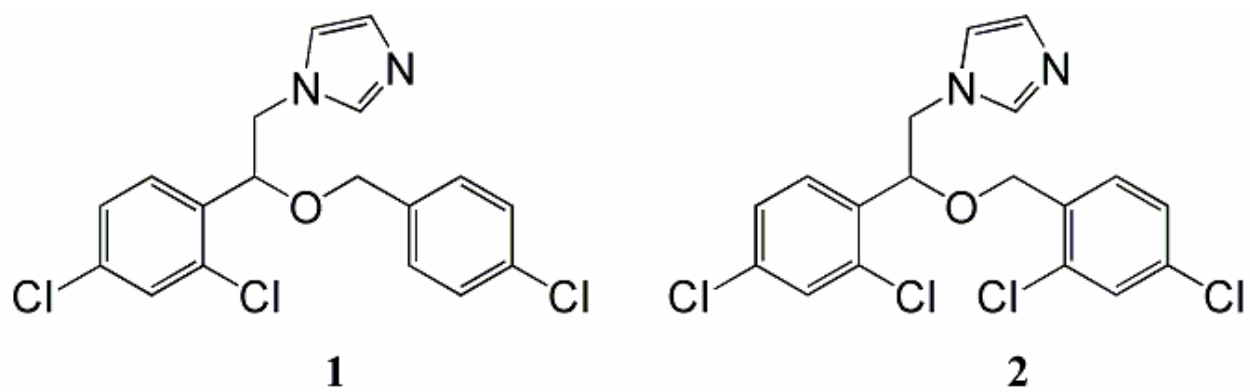
Figure 4.1. Econazole (1) and miconazole (2).

4.3   EXPERIMENTAL

Materials   (2-Hydroxyethyl)-β-cyclodextrin (HE-β-CD), (2-hydroxypropyl)-β-cyclodextrin (HP-β-CD), 2,6-di-o-methyl-β-cyclodextrin (DM-β-CD), heptakis(2,3,6-tri-o-methyl)-β-cyclodextrin (TM-β-CD), α-cyclodextrin (α-CD), and β-cyclodextrin (β-CD) were purchased from Sigma-Aldrich-Fluka at the highest available purities. Econazole free base was purchased form Molecula Ltd. (Dorset, UK). Miconazole free base was purchased from MP Biomedicals (Solon, OH). HPLC grade tetrahydrofuran (THF) and acetonitrile (ACN) were purchased from Aldrich (Milwaukee, WI). PVC (high molecular weight, Selectophore) and dioctyl sebacate (DOS; Selectophore) were purchased from Fluka (Ronkonkoma, NY). Water used in all the experiments was purified with a Milli-Q Synthesis A10 system (Millipore, Bedford, MA). Costar polypropylene 96-well microplates (flat-bottom, 330-μL well volume) and thermal adhesive sealing films were purchased from Fisher Scientific Co. (Pittsburgh, PA).

Equipment   An UltraSpense 2000 microplate dispenser (KD Scientific, Holliston, MA) was used to prepare polymer films in 96-well plates. A Deep Well Maximizer (or BioShaker) (Model M·BR-022 UP, made by Taitec and distributed by Bionexus, Inc., Oakland, CA) was used to speed up the drug distribution kinetics and control the temperature for better reproducibility. An X-LC (Jasco, Inc.) HPLC system was used to determine the econazole and miconazole concentration with a UPLC C_{18} column (1.0 × 50 mm, particle size: 1.7 μM, Waters, Milford, MA). The molecular weights of the cyclodextrins in this study were determined by ESI-MS (Agilent HP 1100 LC-MSD).

Buffer Preparation   The phosphate buffer solutions (20 mM, pH 5.8, 7.4, 8.5) were made by mixing appropriate amounts of 20 mM sodium phosphate dibasic solution and 20 mM sodium phosphate monobasic solution. The phosphate buffer (20 mM, pH 1.8) was made by mixing appropriate amounts of 20 mM sodium phosphate monobasic solution and 20 mM phosphoric acid solution.

High-Throughput Phase-Distribution Studies   Figure 4.2 gives the sequence of operations for the phase-distribution method that measures the binding constants of drug-CD complexes. The plasticized PVC films were prepared in polypropylene 96-well microplates. The detailed process is described elsewhere,[28] with the exception that in this study a microplate dispenser rather than a multichannel pipet was used for solution dispensing. This provided higher throughput and better precision. Briefly, an appropriate amount of the PVC, DOS and drugs were dissolved in THF. Aliquots of 250 μL of this solution were dispensed by the microplate dispenser to microplates. Evaporation of solvent allowed the formation of polymer films at the bottom of each well. The volume of each film has been calculated to be ~2.5 μL.[28] CD-containing aqueous buffers were then manually dispensed over the films with a multichannel pipet. The plates were covered by adhesive sealing films and incubated in a shaker (500 rpm, 25 ºC). In order to determine the equilibration time, the concentration of drug extracted into the aqueous phase was measured as a function of time. Other than for this experiment, all data generated were at equilibrium. To determine the drug concentration, the supernatant from each well was transferred to another plate and injected to the HPLC system by an autosampler. The distribution coefficient, *D*, was then calculated as

$$D = \frac{C_E}{\left(C_{tot} - C_E\right) \cdot \Phi}$$ (4.3)

Add PVC/DOS/drug in THF

96-well plate
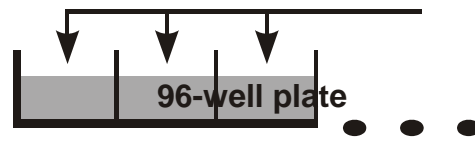
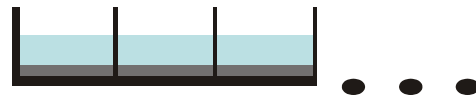**Evaporate THF**
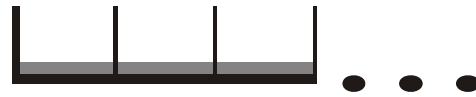
Add CD-containing buffer
Equilibrate (const. T)

Transfer supernatant to
another plate, measure
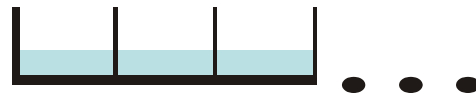**drug conc. by HPLC**

Figure 4.2. General procedure for binding constant measurement.

Here C_{tot} is the drug aqueous concentration if all the target has been extracted to the aqueous phase, C_E is the drug aqueous concentration at equilibrium, and Φ is the phase ratio (aqueous over polymer).

HPLC Method to Determine Econazole/Miconazole Concentration To minimize the ionized form, pH 1.8 samples were diluted 9 times with 20 mM pH 8.5 phosphate buffer; pH 5.8 samples were diluted 3 times with 20 mM pH 8.5 phosphate buffer. The mobile phase was H_2O/acetonitrile (65/35), flowing at 0.2 mL/min through a Waters UPLC C_{18} column. The back-pressure was ~480 bars. To ensure reproducibility, the full-load injection mode was used (injection volume 5 μL; loop volume 1 μL). The peak area was used for the calibration and determination of sample concentration. The time per analysis was ~60 s.

ESI-MS Method to Determine Cyclodextrin Molecular Weights The mobile phase was acetonitrile/H_2O (35/65) with 0.1% formic acid. The samples were introduced into the ESI source at 5 μL/min. All experiments were performed in positive ion mode. Typically, a probe high voltage ~4000 V was applied between the spray needle and the end plate. The drying gas temperature was 350 °C with the flow rate at 10 L/min. The nebulizer pressure was 29 psig. The mass scanning range was 100-3000 with a resolution of 0.15.

Theories to Determine the Stoichiometry n and Binding Constants $K_{1:i}$ ($i = 1$ to n) The distribution of the free drug between the aqueous phase and the film phase is determined by the partition ratio D_0

$$D_0 = \frac{[S]}{[S]_{film}} \tag{4.4}$$

where [S] and [S]$_{film}$ are the free drug concentration in the aqueous phase and film phase, respectively. When the CD is added to the aqueous phase, the drug distribution coefficient is:

$$D = \frac{[S] + \sum\limits_{i=1}^{n} [S\text{-}CD_i]}{[S]_{film}} \qquad (4.5)$$

where n is the stoichiometry, $[S\text{-}CD_i]$ ($i = 1$ to n) is the drug-CD complex concentration in the

aqueous phase in various forms. Dividing Eq. 4.5 by Eq. 4.4

$$\frac{D}{D_0} = 1 + \sum\limits_{i=1}^{n} \frac{[S\text{-}CD_i]}{[S]} \qquad (4.6)$$

From Eq. 4.2, one obtains

$$[S\text{-}CD_i] = [S][CD]^i \prod\limits_{j=1}^{i} K_{1:j} \qquad (4.7)$$

Inserting Eq. 4.7 to Eq. 4.6

$$\frac{D}{D_0} = 1 + \sum\limits_{i=1}^{n} \left([CD]^i \prod\limits_{j=1}^{i} K_{1:j} \right) \qquad (4.8)$$

Plotting D/D_0 versus $[CD]$, the stoichiometry and the binding constants can be obtained from

polynomial fitting analyses. In practice, a degree 1 (linear) fitting should first be performed,

assuming that only 1:1 complex forms

$$\frac{D}{D_0} = 1 + K_{1:1}[CD] \qquad (4.9)$$

A proper fitting should give a straight line with a y-intercept of 1, and the slope can report the

value of $K_{1:1}$. Otherwise a degree 2 (quadratic) fitting should be carried out, assuming that both

1:1 and 1:2 complexes form:

$$\frac{D}{D_0} = 1 + K_{1:1}[CD] + K_{1:1}K_{1:2}[CD]^2 \qquad (4.10)$$

Again, a correct fitting should give a y-intercept of 1, and the $K_{1:1}$ and $K_{1:2}$ values can be obtained from the corresponding coefficients of the polynomial. If the fit is still not satisfactory, fitting analyses with higher degrees should be continued. Note that all the coefficients of the polynomial should have positive values. In this study, the concentration of CD prepared in the aqueous buffer (C_{CD}) is much higher than the drug concentration (C_{tot}), hence the drug-CD complexation does not significantly change the free CD concentration, and [CD] in Eq. 4.8, 4.9 and 4.10 can be reasonably replaced by C_{CD}.

4.4   RESULTS AND DISCUSSION

A kinetic study was first performed to determine the time needed for the phase distribution of econazole to reach equilibrium. The results are shown in Figure 4.3. Clearly, 8-9.5 h is enough for all the distribution experiments being equilibrated. Careful inspection of the curves shows that the equilibration time is shorter when the aqueous phase contains less CD or the specific CD has a weaker ability to extract econazole. All other distribution experiments were allowed to equilibrate for 10 h.

Instructed by Eq. 4.8, the effect of CD concentration on the distribution of econazole was then studied. Figure 4.4 gives the profile of econazole equilibrium concentration versus CD-content in the aqueous phase for six CDs. Each measurement was repeated for four times and the corresponding error bar indicates the standard error of the mean (SEM). The SEM values were then used in error propagations to determine the errors of the calculated distribution coefficients and D/D_0 values. C_{tot} is 88.8 μM in this experiment. Apparently, at higher CD concentration, more econazole is extracted to the aqueous phase. For these six CDs, the ability to
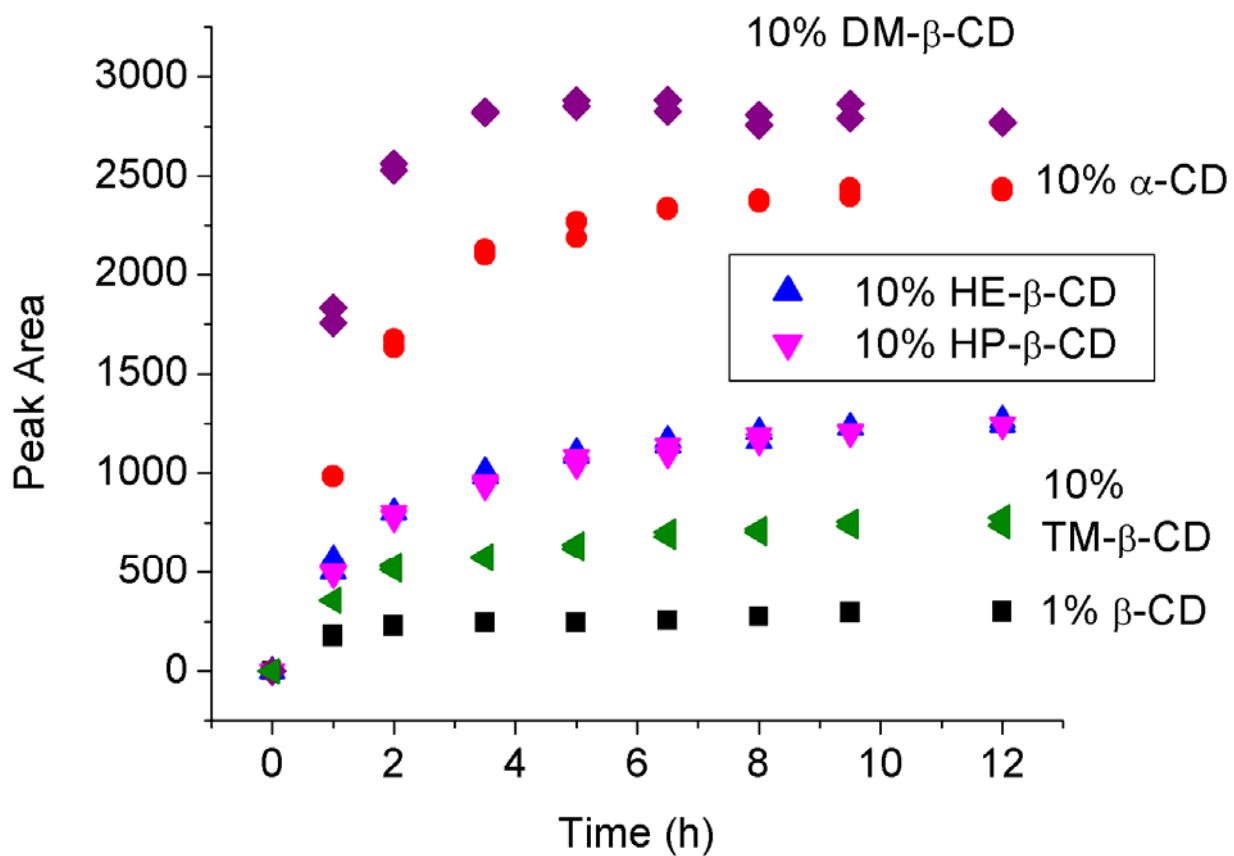
Figure 4.3. HPLC peak area of econazole in the aqueous phase during the distribution equilibration process.
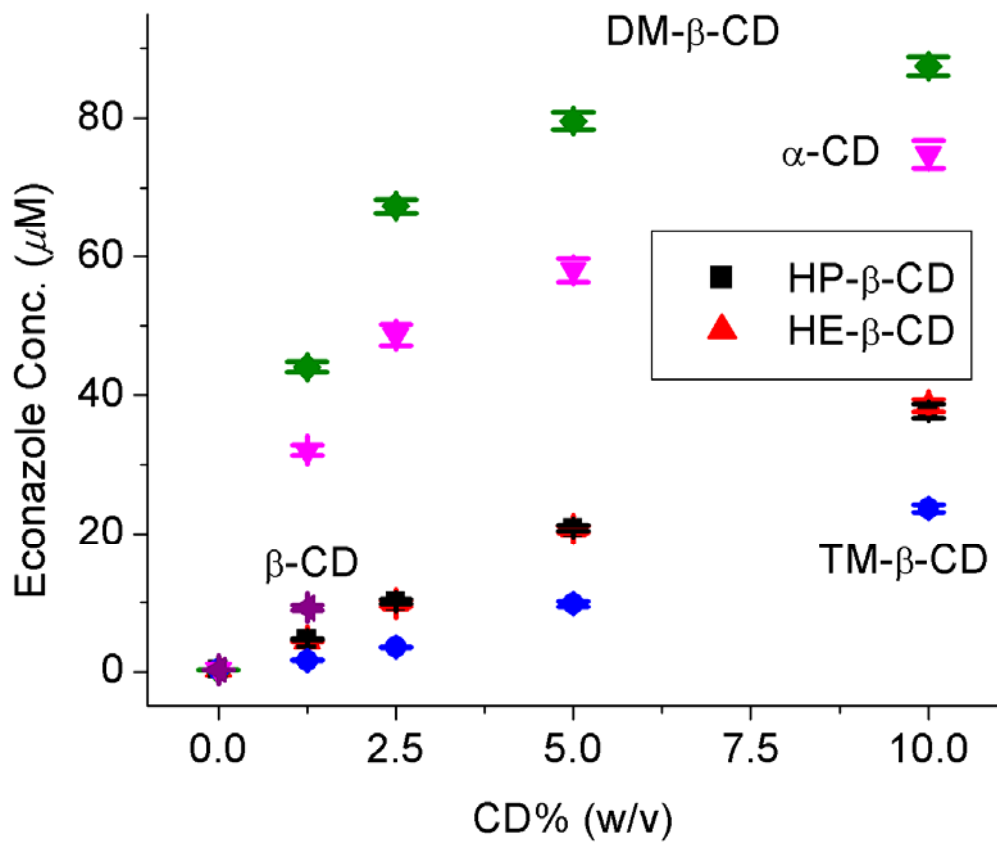
Figure 4.4. Effect of CD concentration on econazole equilibrium concentration in the aqueous phase.

econazole is in the order of DM-β-CD > α-CD > β-CD > HE-β-CD ≈ HP-β-CD > TM-β-CD, which is in good agreement with the previous kinetic study (Figure 4.3) and reported phase-solubility data of several CDs (α-CD > β-CD > HP-β-CD).[30] Quadratic polynomial fitting analyses according to Eq. 4.10 give the $K_{1:1}$ and $K_{1:2}$ values, as shown in Table 4.1. The errors are their standard deviations. Some of the fitted curves are shown in Figure 4.5 and all the coefficients of determination (COD) are listed in Table 4.1. Since β-CD is insoluble at concentrations higher than 1.25% (v/w), no fitting analysis was performed for the calculation of its binding constant. Instead, the equation described in Table 4.1 was used to determine its $K_{1:1}$ value based on the assumption that only 1:1 complex had formed. The econazole-CD binding constants ($K_{1:1}$) discovered by phase-solubility studies have been reported for α-CD, HP-β-CD, and β-CD, which are 2630±260, 1540±150, and 1420±130 M^{-1}, respectively.[30] These values are a little bit off from the data in Table 4.1. However, since the pH and choice of buffer species have a great effect on the determination of binding constant,[30] the literature values measured in pure water should only used for qualitative purposes. Since the binding constant of econazole with β-CD was calculated without using the fitting analysis, to determine this value more accurately, a repeat of experiment with more data points at lower CD concentrations may be necessary. The $K_{1:2}$ values of five CDs are larger than 0, indicating the formation of 1:2 complexes. The relative standard deviation (RSD) of $K_{1:1}$ for econazole/DM-β-CD interaction is so large that $K_{1:1}$ is not significantly different from 0. Another fitting analysis was performed assuming $K_{1:1} = 0$, and the obtained $K_{1:2}$ has a much smaller RSD. This indicates that only the 1:2 complex formed for econazole/DM-β-CD binding. Most studies on imidazole-CD complexation have assumed a 1:1 ratio,[1, 31] but higher order complexes have also been reported.[32-36] For instance, the stoichiometry of econazole/β-CD has been published by several groups to be 1:1,[30, 37] while one study has

Table 4.1. Binding constants of econazole with six CDs.

D_0	Cyclodextrin	M.W. (g/mol)	$K_{1:1}$ (M^{-1})	$K_{1:2}$ (M^{-1})	COD
(3.30±0.12)x10^{-5}	HE-β-CD	~1480[a]	1662±159	17±3	0.9977
	HP-β-CD	~1580[a]	1964±51	13±1	0.9998
	DM-β-CD	~1330[a]	19600±5100	72±23	0.9963
			0[c]	1.94±0.12 x 10^{6} [c,d]	0.9462[c]
	TM-β-CD	1429.54	373±77	46±10	0.9979
	α-CD	972.84	13190±300	1.9±0.4	0.9997
	β-CD	1134.98	3100±160[b]	N/A	N/A

[a] Randomly substituted, and their average molecular weights are determined by ESI-MS.

[b] The stoichiometry of econazole-β-CD is assumed to be 1:1, and its $K_{1:1}$ is calculated as

$$K_{1:1} = \left(\frac{D}{D_0} - 1\right)\Big/ C_{CD}$$

[c] Quadratic fitting with the restriction $K_{1:1} = 0$.

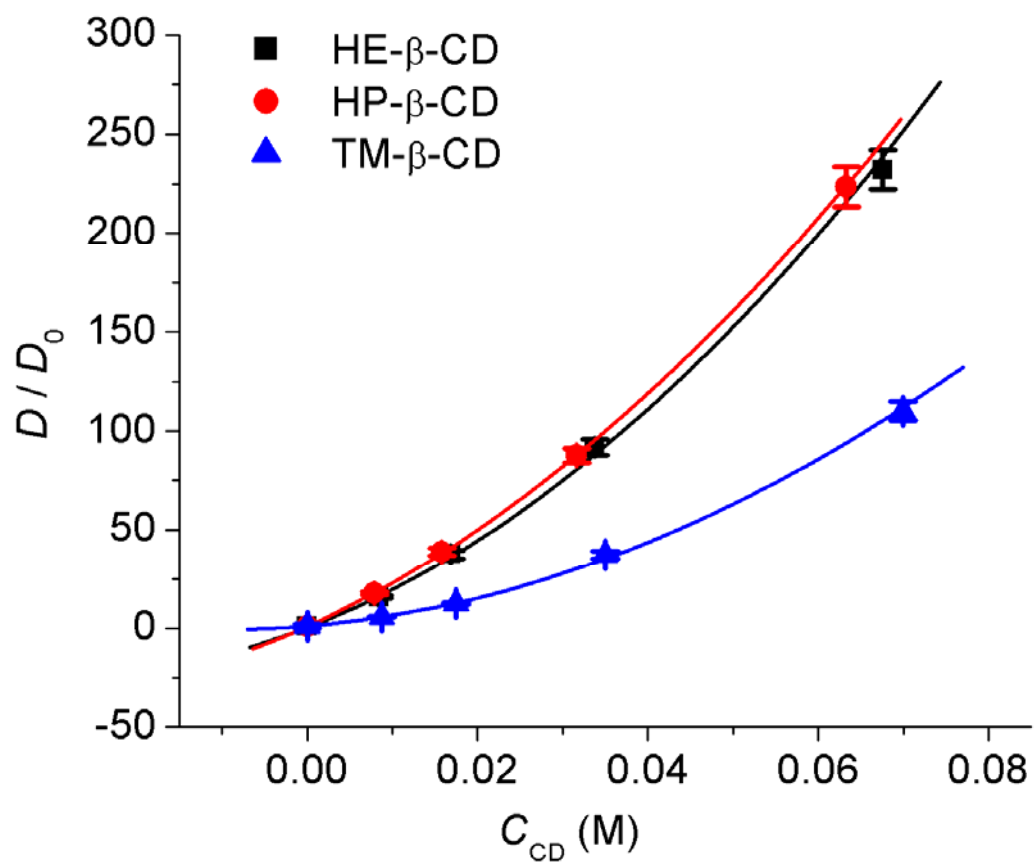[d] This entry should be compared to the product $K_{1:1}K_{1:2,}$ and it has units of M^{-2}.

Figure 4.5. Quadratic polynomial fitting of D/D_0 versus CD concentration.

discovered the formation of 2:3 complex.[32] Our ESI-MS studies have observed the formation of DM-β-CD dimers and trimers, as demonstrated in Figure 4.6. The signals for high-order econazole/DM-β-CD complexes were not discovered which may be due to the limited sensitivity of the instrument.

The drug distribution behavior at various C_{tot} values was studied. The corresponding equilibrium concentrations versus CD-concentration profiles are shown in Figure 4.7. The CD used was HP-β-CD and the pH of the aqueous buffer was 8.5. D_0, $K_{1:1}$ and $K_{1:2}$ values are listed in Table 4.2. At higher C_{tot}, the D_0 value is greater and the $K_{1:1}$ and $K_{1:2}$ values tend to be smaller. This interesting trend may be due to a decreasing drug activity coefficient as concentration is increased. This effect can explain the previous observation that binding constants determined by phase-solubility studies are smaller than by this method, since in phase-solubility experiments, the saturated econazole concentration is much higher than the equilibrium drug concentration in this distribution study.

This method has also been applied in the situation where two mixed drugs are studied at the same time. Since the CD concentration is large with respect to the sum of the drug concentrations, a 'multiplex' approach is possible. Miconazole is an analogue of econazole. Both of them were dissolved in the same polymer film. The extraction profile is shown in Figure 4.8. The values of D_0, $K_{1:1}$ and $K_{1:2}$ are listed in Table 4.2. From the data, miconazole is more lipophilic than econazole, and binds more strongly to HP-β-CD. When mixed with miconazole, the distribution coefficient of econazole is greater, and the binding constants $K_{1:1}$ and $K_{1:2}$ are smaller, which may be attributable to the decreased drug activity coefficient caused by association with miconazole.
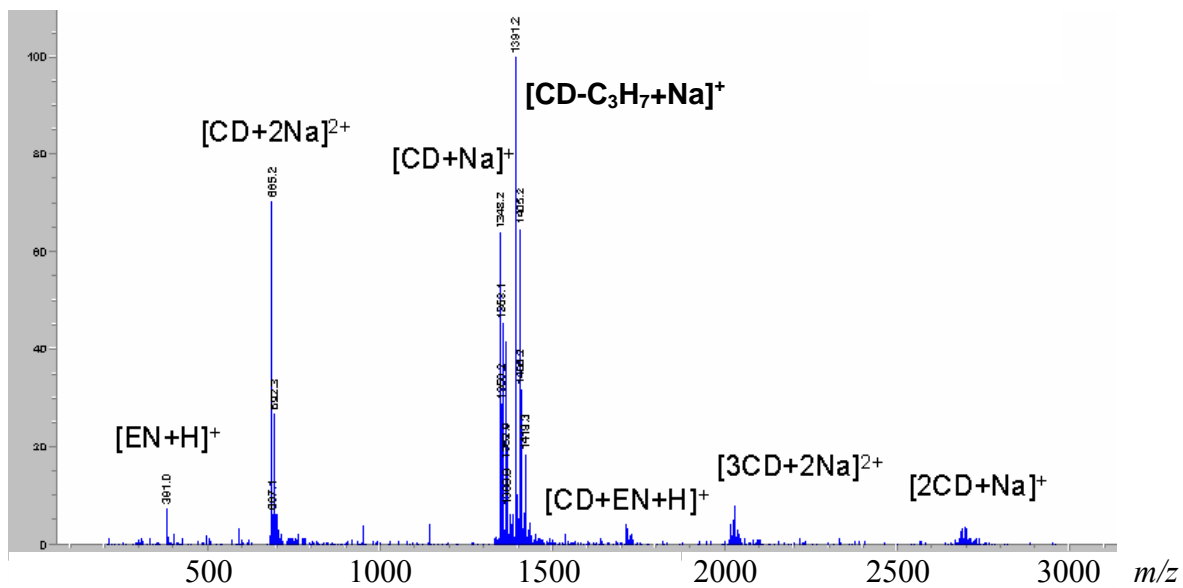
Figure 4.6. ESI-MS spectrum of DM-β-CD (10% w/v) and econazole after distribution

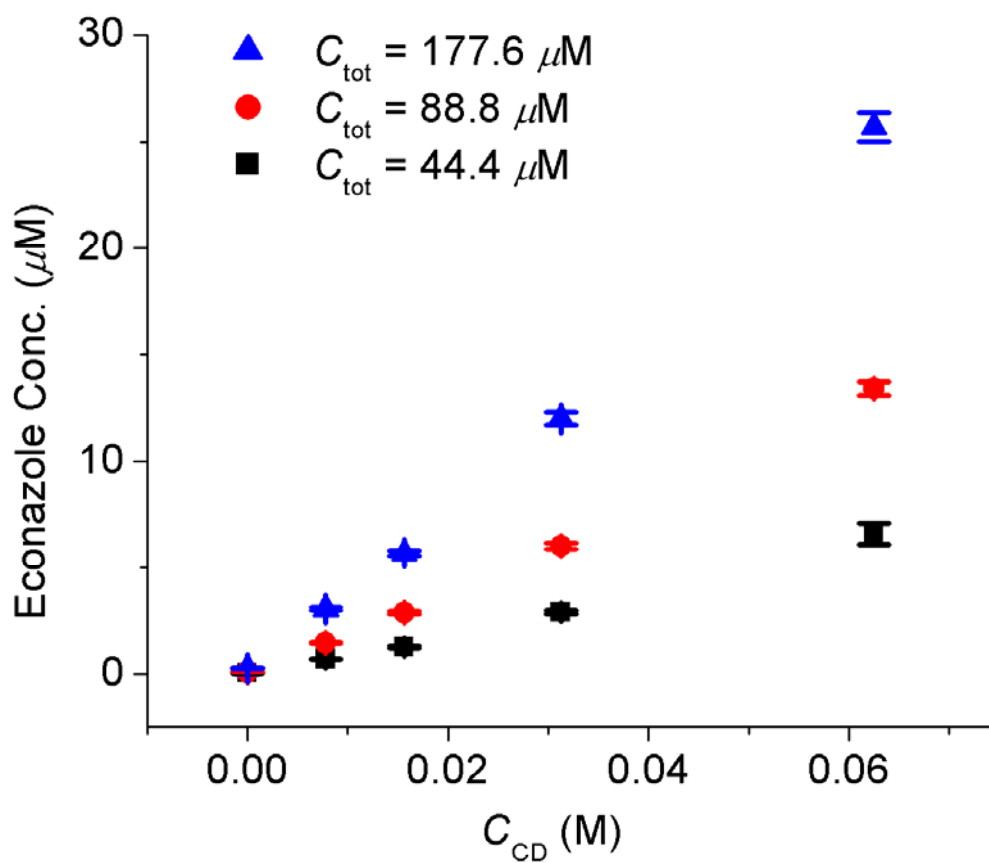equilibration. (DM-β-CD with various degrees of substitution exist)

Figure 4.7. Effect of HP-β-CD concentration on econazole equilibrium concentration in the aqueous phase at various drug concentrations.

Table 4.2. Binding constants of econazole and miconazole with HP-β-CD at various drug concentrations.

Drug	C_{tot} (μM)	D_0	$K_{1:1}$ (M^{-1})	$K_{1:2}$ (M^{-1})	COD
Econazole	44.4	(8.74 ± 0.72)x10^{-6}	1792 ± 100	12 ± 1	0.9999
	88.8	(1.02 ± 0.02)x10^{-5}	1709 ± 38	9.4 ± 0.4	0.99997
	177.6	(1.49 ± 0.12)x10^{-5}	1225 ± 30	7.2 ± 0.4	0.99996
	88.8[a]	(1.37 ± 0.06)x10^{-5}	1498 ± 8	6.8 ± 0.1	1.0000
Miconazole	80.0[b]	(1.46 ± 0.39)x10^{-6}	4052 ± 416	10 ± 2	0.9995

[a] mixed with miconazole

[b] mixed with econazole

Table 4.3. Binding constants of econazole with HP-β-CD at various pH conditions.

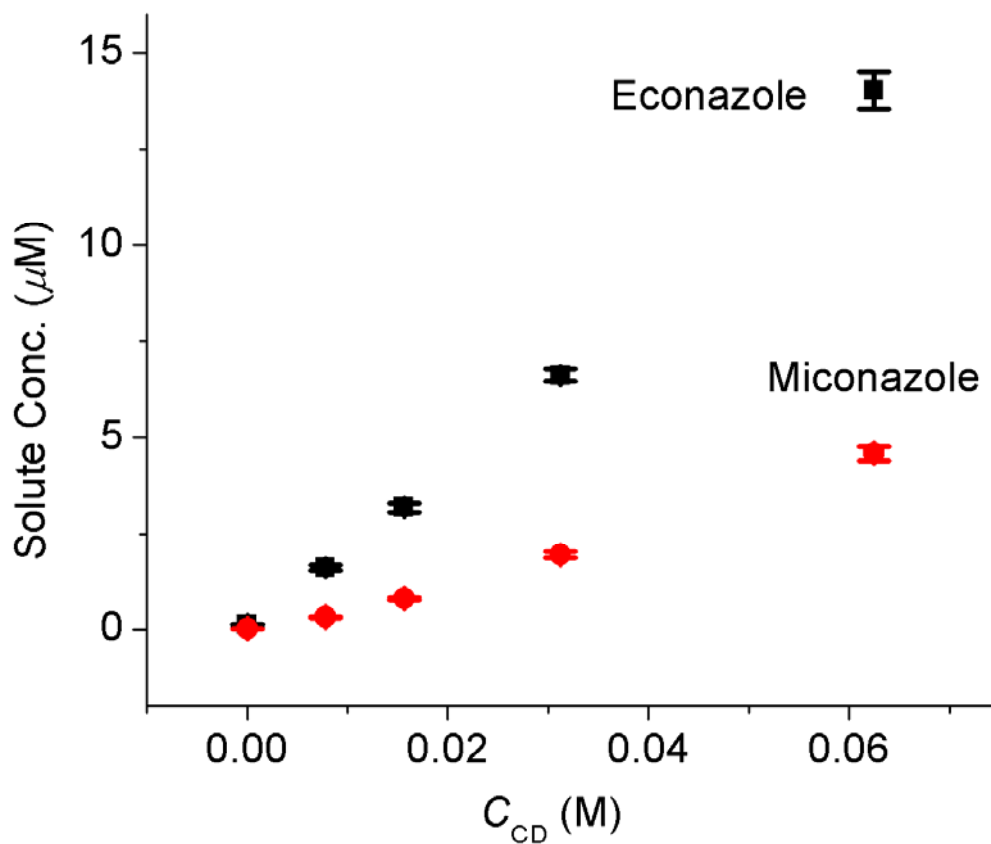| pH	D_0	$K_{1:1}$ (M^{-1})	$K_{1:2}$ (M^{-1})	COD
1.8	(1.36 ± 0.07)x10^{-2}	108 ± 6	0	0.9932
5.8	(1.86 ± 0.14)x10^{-3}	270 ± 9	0	0.9965
7.4	(3.30 ± 0.12)x10^{-5}	1964 ± 51	13 ± 1	0.9998
8.5	(1.02 ± 0.02)x10^{-5}	1747 ± 174	6.4 ± 2.3	0.9977

Figure 4.8. Effect of HP-β-CD concentration on econazole and miconazole (mixed) equilibrium concentration in the aqueous phase.

The binding behavior of econazole to HP-β-CD has been studied at various pH values. The drug equilibrium concentrations versus aqueous CD-concentration profiles are shown in Figure 4.9. The values of D_0, $K_{1:1}$ and $K_{1:2}$ are listed in Table 4.3. The $K_{1:1}$ values at pH 8.5 and 7.4 are not significantly different, but decrease rapidly in an acidic environment. Econazole is a basic compound and has a pKa value of 6.69,[28] hence it can be concluded that increased ionization decreases its binding constant with CDs, which is consistent with literature observations.[37] Moreover, the formation of the 1:2 complex is suppressed when econazole is ionized, as indicated by the values of $K_{1:2} = 0$ at pH 5.8 and 1.8.

Compared to the phase-solubility method, which can require days, this new technique is faster. Moreover, the drug amounts used in solubility experiments are much greater than in this method. For instance, the highest econazole concentration in a phase-solubility study is ~30 mM,[30] but in the phase-distribution experiment, C_{tot} is less than 0.1 mM. In addition, the volume of the CD solution used in a solubility study is typically 10 mL, which is 40 times more than in this distribution experiment. These two factors have led to a 12000-fold decrease in material requirements. The complexation of much less concentrated drug with cyclodextrins may be one of the reasons that the equilibration time is greatly shortened in these phase-distribution studies. For other phase-distribution methods, which study the drug distribution between an organic solvent and an aqueous phase, the solvent-CD complexation may lead to misinterpretation. In addition, entrainment and emulsion can be severe problems for very hydrophobic compounds,[38] and the handling of small volumes of organic solvent may be difficult.[28]

In phase-solubility studies, the accurate and precise determination of the intrinsic solubility (S_0) is highly important for the accuracy and precision of $K_{1:1}$. Similarly for this approach, the variance of D_0 may lead to misinterpretation of n and $K_{1:i}$ as well. Since the drug
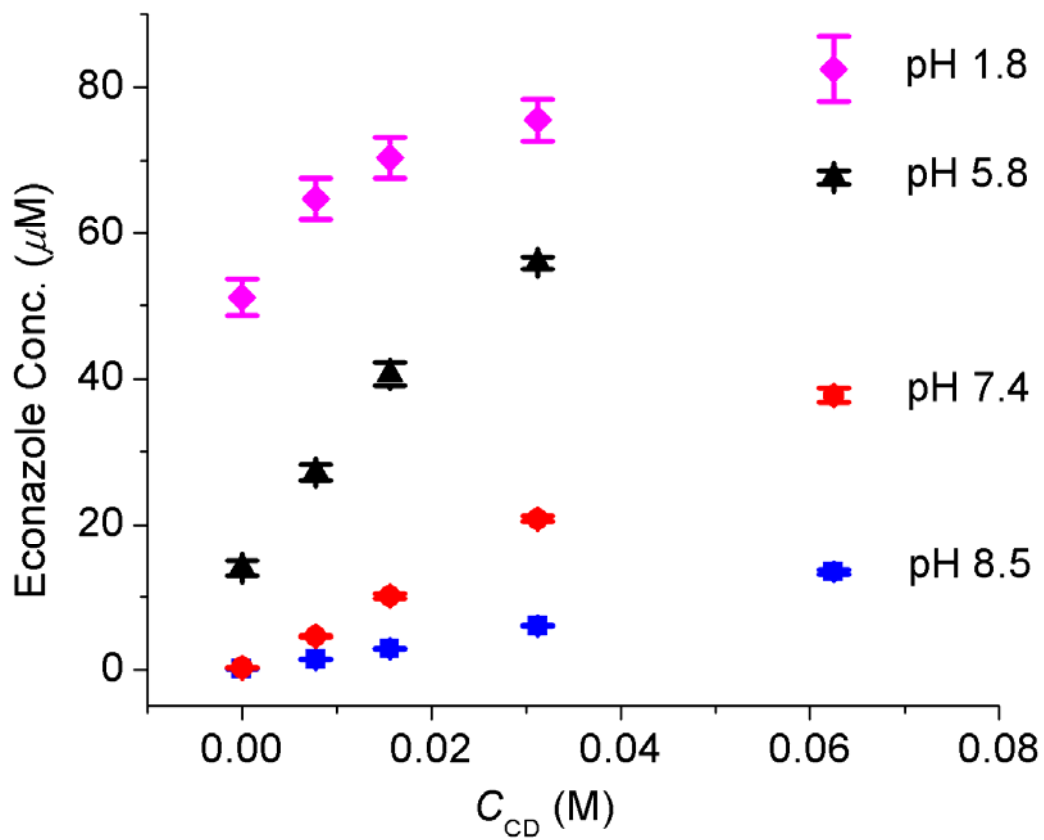
Figure 4.9. Effect of HP-β-CD concentration on econazole equilibrium concentration in the aqueous phase at various pH conditions.

concentration is usually low (~0.01-0.1 μM) when determining D_0, some error is inevitable. Ways to decrease the measurement error of D_0 have been discussed elsewhere.[28] Among them, increasing determination repeats is the easiest to implement, which is convenient when using microtiter plates.

4.5   CONCLUSIONS

A new method to measure the binding constants of drug-CD complexes in the aqueous phase using high-throughput technologies was developed. This method measures the distribution behavior of a drug between a polymer phase and an aqueous phase in 96-well microplates. With four repeats, distribution coefficients of econazole respect to six CD-containing buffers at four different concentrations can be determined simultaneously. Quadratic polynomial correlations have been established to give the binding constants of econazole to the six CDs respectively. Both 1:1 and 1:2 complexes are found and the calculated $K_{1:1}$ values can be correlated to some literature data from phase-solubility studies. The binding constants of econazole to HP-β-CD have been studied at various drug concentrations and pH conditions. At higher econazole concentrations, the drug-CD binding tends to be weaker, which may due to the self-association of the drug. An acidic environment weakens the binding between econazole with HP-β-CD and suppresses the 1:2 complex formation. Compared to the phase-solubility method, our protocol is much faster. Moreover, the material requirement decreases four orders of magnitude. This method has great flexibility as well, for instance, 'multiplex' approaches are possible due to the much lower concentration of the drug relevant to the CD concentration.

4.6 REFERENCE

(1)   Loftsson, T.; Hreinsdottir, D.; Masson, M. *International Journal of Pharmaceutics* **2005**, *302*, 18-28.

(2)   Das, N. G.; Das, S. K. *Drug Delivery Report* **2006**, *Spring/Summer*, 52-55.

(3)   Hedges, A. R. *Chemical Reviews (Washington, D. C.)* **1998**, *98*, 2035-2044.

(4)   Uekama, K.; Hirayama, F.; Irie, T. *Chemical Reviews (Washington, D. C.)* **1998**, *98*, 2045-2076.

(5)   Loftsson, T.; Brewster, M. E.; Masson, M. *American Journal of Drug Delivery* **2004**, *2*, 261-275.

(6)   Hirsch, W.; Fried, V.; Altman, L. *Journal of Pharmaceutical Sciences* **1985**, *74*, 1123-1125.

(7)   Bodor, N.; Buchwald, P. *Journal of Inclusion Phenomena and Macrocyclic Chemistry* **2003**, *44*, 9-14.

(8)   Rao, V. M.; Stella, V. J. *Journal of Pharmaceutical Sciences* **2003**, *92*, 927-932.

(9)   Lipinski, C. A. *Journal of Pharmacological and Toxicological Methods* **2001**, *44*, 235-249.

(10)   Chen, J.; Ohnmacht, C. M.; Hage, D. S. *Journal of Chromatography, A* **2004**, *1033*, 115-126.

(11)   Schou, C.; Heegaard, N. H. H. *Electrophoresis* **2006**, *27*, 44-59.

(12)   Schipper, B. R.; Ramstad, T. *Journal of Pharmaceutical Sciences* **2005**, *94*, 1528-1537.

(13)   Karakasyan, C.; Taverna, M.; Millot, M.-C. *Journal of Chromatography, A* **2004**, *1032*, 159-164.

(14)   Rundlett, K. L.; Armstrong, D. W. *Electrophoresis* **2001**, *22*, 1419-1427.

(15)   Sideris, E. E.; Georgiou, C. A.; Koupparis, M. A.; Macheras, P. E. *Analytica Chimica Acta* **1994**, *289*, 87-95.

(16)   Beni, S.; Szakacs, Z.; Csernak, O.; Barcza, L.; Noszal, B. *European Journal of Pharmaceutical Sciences* **2007**, *30*, 167-174.

(17)   Archontaki, H. A.; Vertzoni, M. V.; Athanassiou-Malaki, M. H. *Journal of Pharmaceutical and Biomedical Analysis* **2002**, *28*, 761-769.

(18)   Koopmans, C.; Ritter, H. *Journal of the American Chemical Society*, ACS ASAP.

(19)   Sheehy, P. M.; Ramstad, T. *Journal of Pharmaceutical and Biomedical Analysis* **2005**, *39*, 877-885.

(20)   Kahle, C.; Holzgrabe, U. *Chirality* **2004**, *16*, 509-515.

(21)   Higuchi, T.; Connors, K. A. *Advan. Anal. Chem. Instr.* **1965**, *4*, 117-212.

(22)   Loukas, Y. L. *Pharmaceutical Sciences* **1997**, *3*, 343-346.

(23)   Loukas, Y. L.; Vraka, V.; Gregoriadis, G. *International Journal of Pharmaceutics* **1996**, *144*, 225-231.

(24)   Masson, M.; Sigurdardottir, B. V.; Matthiasson, K.; Loftsson, T. *Chemical & Pharmaceutical Bulletin* **2005**, *53*, 958-964.

(25)   Eli, W.; Chen, W.; Xue, Q. *Journal of Inclusion Phenomena and Macrocyclic Chemistry* **2000**, *38*, 37-43.

(26)   Senisterra, G. A.; Markin, E.; Yamazaki, K.; Hui, R.; Vedadi, M.; Awrey, D. E. *Journal of Biomolecular Screening* **2006**, *11*, 940-948.

(27)   Hallikas, O.; Taipale, J. *Nature Protocols* **2006**, *1*, 215-222.

(28)   Chen, Z.; Weber, S. G. *Analytical Chemistry* **2007**, *79*, 1043-1049.

(29)   Chen, Z.; Yang, Y.; Werner, S.; Wipf, P.; Weber, S. G. *Journal of the American Chemical Society* **2006**, *128*, 2208-2209.

(30)   Mura, P.; Faucci, M. T.; Manderioli, A.; Bramanti, G. *Journal of Inclusion Phenomena and Macrocyclic Chemistry* **2001**, *39*, 131-138.

(31)   Guillaume, Y. C.; Peyrin, E. *Analytical Chemistry* **1999**, *71*, 2046-2052.

(32)   Pedersen, M.; Bjerregaard, S.; Jacobsen, J.; Rommelmayer Larsen, A.; Mehlsen Sorensen, A. *International Journal of Pharmaceutics* **1998**, *165*, 57-68.

(33)   Pedersen, M. *European Journal of Pharmaceutics and Biopharmaceutics* **1994**, *40*, 19-23.

(34)   El-Barghouthi, M. I.; Masoud, N. A.; Al-Kafawein, J. K.; Abdoh, A. A. *Russian Journal of Physical Chemistry* **2006**, *80,* 1050-1055.

(35)   Peeters, J.; Neeskens, P.; Tollenaere, J. P.; Van Remoortere, P.; Brewster, M. E. *Journal of Pharmaceutical Sciences* **2002**, *91*, 1414-1422.

(36)   Miyake, K.; Irie, T.; Arima, H.; Hirayama, F.; Uekama, K.; Hirano, M.; Okamaoto, Y. *International Journal of Pharmaceutics* **1999**, *179*, 237-245.

(37)   Pedersen, M.; Edelsten, M.; Nielsen, V. F.; Scarpellini, A.; Skytte, S.; Slot, C. *International Journal of Pharmaceutics* **1993**, *90*, 247-254.

(38)   Poole, S. K.; Poole, C. F. *Journal of Chromatography, B: Analytical Technologies in the Biomedical and Life Sciences* **2003**, *797*, 3-19.

APPENDIX A

Z-TEST[1]

The Z-test is a statistical test used in inference which determines if the difference between a sample mean and the population mean is large enough to be statistically significant.

In order for the Z-test to be reliable, certain conditions must be met. The most important is that since the Z-test uses the population mean and population standard deviation, these must be known. The sample must be a simple random sample of the population. If the sample came from a different sampling method, a different formula must be used. It must also be known that the population varies normally (*i.e.*, the sampling distribution of the probabilities of possible values fits a standard normal curve). If it is not known that the population varies normally, it suffices to have a sufficiently large sample, generally agreed to be ≥ 30 or 40.

The test requires the following to be known: σ (the standard deviation of the population), μ (the mean of the population), x (the mean of the sample), and n (the size of the sample).

First, calculate the standard error of the mean (SEM): $\text{SEM} = \sigma / \sqrt{n}$; then calculate the z score for the Z-test: $z = (x - \mu) / \text{SEM}$; finally, the z score is compared to a Z table, a table which contains the percent of area under the normal curve between the mean and the z score. Using this

table will indicate whether the calculated z score is within the realm of chance or if the z score is so different from the mean that the sample mean is unlikely to have happened by chance.

For the Z-test in Table 3.6, $\mu = 0.737$. The value of σ has been experimentally determined to be 0.0135. For each sample, $n = 2$. According to the z table, z scores should be larger than 2.33 to ensure that the sample mean is different from the population mean at the 99% confidence level.

Reference

(1)   Caulcutt, R.; Boddy, R. *Statistics for Analytical Chemists*; Chapman & Hall: London, 1983.

ULTRASPENSE 2000 MICROPLATE DISPENSER USER'S GUIDE

B.1   GENERAL OPERATION

1. Turn the power 'on', the switch is located on the back, right-hand side of the instrument.

2. Check the cleanness of the manifold; make sure channels are clean and free of debris.

3. Attach the manifold to the instrument by pushing the tube to the end while tightening the screw.

4. Insert the manifold into the holder, tighten the screw and adjust height.

5. Verify that the waste container is aligned with the waste dispenser.

6. Using the arrows to navigate through the main menu.

7. When 'Prime' is on the screen, press enter to access the Prime menu. Hit 'Yes' to rinse the instrument with solvent. You may want to do this multiple times.

8. Press 'Esc' to return to the main menu and navigate to 'Run', if you have already programmed your own dispensing process (otherwise go to B.2. first for programming). Select 'enter' to access the Run menu and choose your OWN program. Choose the number of plates (1 or 2) you want to dispense solution (usually 1). Then hit 'enter' to dispense the liquid.

9. Press 'Esc' to return to main menu. To save the liquid that is remaining in the tubing and to return it to the solvent container, access the 'Back' menu from the main menu. Select 'Yes' to return the liquid.

10. 'Prime' the instrument again (several times if needed) with solvent to rinse the instrument, followed by priming with ACN (as needed), and finally, prime the instrument with water several times.

11. When finished, carefully remove the manifold; make sure it is clean; wrap with laboratory tissues and store in a safe place.

12. Wrap the tubes with laboratory tissues and switch the power to 'off'.

13. Empty the waste container. You may need to do that between 'prime's.

14. Turn off the instrument.

B.2   PROGRAMMING

'Program' the dispensing process: You can create a new one by selecting a program that is empty. The instrument can save up to 16 programs.

1. Name your program (2 letters)

2. Choose a starting position.

3. Choose an ending position.

4. Select columns you want liquid dispensed into. Columns 1-12 will display a 1 or 0. A 1 means liquid will be dispensed into that column, a 0 means that it will not.

5. Choose the sample volume, units are microliters.

6. Choose pump speed (1-3). If unsure, '2' is probably sufficient.

7. Choose prime volume. If unsure, choose 50 μL.

8. When through programming, press 'Esc' to get back to main menu.

B.3   SETUP

'Setup' some basic parameters of the dispenser: For instance, the position of the manifold (if you change one), the pumping speed (1, 2, 3: 100-3800. Having been optimized so it is not suggested to change them.), minimal volume (DO NOT change it unless you have read the detailed manual, since it is related to the actual volume it dispenses.), the prime volume, the prime speed, etc. Please be advised to read the manual first before you 'setup' the instrument.

B.4   TROUBLESHOOTING

When the precision of the solvent dispensing is not satisfactory, it is necessary to check the performance of the dispenser. Several factors may affect the dispensing precision.

1. Bubbles in the tubing.

Solution: 'Prime'.

2. Polymer debris in the glass tips of the manifold.

Solution: Remove the debris using a capillary with an outer diameter of ~360 μm. Gas dusters may also help.

3. Solvent droplets remaining at the end of the glass tips (the most frequently occurred problem).

Solution: Keep the outside of the tips clean, especially when finishing an experiment. If necessary, ultrasonication may help. There is an alternative manifold that is equipped with stainless steel tips. It has been tested that the droplet problem was less severe when that manifold was used. However, other problems may occur and the precision was not improved. KD Scientific has been working on glass tips with ceramic coatings to solve the problem.

To check the precision of the solvent dispensing, generally two approaches can be performed. Since the viscosity of a solution may have a great effect on the precision of the dispensing, the 2nd approach is necessary for the preparation of PVC/DOS films.

1. Dissolve a reference compound in water and dispense the solution into a 96-well UV-transparent microplate. Check the UV absorbance of each well by a microplate reader.

2. Dispense the PVC/DOS/THF solution into a 96-well polypropylene microplate. After the THF is dry, the weight of film in each well is measured to evaluate the precision.

APPENDIX C

SOME TIPS IN THE EXPERIMENTAL SECTION TO IMPROVE REPRODUCIBILITY

C.1   POLYMER FILM PREPARATION

PVC is hard to dissolve in THF when the PVC/plasticizer ratio is larger than 1:1. To prevent from PVC agglomeration, it is necessary to intensively shake the flask immediately after a certain amount of THF is dispensed into the flask. It may take more than one day to dissolve if PVC agglomerates.

Ligand and/or solute can be prepared in the polymer/plasticizer/THF solution or in pure THF respectively. When prepared in the PVC/plasticizer/THF solution, only one dispensing is needed to make the polymer films hence the precision of the ligand (and/or solute) concentration in the films may be better. However, flexibility may be a problem if ligand (and/or solute) concentration-dependent experiments are performed. When ligand and solute are prepared in pure THF respectively, it is essential to dispense them first prior to dispensing the polymer/plasticizer solution. The plates are placed in the hood to allow the THF to evaporate. The polymer/plasticizer solution should then be dispensed but before the wells are completely dry. Gentle shaking may be necessary to allow the compounds in the wells to dissolve again. It is important to ensure that there is no compound remaining on the walls of the wells that is not

dissolved. Some covering is necessary when the plate is again placed in the hood for THF evaporation. Laboratory tissues are usually used. Covering will make the THF evaporation slower to ensure better reproducibility of the films. It has been observed that the solute distribution behavior may be affected by the film drying process.

C.2 AQUEOUS SOLUTION DISPENSING

For better flexibility, multi-channel pipettes are usually used to dispense aqueous solutions. Two pipettes can be basically used to deliver 50-250 μL aqueous solution into each well: a 100 μL x 12 pipette and a 1 mL x 12 pipette. Note that it is not necessary to use all the channels. The former pipette is ideal when less than 100 μL solution is dispensed into each well. The latter one is more convenient when more than 200 μL solution in each well is dispensed, especially with the 'multi-dispensing' mode. However, the precision may be poorer in this mode. The pipettes need to be calibrated regularly. It has been found that the delivery volume may become less for the channels at the two sides after a certain period of time.

In the film preparation process and when the THF evaporates, the polymer film will form not only at the bottom but also on the wall of each well. Hence it is desired that the dispensed volume of the aqueous solution is at least 50 μL more than the maximum volume of the THF solution in a well to ensure that the whole film will be covered by the aqueous solution.

Cyclodextrin solutions are extremely adhesive in the pipette tips. The 100 μL x 12 pipette is suggested in this case.